Bioactive Materials 64 (2026) 655–685

Contents lists available at ScienceDirect

Bioactive Materials

journal homepage: www.keaipublishing.com/en/journals/bioactive-materials

Design and applications of barrier membranes for guided bone regeneration

Yue Liu [a,b,d,1], Hao Zhang [b,1], Lingkun Zhang [b,*], Jianmin Han [a,d,**], Jian Yang [b,c,e,***]

[a] Tianjin Medical University School and Hospital of Stomatology & Tianjin Key Laboratory of Oral Soft and Hard Tissues Restoration and Regeneration, No.12 Qixiangtai Road, Heping District, Tianjin, 300070, PR China
[b] Department of Materials Science and Engineering, School of Engineering, Westlake University, Hangzhou, Zhejiang, 310030, PR China
[c] Research Center for Industries of the Future, Westlake University, Hangzhou, Zhejiang, 310030, PR China
[d] Tianjin Medical University Institute of Stomatology, No.12 Qixiangtai Road, Heping District, Tianjin, 300070, PR China
[e] Center for Biobased Materials, Muyuan Laboratory, Zhengzhou, Henan, 450016, PR China

ARTICLE INFO

Keywords:
Guided bone regeneration
Barrier membranes
Material innovation
Structural design
Clinical translation

ABSTRACT

Despite the placement of millions of dental implants annually, one-quarter to one-half of cases require concurrent guided bone regeneration (GBR), where a recent meta-analysis of 100 studies reported an approximately 26% complication rate that exposes the structural and biological limits of current barrier membranes. Conventional collagen and PTFE-based membranes function predominantly as passive occlusive barriers, lacking the bioactivity, controllable degradation, and immunomodulatory capacity demanded by the dynamic alveolar microenvironment, in which up to 50% of ridge width can be lost within 12 months post-extraction. Addressing this gap requires reframing GBR membranes as programmable interfaces. This review presents a three-lens framework — alveolar-bone-specific osteoimmune biology, metabolically active and stimuli-responsive material platforms, and translational bottlenecks — to systematically chart the field. We synthesize recent advances across four next-generation material families (polymer composites, biodegradable Mg/Zn alloys, MXene-based systems, and citrate-based polymers), four hierarchical structural strategies (bilayer, Janus, gradient, and 4D-printed architectures), and complementary functionalization strategies that include surface chemistry tailoring, bioactive ion release, and stimuli-responsive triggers, explicitly mapping how each modulates mechanical retention, degradation kinetics, antibacterial activity, and macrophage M1-to-M2 polarization. We further evaluate the clinical performance of these material platforms in alveolar ridge augmentation and identify platform-specific post-market follow-up endpoints required for regulatory translation. Finally, we articulate six open mechanistic questions and a near-term agenda integrating artificial intelligence/machine learning-driven design, microfluidic oral-microenvironment models, and standardized large-animal alveolar protocols. This framework repositions GBR membranes toward programmable, osteoimmune-active regenerative platforms, charting an actionable path from bench to clinic.

1. Introduction

Dental implantation is a well-established clinical approach for replacing missing teeth, with several million implants placed globally each year and a substantial proportion of cases (estimated at one-quarter to one-half) requiring concurrent or staged bone augmentation due to inadequate ridge volume; a recent systematic review and meta-analysis of 100 studies further reported a pooled complication rate of approximately 26% for guided bone regeneration (GBR) procedures [1], highlighting both the clinical importance and the residual technical challenges of this intervention. Adequate alveolar bone volume is essential for stable implant placement and long-term osseointegration.

Peer review under the responsibility of editorial board of Bioactive Materials.
* Corresponding author.
** Corresponding author. Tianjin Medical University School and Hospital of Stomatology & Tianjin Key Laboratory of Oral Soft and Hard Tissues Restoration and Regeneration, No.12 Qixiangtai Road, Heping District, Tianjin, 300070, PR China.
*** Corresponding author. Department of Materials Science and Engineering, School of Engineering, Westlake University, Hangzhou, Zhejiang, 310030, PR China.
E-mail addresses: zhanglingkun@westlake.edu.cn (L. Zhang), hanjm@tmu.edu.cn (J. Han), yangjian07@westlake.edu.cn (J. Yang).
[1] Yue Liu and Hao Zhang contributed equally to this work.

https://doi.org/10.1016/j.bioactmat.2026.05.008
Received 26 January 2026; Received in revised form 2 May 2026; Accepted 4 May 2026
Available online 21 May 2026

However, alveolar bone defects resulting from periodontal disease, periapical pathology, trauma, or tumor resection pose significant challenges to successful implant restoration [2]. Consequently, GBR has become a fundamental strategy for alveolar ridge augmentation. During this procedure, a barrier membrane covers the bone graft materials within the defect. This isolates the regenerative space and prevents soft tissue invasion, thereby facilitating bone formation [3,4]. The biological foundation of GBR lies in the principle of cell occlusivity, which enables selective repopulation of osteogenic cells. Clinically, GBR adheres to the widely accepted PASS (primary closure, angiogenesis, space maintenance, and stability) principle [5,6]. The GBR membrane plays a pivotal role in fulfilling these principles by maintaining the regenerative space, protecting the developing vascular network, and preventing the infiltration of competing soft tissues [6].

Currently, clinical GBR membranes are categorized as resorbable or non-resorbable [7]. Resorbable collagen membranes are predominantly used in clinical practice due to their excellent biocompatibility and the elimination of secondary surgical removal [7,8]. However, their rapid degradation and limited mechanical strength may compromise long-term space maintenance [9]. Conversely, non-resorbable alternatives, such as polytetrafluoroethylene (PTFE) membranes and titanium meshes, offer high mechanical strength and superior space-maintaining capabilities. Nevertheless, they carry an elevated risk of wound exposure and necessitate secondary surgical removal [10]. Crucially, these conventional materials are largely biologically inert, lacking the capacity to modulate immune responses, angiogenesis, and osteogenesis. To address these limitations, recent research has shifted toward developing bioactive and multifunctional GBR membranes that integrate structural stability with biological responsiveness. Advances in polymer chemistry, surface functionalization, and multiscale structural design enable precise regulation of biocompatibility, degradation kinetics, and localized therapeutic delivery. These innovations synchronize material degradation with tissue regeneration.

Complementing prior reviews [11,12], this work explicitly frames GBR membrane development through three complementary lenses: (i) the alveolar-bone-specific biological microenvironment (immune, vascular, and microbial), (ii) the emergence of metabolically active and stimuli-responsive material platforms beyond inert barrier function, and (iii) the regulatory and manufacturing bottlenecks gating clinical translation. To support this framework, we draw on recent literature (2015-2026) selectively, with earlier seminal studies retained for historical context. Guided by these three lenses, the review opens by establishing the alveolar-bone-specific biological microenvironment and the design requirements that emerge from it. The discussion then moves to the four clinical paradigms — rigidity, bacterial exclusion, biocompatibility, and tunability — and maps each onto its underlying material bottleneck. The core of the review synthesizes recent research progress along three complementary axes: emerging material platforms, hierarchical structural architectures, and functionalization strategies. The final chapters bridge bench to clinic by examining the regulatory and translational hurdles that gate adoption and distilling emerging directions and open questions (Scheme 1).

2. Structural characteristics and regeneration of alveolar bone

2.1. *Biological and structural basis of alveolar bone defects and regeneration*

2.1.1. *Hierarchical anatomy and turnover of alveolar bone*

Serving as the primary periodontal support, the alveolar bone comprises a distinct hierarchical architecture [13]: the lamellar socket walls mediate rapid mechanoadaptation via Sharpey's fibers [14], the trabecular core sustains local metabolic homeostasis, and the dense cortical plates provide rigid resistance to masticatory loading (Fig. 1A) [15].

As a highly metabolically active tissue, alveolar bone undergoes remodeling approximately three to six times faster than non-oral skeletal sites, with the exact ratio depending on species, anatomical site, and

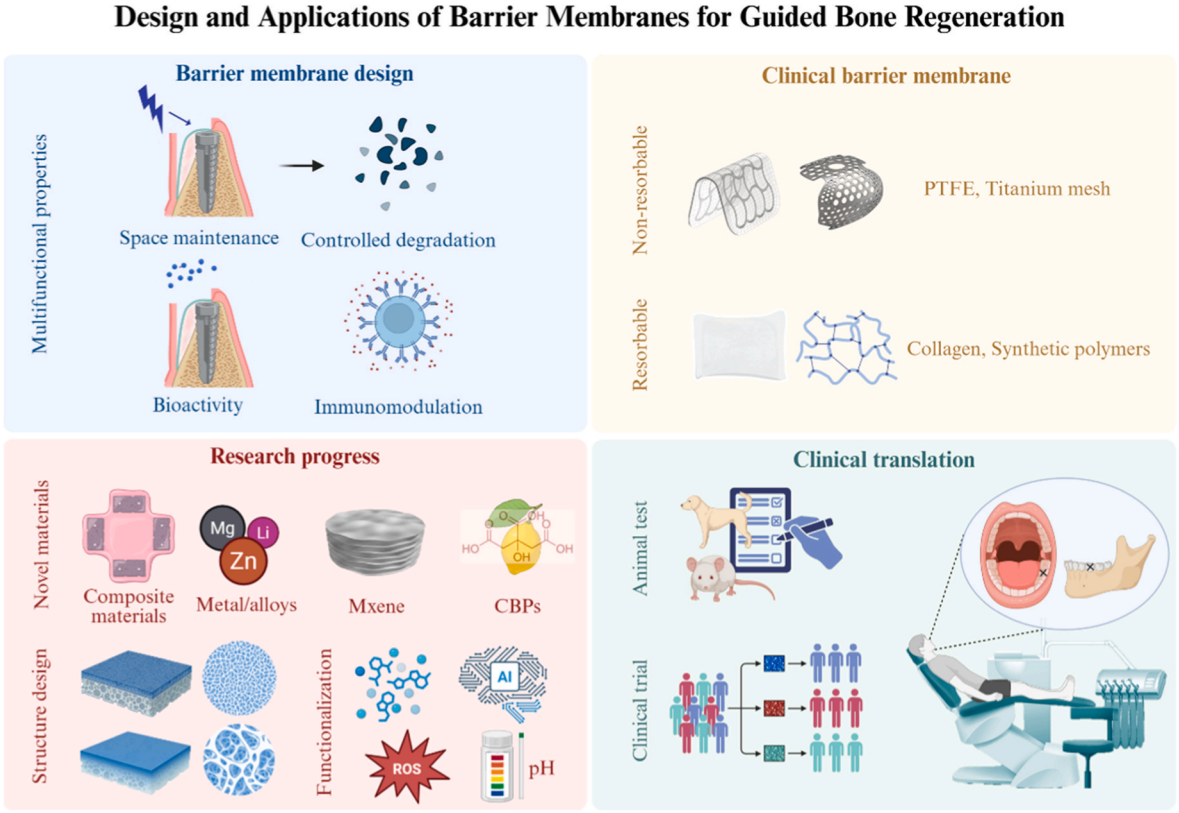

Scheme 1. Schematic illustration of the design and applications of barrier membranes for GBR.

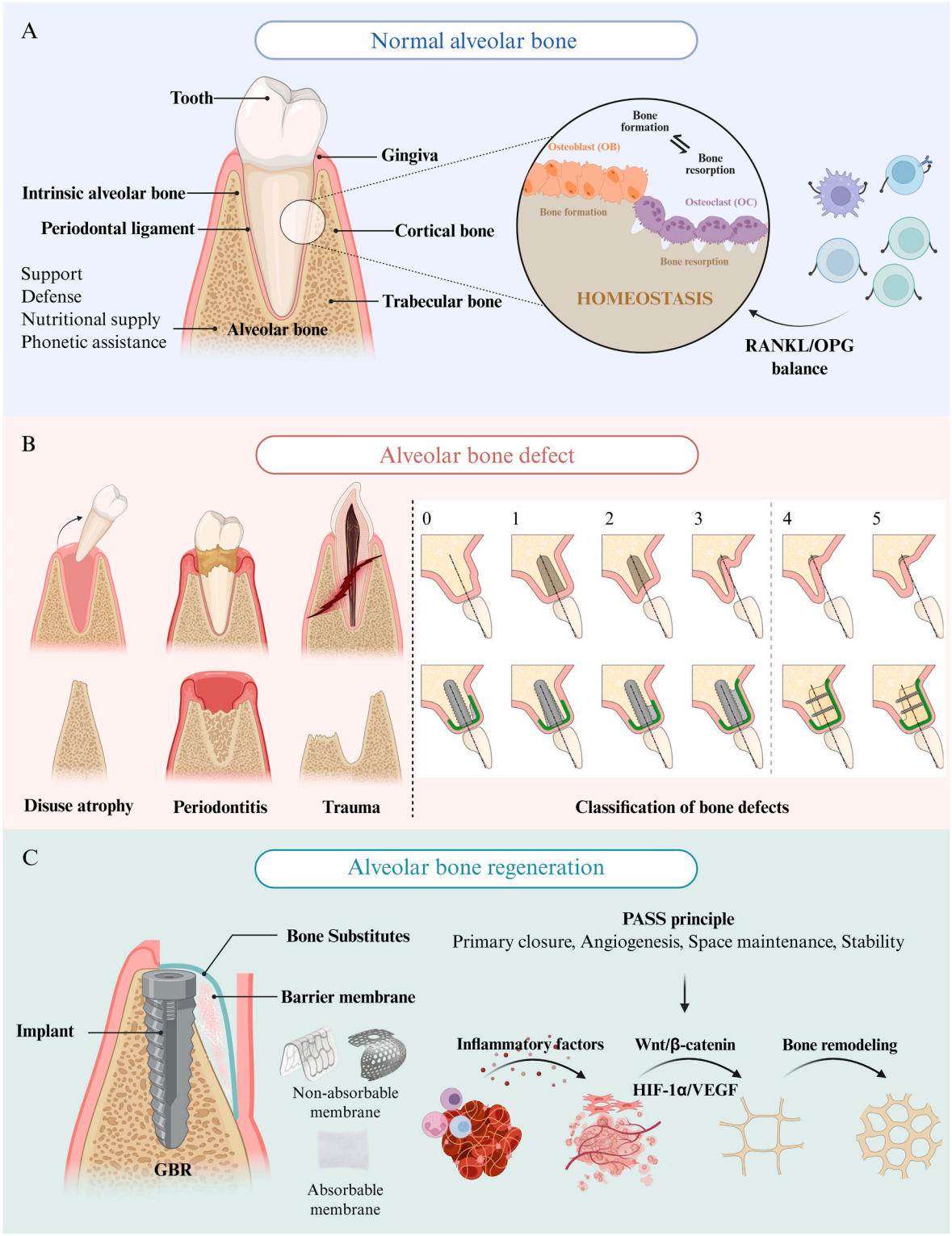

Fig. 1. Alveolar bone defects and the mechanisms of alveolar bone regeneration in GBR. A) Anatomy of the natural alveolar bone and bone homeostasis, illustrating the periodontal-bone-tooth complex (cortical plate, trabecular core, periodontal ligament) and the four physiological functions (mechanical support, defense, nutritional supply, phonetic assistance), with the RANKL/OPG-balanced osteoblast-osteoclast homeostasis maintaining bone-formation/resorption equilibrium. B) Causes and classifications of alveolar bone defects. Class 0: Site with a ridge contour deficit and sufficient bone volume for standard implant placement. Class 1: Intra-alveolar defect between the implant surface and intact bone walls. Class 2: Peri-implant dehiscence, in which the volume stability of the area to be augmented is provided by the adjacent bone walls. Class 3: Peri-implant dehiscence occurs when the surrounding bone walls fail to provide sufficient volume stability for the augmentation site. Class 4: Horizontal ridge defect requiring bone augmentation before implant placement. Class 5: Vertical ridge defect requiring bone augmentation before implant placement [31]. Copyright 2014. C) Mechanisms of alveolar bone regeneration in GBR: Under physiological conditions, the alveolar bone maintains a state of homeostasis. After tooth extraction, progressive alveolar bone resorption frequently results in horizontal ridge deficiencies, creating the need for GBR to re-establish bone contour and support implant placement. The bone regeneration process of GBR primarily involves four stages: (1) the formation of the blood clot and inflammatory response. (2) granulation tissue formation and vascularization. (3) woven bone formation. (4) bone remodeling and lamellar bone formation.

measurement method, adapting to mechanical loading in accordance with Wolff's law [16–19]. However, following tooth extraction, the loss of periodontal-ligament (PDL) stimulation leads to rapid resorption. The PDL niche additionally harbors PDL-derived stem cells (PDLSCs) with osteogenic-immunomodulatory profiles distinct from long-bone bone marrow mesenchymal stem cells, a heterogeneity revisited in Section 6. Clinical evidence indicates that alveolar ridge width can decrease by approximately 50% within the first 12 months post-extraction, with much of the horizontal resorption occurring within the first three months, followed by significant vertical height loss within the first six months [19,20]. Consequently, long-term tooth loss often causes progressive alveolar ridge atrophy, posing a significant challenge for implant rehabilitation.

2.1.2. Cellular orchestration of bone remodeling

At the cellular level, alveolar bone remodeling involves osteoblasts (controlled by Wnt/β-catenin, BMP-Smad, and Runx2/Sp7 transcriptional networks), osteoclasts (differentiated from monocytic precursors via M-CSF/RANKL signaling and resorbing bone matrix through integrin-αvβ3-mediated podosome formation), osteocytes (the principal mechanosensors that secrete sclerostin to restrain Wnt-driven osteogenesis under low-load conditions), and osteoprogenitor cells, which collectively maintain a tightly regulated balance between bone formation and resorption, broadly consistent with general bone homeostasis mechanisms (Fig. 1A; Table 1) [21,22]. This dynamic remodeling is essential for maintaining skeletal homeostasis and regenerative potential. Unlike other skeletal sites, alveolar bone is uniquely influenced by its microbiota-dependent immune microenvironment [21,23]. Immune cells, including B and T lymphocytes, regulate osteoclastogenesis via the receptor activator of nuclear factor kappa-B ligand (RANKL)/osteoprotegerin (OPG) axis, with Th17-derived IL-17 and IL-1β further amplifying RANKL signaling under inflammatory states. Inflammatory conditions such as periodontitis — driven in part by oral dysbiotic species that activate TLR2/TLR4 cascades on resident macrophages — exacerbate bone resorption, highlighting the critical role of immune regulation in alveolar bone health [24–27].

2.1.3. Defect etiology and clinical classification

Clinically, alveolar bone defects present a common challenge, significantly impacting both the primary stability and long-term success of dental implants [28]. The etiology of these defects is multifactorial, encompassing physiological resorption following tooth loss, periodontal diseases, trauma, and tumor resection (Fig. 1B) [29]. Notably, periodontal disease-related defects are strongly associated with oral microbiome dysbiosis. This triggers persistent host inflammatory responses and osteoclast activation, ultimately causing progressive alveolar bone destruction [30]. These defects are commonly categorized into horizontal, vertical, and combined defects, which largely dictate the choice of bone augmentation strategy [31]. Among available techniques, GBR is widely adopted for horizontal ridge augmentation due to its predictable outcomes and relatively low surgical morbidity, accounting for approximately 40% of clinical cases [32–34]. Beyond geometric classification, three anatomically-defined biomechanical factors govern membrane choice and surgical protocol: (i) defect biomechanics — the residual lingual or palatal bone wall provides primary structural anchorage, with single-wall defects mandating rigid space maintenance; (ii) residual bone height and width — defects with horizontal residual bone width below 4 mm or vertical bone height below 5 mm require staged augmentation rather than simultaneous implant placement; and (iii) overlying soft-tissue thickness — keratinized tissue thickness below 2 mm correlates with elevated risk of membrane exposure (the lamellar/trabecular/cortical hierarchy described above provides anatomical context for these biomechanical thresholds) and necessitates either soft-tissue augmentation prior to GBR or use of low-stiffness, dehiscence-tolerant membrane chemistries. These three factors, rather than defect class alone, dictate the membrane mechanical profile (rigid d-PTFE-Ti vs resorbable collagen) and the use of additional fixation hardware [35,36].

2.1.4. Temporal cascade of GBR-mediated bone healing

The underlying bone regeneration process in GBR is highly complex and temporally orchestrated, involving four overlapping stages: inflammation, angiogenesis, stem cell recruitment and differentiation, and bone remodeling. Within 24 h postoperatively, a blood clot fills the defect space, serving as a provisional matrix. Platelet-derived factors subsequently recruit inflammatory and progenitor cells to initiate early healing [10,37]. This phase is followed by the formation of vascularized granulation tissue and the recruitment of bone marrow mesenchymal stem cells (BMSCs) from surrounding bone marrow and periosteum. Adequate angiogenesis critically supports osteogenesis via signaling pathways such as the hypoxia-inducible factor 1α (HIF-1α)/vascular endothelial growth factor (VEGF) axis [37–40]. Over subsequent weeks (weeks 2-8), osteoprogenitor cells differentiate into osteoblasts under Runx2/Sp7-dependent transcriptional programs, driving osteoid deposition and woven bone formation, while osteoclasts initiated through M-CSF/RANKL begin coordinated remodeling. This woven bone is gradually remodeled into functionally competent lamellar bone over a period of several months that varies with defect size, location, and patient factors (Fig. 1C) [37,41–44].

Each stage is characterized by distinct molecular timing markers that should guide membrane bioactive-release design: the early inflammatory phase (0-72 h) is driven by NLRP3 inflammasome activation and IL-1β/TNF-α/IL-6 secretion; the angiogenic phase (day 3-7) is dominated by HIF-1α stabilization, VEGF and angiopoietin-2 (Ang-2) signaling, and pericyte recruitment; the osteogenic phase (day 7-28) is marked by Runx2/Sp7 transcriptional activation and matrix deposition genes (COL1A1, ALP, BGLAP); and the remodeling phase (>28 d) involves osteoclast-driven resorption tracked by TRAP and Cathepsin K, balanced

Table 1
Cellular and molecular mechanisms underlying alveolar bone regeneration relevant to GBR membrane design.

Cell type	Functional effect	Implication for GBR membrane design	Refs
Osteoblast	Differentiation, matrix mineralization	Surface stiffness >30 kPa and bioactive ion release (e.g., Sr^{2+}, Mg^{2+}) sustain osteogenic transcriptional programs	[21, 52–54]
Osteoclast	Bone resorption via podosome formation	Controlled OPG-like cues or RANKL antagonism via locally released Mg^{2+}/Zn^{2+} may rebalance osteoclast activity	[21, 23–27]
Osteocyte	Mechanical adaptation; suppresses Wnt under low load	Membranes preserving load transmission to underlying bone may reduce sclerostin-driven Wnt suppression	[16–19]
M1 macrophage	Acute inflammation, pathogen clearance	Membrane debris and bacterial colonization should not perpetuate M1 beyond the 48-72 h transition window	[46,47]
M2 macrophage	Tissue repair; angiogenesis-osteogenesis coupling	Material stiffness, hydrophilicity, and ion cues that bias toward M2 phenotype prolong reparative cytokine output	[49–54, 56]
Endothelial cell	Vascular sprouting, vessel maturation	Pore architecture (>200 μm) and HIF-1α-stabilizing cues (e.g., DFO, hypoxia-mimetics) support timely vascular ingrowth	[37–40]
PDLSCs	Cementogenic and osteogenic differentiation; PDL regeneration	PDL niche-mimetic cues (collagen-rich interfaces, mechanical anisotropy) sustain PDLSCs commitment for periodontal-defect applications	[13,14]

against continued osteoblast activity. Synchronizing release kinetics of bioactive cues and degradation profiles to these molecular windows is a central design objective for next-generation bioactive GBR membranes [45].

2.1.5. Vascular, immune, and osteogenic crosstalk and implications for membrane design

Emerging research in osteoimmunology has demonstrated that biomaterials actively modulate the local immune environment, with macrophages as the principal effectors. While initial M1-driven inflammation — mediated by TLR4/NF-κB signaling and a glycolytic metabolic shift that supports rapid cytokine production (IL-6, TNF-α, IL-1β) — is necessary to clear damaged tissue and recruit progenitor cells, prolonged M1 activity impairs osteogenesis [46,47]. Thus, a timely M1-to-M2 transition is critical. M2 macrophages — metabolically reprogrammed toward fatty-acid β-oxidation and oxidative phosphorylation under IL-4Rα/STAT6 and arginase-1 signaling — orchestrate tissue repair by coupling angiogenesis with osteogenesis (via VEGF/HIF-1α stabilization) and activating TGF-β/BMP-Smad pathways through the secretion of IL-10, TGF-β, and BMP-2 [48–50]. Transcending their traditional role as passive barriers, GBR membranes actively instruct these polarization dynamics through their inherent physicochemical properties [46,51]. Specifically, material stiffness, surface chemistry, and ionic cues collectively dictate macrophage fate via mechanotransduction, specific protein adsorption, and intracellular signaling cascades [52–54]. Ultimately, this highlights a mechanistically intertwined triad of immune, vascular, and osteogenic processes: macrophage polarization influences HIF-1α/VEGF-driven angiogenesis, which in turn influences osteoprogenitor recruitment and the osteoblast-osteoclast balance. These findings emphasize that successful GBR depends not only on mechanical space maintenance but also on the biomaterial's capacity to regulate the local microenvironment.

Therefore, an ideal GBR membrane must act as more than a mere physical barrier; it should actively support vascularization, modulate immune responses, and coordinate its degradation kinetics with new bone formation. These biological criteria establish the foundational design principles for the advanced GBR membranes discussed in the following sections [55].

2.2. Design requirements and standards for GBR membranes

2.2.1. Mechanical stability and space maintenance

Mechanical stability is the primary functional requirement of GBR membranes, as membrane collapse or deformation can compromise the regenerative space, disrupt blood clot stabilization, and ultimately reduce the volume of newly formed bone [55]. Specifically, the compressive and elastic moduli are pivotal parameters that dictate the membrane's capacity to resist complex biomechanical loading within the oral microenvironment. Furthermore, adequate tensile strength in a hydrated state is paramount to ensure excellent surgical handlability (e.g., conformability and suturability) and long-term *in vivo* structural integrity [55].

2.2.2. Controlled degradation and temporal matching with bone regeneration

The degradation profile of GBR membranes is a critical design parameter that directly dictates clinical performance. Ideally, the membrane's resorption kinetics must precisely align with the temporal requirements of bone regeneration. Premature degradation compromises early-stage mechanical stability and space maintenance, whereas excessively slow resorption interferes with tissue remodeling and integration [55,57]. An ideal GBR membrane should maintain its barrier function and provide stable mechanical support throughout the bone regeneration process, which typically lasts 3 to 6 months after surgery [37]. Consequently, increasing research efforts focus on engineering membranes with programmable degradation profiles via strategic material selection, cross-linking techniques, or composite designs.

2.2.3. Multifunctional design for osteoimmune-driven regeneration

Driven by advances in materials science, GBR membranes have evolved from inert physical barriers into bioactive, multifunctional interfaces. Emerging evidence in osteoimmunology demonstrates that successful regenerative outcomes are strongly dictated by the biomaterial's interaction with the local immune microenvironment. Rather than viewing tissue repair as isolated events, modern membrane design recognizes an interconnected biological triad: immune modulation, angiogenesis, and osteogenesis. Specifically, actively inducing macrophage polarization toward a pro-healing (M2) phenotype is a mechanistic prerequisite for early robust angiogenesis, which subsequently couples with and accelerates new bone formation [48]. To actively orchestrate this complex cellular cascade, the membrane's physicochemical properties, pore architecture, and surface chemistries are explicitly tailored. Contemporary engineering strategies focus on incorporating bioactive components to directly enhance endothelial and stem cell functions [55,58,59]. Ultimately, recognizing that no single monolithic material can simultaneously satisfy the stringent demands for mechanical stability, temporal degradation, and multifaceted biological signaling, modern GBR design has increasingly shifted toward hierarchical solutions. Multilayered and composite architectures are now extensively employed, allowing researchers to synergize robust structural barrier functions with spatiotemporally controlled osteoimmunomodulatory activities [48,60].

Overall, GBR membrane design has progressed from inert barriers to multifunctional bioactive systems, specifically tailored to the unique biological and immunological characteristics of alveolar bone. A comprehensive understanding of how material properties interact with the local mechanical, cellular, and immunological microenvironment is essential for rationally developing next-generation GBR membranes with superior regenerative efficacy. Before such next-generation designs can be properly framed, however, it is essential to map how each clinical paradigm has historically constrained current membrane chemistries — the focus of the following discussion.

3. Clinical paradigms and material bottlenecks of current membranes

Despite the commercial proliferation of GBR membranes over the past decades, clinical decision-making remains heavily challenged by inherent material trade-offs. Historically, commercially available options are categorized by their degradation behavior (non-resorbable vs. resorbable) and origin (polymers, metals, naturally derived) (Tables 2 and 3). However, because no single material currently satisfies all the stringent requirements for ideal bone regeneration, selecting an appropriate membrane requires carefully balancing mechanical stability against tissue integration and complication risks. Therefore, this section critically analyzes current representative membranes through the lens of their primary clinical limitations and material bottlenecks.

3.1. Rigidity and soft tissue morbidity

For large or complex vertical alveolar ridge augmentations, rigid structural support is paramount. Titanium meshes and titanium-reinforced PTFE membranes have long been the mainstays for such demanding defects [61,62]. Owing to its high mechanical strength and corrosion resistance, titanium provides excellent space-making capability and limits bacterial adhesion [63,64]. Clinical studies confirm their efficacy in achieving greater vertical bone gain compared to non-rigid alternatives [65], while forming a protective pseudo-periosteum that mitigates complete graft failure even upon exposure [63,66]. However, this necessary rigidity introduces a significant clinical dilemma: soft-tissue morbidity. The stiffness of these non-resorbable barriers frequently causes soft-tissue irritation, leading

Table 2
A summary of commercially non-resorbable GBR membranes.

Product name	Manufacturer	Regulatory status	Composition and structure	Bacterial barrier	Surgical operability
RPM™ - Reinforced PTFE Mesh	Osteogenics Biomedical (USA)	FDA cleared, CE certification	Macropores (0.66 mm) d-PTFE permit limited vascular and cellular penetration.	Yes	Moderate; requires trimming and fixation screws
Cytoplast™ Ti-150/ Ti-Reinforced	Osteogenics Biomedical (USA)	FDA approved, CE certification	d-PTFE (provides barrier function) + titanium frame (provides rigidity and structural stability).	Yes	Good; easily shaped but requires fixation
Titanium T-Barrier	B&B Dental (Italy)	CE certification	Titanium (Grade 2) - available in multiple sizes and shapes.	Yes	Moderate; requires contouring and screw fixation
NeoGen® Non-Reinforced Membrane	Neoss (Sweden)	CE certification	Bilayer PTFE; flexible and easily shaped.	Yes	Excellent; soft and flexible PTFE membrane, easy to trim and adapt to defect morphology
NeoGen® Ti-Reinforced membrane	Neoss (Sweden)	CE certification	Trilaminar design: outer PTFE layer, inner PTFE layer, intermediate malleable titanium mesh	Yes	Good; malleable mesh allows easy shaping
NeoGen® Cape PTFE Membrane	Neoss (Sweden)	CE certification	Prefabricated PTFE + titanium membrane connected to implant abutment	Yes	Excellent; minimal trimming and simplified placement
Customized Titanium Membrane	NeoBiotech (USA)	CE certification	Patient-specific titanium membrane (~0.12 mm thick), CAD-CAM fabricated	Yes	Good; customized shape reduces intraoperative adjustment
Cytoflex® Ti-Enforced	Unicare Biomedical (USA)	FDA cleared	Microporous ePTFE membrane reinforced with titanium frame	Yes	Good; flexible but reinforced for stability
Cytoflex® Tef-Guard®	Unicare Biomedical (USA)	FDA approved	Microporous ePTFE membrane without metal reinforcement	Yes	Excellent; flexible and easily sutured

Notes: The information presented in the table has been compiled from multiple sources, including manufacturer-provided technical data sheets, regulatory agency databases, and peer-reviewed literature.

to high rates of wound dehiscence — particularly when sharp edges are produced during manual shaping [63]. Furthermore, the mandatory secondary surgical removal inevitably increases patient morbidity, surgical trauma, and treatment costs. Consequently, their use is strictly reserved for scenarios where the demand for structural support outweighs the severe drawbacks of non-resorbable rigidity.

3.2. Bacterial exclusion and vascular permeability

PTFE, widely used since its introduction by Gottlow et al. in 1986 [67], exemplifies a critical microstructural paradox in non-resorbable polymer design. The classic expanded PTFE (e-PTFE) features a highly porous architecture (nodes interconnected by fibrils) [68] that facilitates excellent collagen fiber infiltration and membrane stabilization [69–71], historically earning it the title of the GBR "gold standard" [61]. However, this porosity acts as a double-edged sword: upon inevitable membrane exposure, e-PTFE becomes highly susceptible to bacterial colonization, often leading to severe infections and compromised bone regeneration [72].

To counteract this, dense PTFE (d-PTFE) membranes were developed with markedly reduced pore sizes (0.2-0.3 μm), effectively preventing bacterial penetration even during exposure [73–78]. Yet, solving the infection problem created a new biological bottleneck: the extremely dense structure severely impedes vascular infiltration and nutrient diffusion, thereby slowing de novo bone formation [79]. This ongoing struggle to balance soft-tissue exclusion against nutrient permeability highlights the fundamental limitations of static PTFE architectures.

3.3. Biocompatibility and biomechanical limitations

Driven by the desire to eliminate secondary surgeries, Langer et al. (1993) pioneered the shift toward resorbable biomaterials [80]. Currently, collagen membranes (typically bovine or porcine type I/III) dominate the resorbable market due to their unparalleled biocompatibility and low complication rates [31,81–84]. Structurally, collagen membranes utilize a bilayer design to simultaneously prevent epithelial down-growth and support osteogenesis.

Despite these biological advantages, collagen membranes suffer from a fatal flaw: biomechanical vulnerability. They intrinsically lack load-bearing capacity, exhibiting dry tensile strengths often below 10 MPa, which dramatically plummet upon physiological hydration. Furthermore, their rapid enzymatic degradation (typically within 4-12 weeks) frequently leads to premature spatial collapse [85]. Therefore, various cross-linking strategies (ultraviolet, enzymatic, chemical) have been employed to prolong their structural persistence (up to 4-6 months, Table 3) [86,87]. However, excessive chemical modification often compromises the membrane's inherent cytocompatibility, alters cellular responses, and complicates tissue integration, leaving the long-term biological safety of highly cross-linked collagen heavily debated [88].

3.4. Tunability and microenvironmental toxicity

Synthetic biodegradable polymers — such as polylactic acid (PLA), polylactic-co-glycolic acid (PLGA), and polycaprolactone (PCL) — were introduced to overcome the unpredictable degradation of natural collagen [89–91]. These platforms offer precise molecular control over degradation kinetics and mechanical stiffness [92]. However, their clinical adoption is fundamentally bottlenecked by microenvironmental toxicity and biological inertness. Standalone synthetic polymers possess highly hydrophobic surfaces that hinder initial cell adhesion. More critically, their bulk degradation via ester bond hydrolysis releases acidic by-products [93]. This localized acidification provokes severe sterile inflammatory cascades, directly jeopardizing osteoblast function and local angiogenesis. Because these basic polymer platforms cannot overcome their inherent chemical limitations alone, their future utility strictly depends on evolving into multifunctional composite systems.

In conclusion, the current landscape of GBR membranes is defined by a series of compromises. Non-resorbable barriers offer unmatched stability but demand secondary surgeries and risk soft-tissue complications. Conversely, resorbable natural and synthetic polymers provide procedural convenience but struggle with biomechanical failure, unpredictable degradation, or acidic microenvironments. These inherent material bottlenecks underscore a compelling, unmet clinical need: the development of next-generation, actively modulated membranes that seamlessly integrate robust mechanical support, spatiotemporally matched degradation, and proactive biological cues for efficient bone regeneration. Three complementary axes of innovation — emerging material platforms, hierarchical structural architectures, and active functionalization strategies — have emerged to address these compromises and form the focus of the following discussion.

Table 3
A summary of commercially resorbable GBR membranes.

Product name	Manufacturer	Composition	Regulatory status	Structure	Mechanical properties	Degradation time
Bio-Gide®	Geistlich (Switzerland)	Porcine type I/III collagen	CE/MDR certification, FDA cleared, NMPA registration	Bilayer structure: dense surface blocks soft tissue, porous surface promotes osteogenesis.	4-8 MPa (dry); 1-2 MPa (wet) [94,95]	~8-16 weeks
HEAL-ALL®	ZH-Bio (China)	Porcine type I collagen	NMPA registration	Thicknesses: 0.2 mm (for smaller defects)/ 0.4 mm (for larger defects).	7-8 MPa (dry); ~5 MPa (wet) [96]	~8-12 weeks
Megreen®	Reshine-Bio (China)	Bovine pericardium tissue	NMPA registration	Smooth surfaces and rough surfaces	Not available	Not available
Bixiu®	Huamai Medical (China)	Sheep rumen mucosal matrix	NMPA registration	Three-layer structure: porous - dense - porous	Not available	4-6 months
Jason® Membrane	Botiss (Germany)	Porcine pericardium collagen	CE certification, NMPA registration	~0.15 mm thick, with a rough and porous structure (pore size: 78.90 ± 75.89 μm) [97,98]	~13 MPa [99]	>12 weeks
Creos Xenoprotect®	Nobel Biocare (Sweden)	Porcine type I collagen	FDA approved, CE marked	Bilayer design preserving native collagen matrix; high tensile and tear resistance.	High suture retention when hydrated (6.1 N). High force at break, wet (21.2 N).	Not available. The literature presents images of membrane degradation in animal models [100].
OSSIX® Plus	Dentsply Sirona (USA)	Porcine type I collagen	FDA cleared	Thickness: 0.18-0.25 mm. Pore size: ~0.46 μm [97]	~5.13 MPa (dry); ~1.2 MPa (wet) [94]	4-6 months. Resists degradation for 3-5 weeks when exposed
BioMend®	ZimVie (USA)	Bovine tendon type I collagen	FDA approved	Thin, mildly rigid, and suturable.	Significantly higher than porcine collagen membranes	~8 weeks
BioMend Extend®	ZimVie (USA)	Bovine tendon type I collagen	FDA approved	Good space maintenance and tear resistance; suturable and easy to handle	Significantly higher than porcine collagen membranes	~18 weeks
T-Barrier Collagen	B&B Dental (Italy)	Equine collagen	CE marked	No pin fixation needed	Not available	~6-8 weeks
NaturesQue ColTect P®	BEGO (Germany)	Porcine peritoneum/ abdominal collagen	Uncleared	Minimally cross-linked; stiff dry state becomes pliable when hydrated.	Not available	~12-16 weeks
Cytoflex Resorb®	Unicare Biomedical (USA)	PLGA	FDA approved	Thickness ≈ 370 μm	Not available	~2-6 months

Notes: The information presented in the table has been compiled from multiple sources, including manufacturer-provided technical data sheets, regulatory agency databases, and peer-reviewed literature. Some commercial membrane products do not disclose complete mechanical data. Mechanical values represent typical ranges reported for collagen-based GBR membranes under dry and wet conditions in the literature. There are differences among the experiments.

4. Research progress and trends of novel GBR membranes

In response to the limitations of existing GBR membranes, increasing research efforts have been directed toward the development of next-generation membranes. Recent advances in GBR have driven the development of novel barrier membranes that extend beyond conventional passive barriers, with increasing emphasis on material innovation, structural design, and functional integration to better meet the complex biological requirements of alveolar bone regeneration.

4.1. Progress in material design

Material composition fundamentally determines the mechanical, degradation, and biological behavior of GBR membranes. Table 4 summarizes representative materials, broadly categorized into polymer-based composites, biodegradable metal alloys, MXene-based systems, and citrate-based polymers (CBPs).

4.1.1. Composite systems

Single-component matrices rarely satisfy the triple demand of mechanical support, controlled biodegradation, and biological induction simultaneously, motivating the extensive development of composite GBR membranes. These composite systems integrate the processability, mechanical stability, and biodegradability of polymeric matrices with the bioactivity and osteoconductivity of functional fillers, thereby achieving a balanced triad of space maintenance, physical barrier integrity, and biological induction [121]. Equally critical is the choice of fabrication route — electrospinning, 3D/4D printing, freeze-drying, and solvent casting — which dictates fiber diameter, pore architecture, mechanical anisotropy, and growth-factor retention; the same composite formulation can therefore yield substantially different *in vivo* behavior depending on how it is processed.

Synthetic-polymer matrices. Synthetic biodegradable polymers, such as PCL, PLA, and PLGA, offer highly tunable mechanical properties but are inherently limited by a lack of osteoinductivity, with PLA and PLGA additionally producing acidic degradation by-products that may locally acidify the microenvironment. To bridge this gap, inorganic compounds, including nano-hydroxyapatite (nHA, $Ca_{10}(PO_4)_6(OH)_2$; stoichiometric Ca/P = 1.67), β-TCP, silica, and bioactive glass (BG), are frequently incorporated. These functional fillers gradually release bioactive ions (e.g., Ca^{2+}, PO_4^{3-}, soluble silicon species), providing nucleation sites for mineralization and promoting osteogenic differentiation [122,123]. Furthermore, basic inorganic phases buffer the acidic degradation of polyesters, creating a more favorable microenvironment for bone formation [124]. Studies consistently show that while moderate inorganic loading enhances both osteogenic activity and mechanical strength, excessive concentrations lead to particle aggregation and structural compromise [125–131].

Bioactive inorganic fillers. Beyond basic calcium phosphates, BG has emerged as a promising filler due to its tunable release of diverse bioactive ions (e.g., Si, Ca, P, Mg, Mn), which not only stimulate bone regeneration but also facilitate angiogenesis and favorably modulate the local immune microenvironment. Han et al. developed a multifunctional composite membrane (PPMnBG) by incorporating manganese-containing BG (Mn-BG) into a PLGA/PCL matrix. In an alveolar bone defect model, this material demonstrated a notable capacity to promote bone regeneration [132]. It not only supported cell adhesion and proliferation but also enhanced osteogenic differentiation, alleviated oxidative stress, and favorably remodeled the immune microenvironment by modulating macrophage metabolism (Fig. 2A).

2D-material reinforcements. To further enhance cellular affinity without compromising mechanical stability, synthetic polymers are often functionalized with natural extracellular matrix (ECM) components like collagen, recombinant human-like collagen (RHC), and gelatin. These additions significantly improve surface hydrophilicity and provide essential integrin-binding motifs for cell adhesion [133–138]. Advanced composite platforms have also integrated therapeutic metal ions (e.g., Sr^{2+} to simultaneously promote osteoblasts and inhibit osteoclasts) and 2D functional graphene-family materials, such as thermal pyrolysis graphene (TPG) — exemplified by the nTPG/PLGA/PCL system (Fig. 2B), in which Sr^{2+} release supports osteoblast activity [139] and TPG couples mechanical reinforcement with active immunomodulation [140].

Natural-polymer composites. In contrast to synthetic polymer-dominated platforms, natural material-based composites rely on biologically derived macromolecules (primarily collagen, CS, and SF) to

Table 4
Comparison of representative materials for GBR membranes.

Materials	Tensile strength	Degradation time	Advantages	Limitations	References
PCL-based membrane	1-10 MPa	12-36 months. Can be accelerated by combining with gelatin, β-TCP, or HA.	Good mechanical stability and controllable structure.	Slow degradation; Acidic degradation products may cause inflammation.	[101–104]
PLGA-based membrane	0.27-5.3 MPa	2-6 months (depending on LA/GA ratio).	Tunable degradation rate.	Acidic degradation products may cause inflammation.	[102,105,106]
Collagen-based membrane	Normally less than 10 MPa. Can be enhanced (up to 22.3 MPa or higher) by modification.	4-12 weeks	Excellent biocompatibility, easy integration with host tissue.	Rapid degradation, limited mechanical strength. Pure collagen membranes lack biological activity.	[10,95,107,108]
CS-based membrane	Most are ~10 MPa. Can be reinforced with HA or polymers.	6-12 weeks. Can be reinforced with HA or polymers	Antibacterial activity, good biocompatibility.	Mechanical properties and bioactivity are still limited.	[102,109,110]
Silk fibroin (SF)-based membranes	Less than 10 MPa. Related to structure and process.	2-6 months (depending on β-sheet crystallinity)	Good biocompatibility	Limited osteoinductivity	[111,112]
Magnesium-based membrane	Up to hundreds of MPa	Less than 6 months. Coating treatment can extend the degradation time.	Excellent mechanical strength, biodegradable metal; Promotes osteogenesis and angiogenesis.	Rapid corrosion and hydrogen evolution	[113,114]
Zinc-based membrane	Up to hundreds of MPa	6-12 months; Can be modified through alloying.	Excellent mechanical strength, biodegradable metal; Promotes osteogenesis.	Pathways of degradation products remain unclear. Biological reactions are debated.	[114–116]
MXene-based membrane	Tens to hundreds of MPa (Up to 755 MPa)	MXene undergoes slow metabolic degradation *in vivo*, and the composite membrane depends on the polymer matrix.	Electrical conductivity, photothermal conversion, multifunctional activity (antibacterial, osteogenic, anti-inflammatory)	Unclear *in vivo* stability and degradation behavior	[117,118]
CBPs-based membrane	1-2 MPa	1-24 months (highly adjustable).	Excellent biocompatibility and metabolic activity.	Wet mechanical strengths are weak, limited processability.	[119,120]

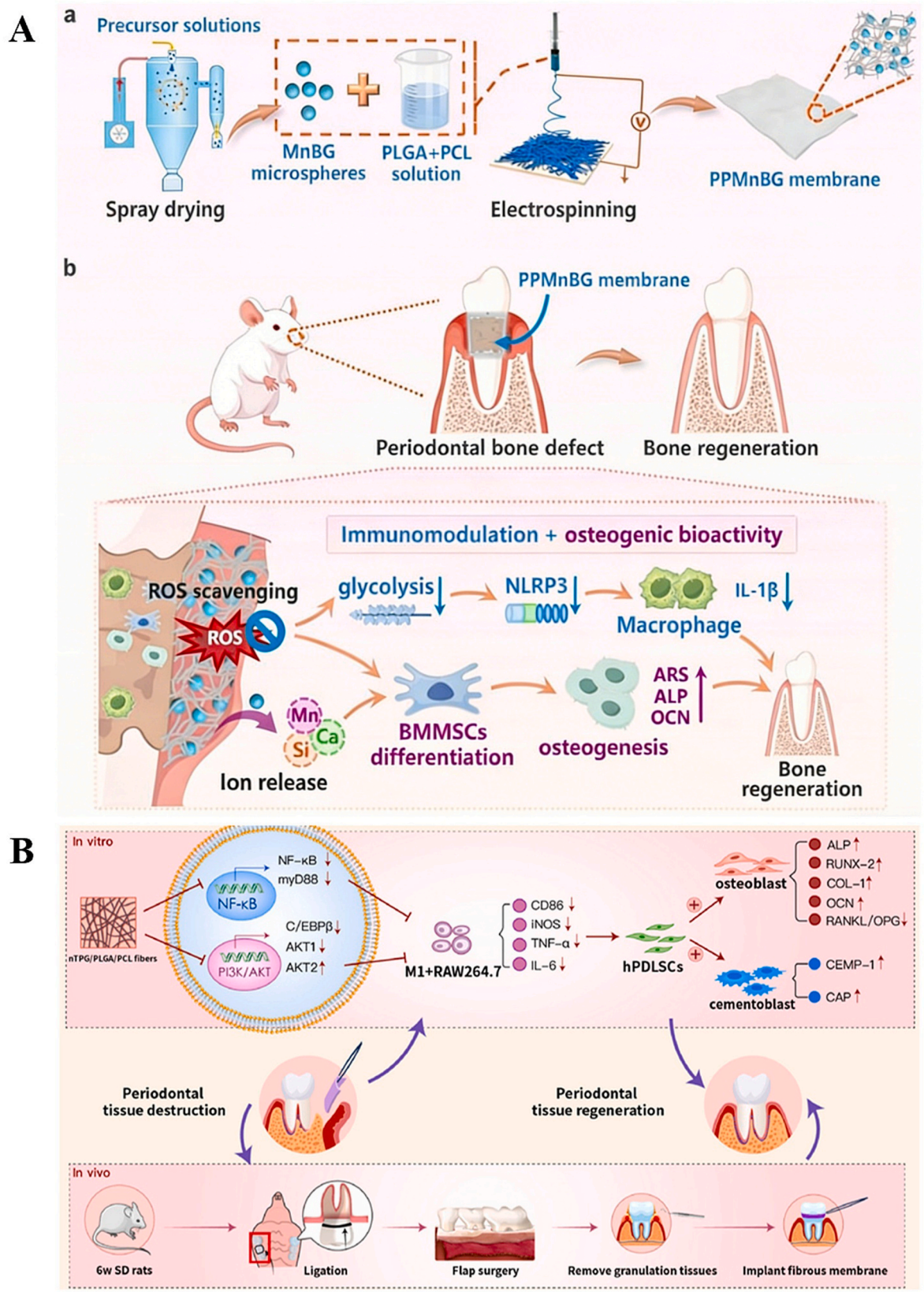

Fig. 2. Composite material systems combining synthetic polymers with bioactive inorganic and 2D-material fillers. A) Preparation and therapeutic mechanism of the PPMnBG membrane (manganese-doped bioactive glass embedded in PLGA/PCL nanofibers) — schematics show electrospinning fabrication and the proposed antioxidative-immunomodulatory pathway driving periodontal-bone regeneration [132]. Copyright 2025. B) Graphical model of the nTPG/PLGA/PCL nanofiber membrane (thermal pyrolysis graphene as a 2D conductive functional filler) — illustrates how immune-microenvironment regulation translates into accelerated periodontal tissue regeneration [140]. Copyright 2024.

closely recapitulate the native extracellular environment of alveolar bone and periodontal tissues. While these materials provide excellent biocompatibility, their clinical application in challenging defects is often restricted by rapid enzymatic degradation and limited mechanical strength [10,95].

Mineralized natural matrices. Consequently, incorporating inorganic minerals into natural matrices is a primary strategy for reinforcement. For example, mineralized collagen or zinc-doped nHA-collagen systems exhibit markedly increased tensile strength and delayed degradation profiles, extending their effective barrier lifespan [107,141]. Similarly, CS or SF with calcium phosphates, BG, metal oxides, or synthetic polymers (e.g., PCL) dramatically improves membrane stiffness and imparts multidimensional bioactivities, transforming them from passive barriers into active regulators of the osteogenic and antimicrobial microenvironment [142–150]. Recently, eggshell membranes (ESMs) have attracted attention as a highly biomimetic and cost-effective alternative [151–153]. However, due to their inherent thinness and low mechanical strength, ESMs require composite modifications, such as PLGA/nHA lamination or self-mineralization, to function effectively as GBR barriers [154,155].

Collectively, composite systems remain the most extensively studied class of GBR membrane composites [8,11,55]. Synthetic polymer-based composites offer precise tunability but require bioactive fillers to compensate for their inherent biological inertness, while natural

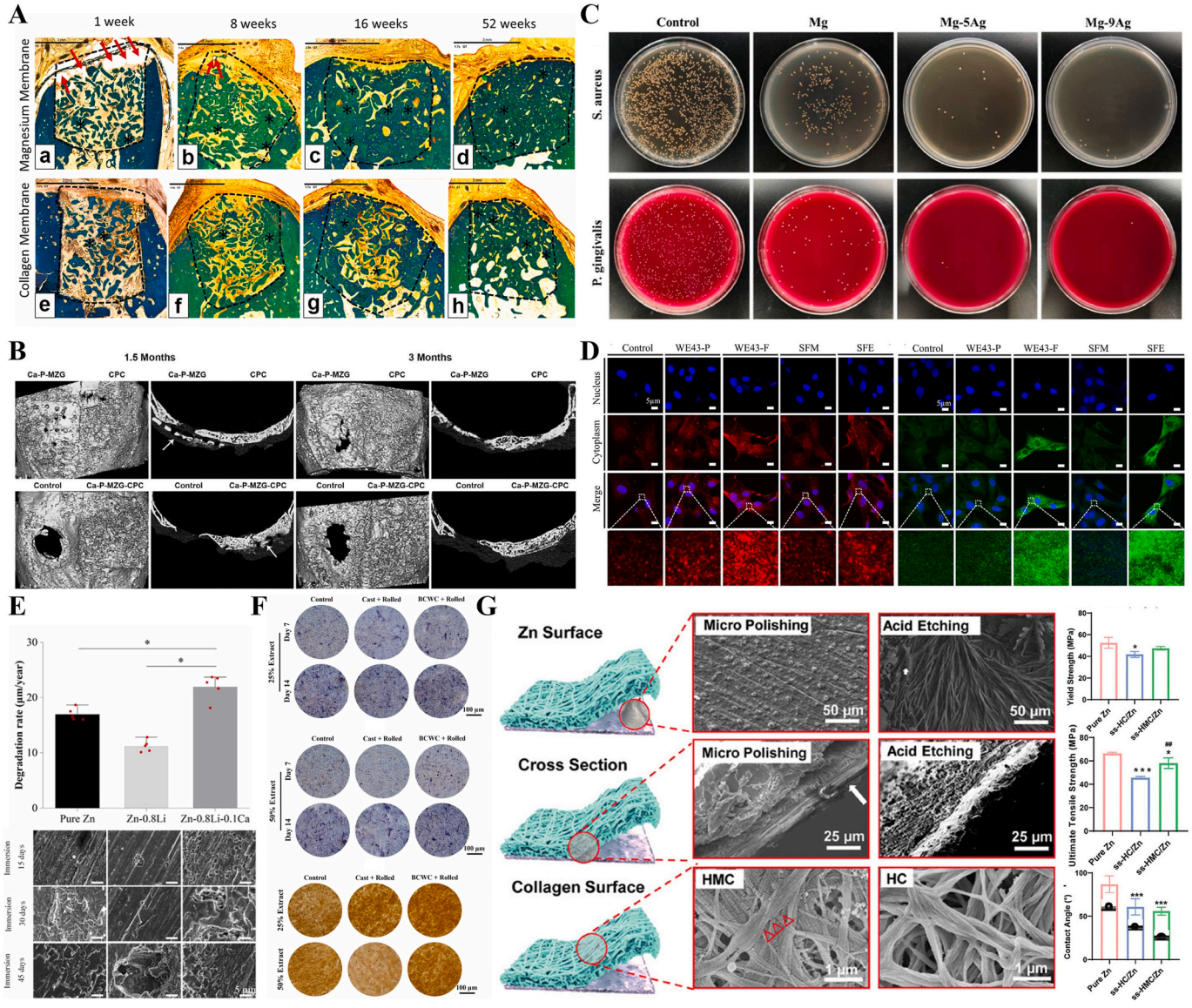

Fig. 3. Research progress on biodegradable metal-based GBR membranes. A) Representative scanned Goldner's Trichrome histology images of the GBR performance study on beagles. Dotted Line = edges of the defect site; Asterisks (*) = particles of bone filler material within the defect site; Red Arrow = void/cavity/gas space; (a), (b), (c) and (d) are presenting the magnesium membrane where we can see that it is degrading/reabsorbing over time, and by 8 weeks (b), only small residual particles of the magnesium membrane are left, surrounded by new bone and little part of void space. At 16 weeks (c) and 52 weeks (d), the magnesium membrane is completely absorbed and replaced by new bone. (e), (f), (g), and (h) presented a collagen membrane at all time points — 1 week (e), 8 weeks (f), 16 weeks (g), and 52 weeks (h). In each image, the scale bar represents 3 mm [157]. Copyright 2022. B) Micro-CT overview and parameters quantification of the critical-sized rabbit calvarial defect (white arrow represents residual Ca-P coated MZG membrane at 1.5 months after the surgery) [159]. Copyright 2021. C) *In vitro* antibacterial performances of Mg alloys (*S. aureus* and *P. gingivalis* grown in Mg alloy extracts after 24 h) [113]. Copyright 2024. D) Immunofluorescence staining of ALP and RUNX2 in BMSCs cultured with extracts from control and the four sample groups [161]. Copyright 2025. E) Degradation rates and degradation morphology under SEM [168]. Copyright 2024. F) Expression of osteogenic activity *in vitro* (Cast: traditional casting; BCWC: bottom circulating water-cooled casting) [170]. Copyright 2024. G) Characterization (SEM, yield strength, ultimate tensile strength, and contact angles) of pure Zn, ss-HC/Zn, and ss-HMC/Zn [56]. Copyright 2025.

material-based composites provide superior biocompatibility but often sacrifice mechanical robustness. Despite these advances, the mechanical strength of polymer-based composites remains fundamentally constrained by the polymer matrix, motivating the exploration of biodegradable metals as an alternative strategy for applications demanding robust structural support.

4.1.2. Biodegradable metals

Biodegradable metals have emerged as a unique class of GBR membrane materials by simultaneously providing mechanical support and bioactive degradation products, thereby offering unique advantages over conventional polymer-based membranes.

Magnesium and its alloys. Magnesium and its alloys are considered candidates for GBR membranes because they combine biocompatibility, degradability, and osteogenic/osteoconductive potential. With an elastic modulus around 41-45 GPa, magnesium is substantially softer than titanium (~110 GPa) or stainless steel, although still higher than cortical bone (~14-20 GPa). This narrower modulus gap offers partial mitigation of the "stress shielding" effect typically associated with rigid metallic implants [156]. Furthermore, the natural degradation of magnesium — typically in the 0.2-3.2 mm/year range for pure Mg/Mg-based alloys depending on alloy composition, surface treatment, and immersion medium — proceeds via $Mg + 2H_2O \rightarrow Mg(OH)_2 + H_2\uparrow$ (in Cl^--rich physiological media, $Mg(OH)_2$ is partially solubilized as soluble $MgCl_2$), releasing osteogenic Mg^{2+}, while the localized alkaline microenvironment offers inherent antibacterial properties [157].

However, the rapid *in vivo* corrosion of pure magnesium remains a primary obstacle. Two complementary *in vivo* studies by Rider et al. assessed this issue: a corrosion-kinetics study in Yucatan minipigs and a GBR performance study in beagle dogs. While the corrosion-kinetics study showed that pure magnesium membranes maintained their shape during the initial 4 weeks but underwent progressive resorption by week 8, the performance study confirmed bone regeneration outcomes comparable to those achieved with a resorbable collagen membrane (Fig. 3A) [157].

To stabilize degradation, researchers have explored surface modifications. Shan et al. applied a micro-arc oxidation (MAO) treatment to pure magnesium membranes, reducing the 14-day degradation rate to approximately 0.16 mm/year. *In vivo*, the membranes exhibited superior bioactivity and bone regeneration compared to pure titanium membranes at 2 weeks post-surgery [158].

Alloying is another effective strategy to match degradation kinetics with bone regeneration timelines. Calcium phosphate-coated magnesium alloys (Ca-P-MZG) have demonstrated progressive degradation and significantly enhanced new bone formation without inflammatory reactions at 1.5 months (Fig. 3B) [159]. To augment their antibacterial properties, researchers have also fabricated magnesium-silver (Mg-Ag) alloy membranes, which showed potent activity against *Porphyromonas gingivalis* (*P. gingivalis*) and *Staphylococcus aureus* (*S. aureus*) (Fig. 3C) [113]. Additionally, Luo et al. demonstrated that incorporating 1 wt% gallium (Mg-1wt%Ga) significantly enhanced osteogenic gene expression and matrix mineralization [160]. Beyond standalone membranes, magnesium alloys can also be integrated into composite systems to create multifunctional constructs capable of supporting large-scale alveolar bone defects. As a representative example of compositing magnesium alloys with bioactive coatings, Zhai et al. [161] designed a porous magnesium alloy scaffold combined with an electrospun SF membrane. By functionalizing the surface with epigallocatechin gallate (EGCG) and polydopamine (PDA), this system (SFE) upregulated osteogenic markers including ALP and RUNX2 in BMSCs (Fig. 3D), inhibited bacterial growth, and demonstrated bone regeneration in a rat maxillary defect model. Following the CE certification of NovaMag (botiss biomaterials, MDR Class III), recent post-market clinical case series have documented patient outcomes for Mg-membrane GBR [162,163].

Despite these advances, the rapid degradation of magnesium in physiological fluids may lead to premature loss of barrier function, excessive local alkalinity, and hydrogen accumulation, which can result in subcutaneous gas cavity formation and disruption of the healing process [164]. These issues remain critical challenges for the clinical translation of magnesium-based membranes.

Zinc and zinc alloys. Compared to magnesium, zinc — with an elastic modulus of ~108 GPa and reported degradation rates in the 0.05-0.3 mm/year range for Zn-Mg or Zn-Li binary alloys, depending on alloy composition and immersion medium — shows a milder degradation rate in physiological environments. This allows it to maintain structural support for the duration required for bone regeneration while minimizing adverse reactions such as gas accumulation or alkaline stimulation caused by rapid corrosion [165].

Despite these advantages, pure zinc possesses limited mechanical properties, poor plasticity, and a non-uniform degradation profile that often fails to synchronize with bone regeneration (Fig. 3E) [166–168]. To address these deficits, researchers have turned to alloying. The addition of elements like Cu, Ag, and Mg can enhance mechanical strength while simultaneously modulating corrosion resistance and biological reactivity [114]. Lithium (Li) is regarded as one of the most effective elements for strengthening zinc-based alloys. For instance, the Zn-Li binary alloy achieves compressive yield strength (CYS) up to ~457 MPa and ultimate tensile strength (UTS) ranges from 430 to 520 MPa. The highest UTS of ≈520 MPa is achieved in the Zn-0.4Li alloy. Zn-0.8Li, despite achieving high compressive strength, has been reported to fracture before yielding under tensile loading and therefore does not reliably provide a measurable UTS [167]. Because this specific alloy suffers from low plasticity and excessively slow degradation, Liu et al. [168] introduced trace amounts of calcium to successfully improve its ductility and optimize the degradation rate.

Ensuring biocompatibility remains a critical step for the clinical application of zinc-based alloys. A dynamic evaluation of a Zn-4Ag alloy membrane revealed that the material maintained excellent cytocompatibility as long as the Zn^{2+} concentration in the degradation medium remained below 90 μM, Ag^+ below 0.5 μM, and the pH did not exceed 9.0-a relatively narrow safety window that illustrates the delicate balance required in Zn alloy biocompatibility design [169]. This underscores that well-designed alloy compositions can prevent ion-induced cytotoxicity. Building on this, a high-plasticity Zn-0.3Ca alloy achieved an optimal balance: the micro-addition of calcium improved plastic deformability, provided potent inhibitory effects against oral pathogens like *S. aureus* and *P. gingivalis*, and maintained excellent osteoconductivity *in vivo* (Fig. 3F) [170].

Finally, composite designs offer a pathway to modulate degradation while maintaining the osteogenic space. For example, a bilayer self-induced GBR membrane (ss-HMC/Zn) — constructed by combining pure zinc with hierarchical mineralized collagen (HMC) via self-assembly — exhibited robust mechanical stability alongside enhanced osteogenic performance (Fig. 3G) [56].

Moving forward, while zinc-based membranes demonstrate highly attractive prospects, their clinical application depends on mitigating potential cytotoxicity from excessive Zn^{2+} release [171]. Future research should focus on elucidating *in vivo* ion metabolic pathways and further optimizing alloy compositions to achieve a seamless balance between degradation and tissue regeneration.

Iron-based alloys. In addition to magnesium- and zinc-based alloys, iron-based biodegradable metals have also attracted increasing attention. Iron-based alloys (e.g., Fe-Mn) exhibit high mechanical strength (tensile ~250-500 MPa), rigidity, and elastic moduli ranging from ~30 to 80 GPa for moderate-porosity scaffolds (lower for high-porosity Fe-Mn) and ~160-200 GPa for dense Fe-Mn alloys (compared to ~14-20 GPa for cortical bone), along with a slow *in vivo* degradation rate, which may require more than 3-5 years for complete resorption. Although these features may theoretically benefit orthopedic scenarios requiring prolonged mechanical support, this timeline far exceeds the temporal requirements of alveolar bone regeneration [172]. However, their excessive stiffness limits flexibility and conformability, and their slow

degradation is far from meeting clinical GBR requirements. Moreover, the difficulty of fabricating ultrathin, homogeneous membrane structures poses an additional challenge. Consequently, the application of iron-based materials in GBR membranes remains at a very early experimental stage. Overall, Fe-based GBR membranes still face significant challenges, and their clinical potential requires further systematic investigation. Notably, in contrast to magnesium- and zinc-based systems, the iron-based GBR evidence base remains predominantly limited to *in vitro* and small-animal characterization, with no large-animal alveolar bone studies or clinical reports specifically targeting GBR indications reported to date.

In summary, magnesium-, zinc-, and iron-based materials exhibit markedly different degradation behaviors and biological responses. Magnesium alloys degrade relatively rapidly and release Mg^{2+} that stimulates osteogenesis and angiogenesis, but uncontrolled corrosion and hydrogen evolution may compromise structural stability. Zinc-based alloys typically exhibit slower and more uniform degradation while providing antibacterial activity and osteogenic stimulation through Zn^{2+} release; however, excessive zinc concentrations may induce cytotoxic effects. In contrast, iron-based alloys possess excellent mechanical strength but degrade extremely slowly, often exceeding the timeframe required for bone regeneration. Consequently, current research primarily focuses on magnesium and zinc alloys, where alloying strategies and surface modifications are being explored to achieve a balance between corrosion control, mechanical integrity, and biological activity.

4.1.3. MXene

MXenes, a rapidly emerging family of two-dimensional transition metal carbides and nitrides, have recently been introduced into GBR membrane design. This is due to their unique physicochemical properties, including high surface area, single-layer thickness of ~1-3 nm, in-plane electrical conductivity reaching 6000–15,000 S/cm in solution-processed films (although composite/in-vivo conductivity typically decreases by 1-2 orders of magnitude from these maximum film values), and potential immunomodulatory effects [173–175]. The layered structure, combined with abundant surface terminal groups (e.g., -O, -OH, -F), endows MXenes with excellent interfacial activity and supports cell adhesion [176]. For instance, the porous MXene membrane exhibited a water contact angle of 39°, indicating superior hydrophilicity and potential for cell attachment [176]. Furthermore, their inherent conductivity provides a physical basis for achieving electrostimulation-enhanced bone regeneration. Applied electrical fields promote the osteogenic differentiation of bone marrow mesenchymal stem cells (BMSCs) and activate angiogenic pathways [175].

MXenes also exhibit exceptional antimicrobial potential. For example, $Ti_3C_2T_x$ membranes demonstrated high bactericidal efficacy against *Escherichia coli* and *Bacillus subtilis* [177]. However, these are non-oral pathogens, and further evaluation against oral-specific microbes such as *P. gingivalis* and *Fusobacterium nucleatum* is warranted; recent MXene-based hydrogels have shown direct antibacterial activity against *P. gingivalis* in periodontitis treatment [178]. Leveraging their photothermal conversion properties, MXenes provide synergistic photothermal and antibacterial functions, further enhancing the anti-infective capabilities of GBR membranes [179].

Fabrication strategies. Several fabrication and structural optimization strategies have validated the feasibility of using MXenes in GBR. Zhang et al. fabricated freestanding, multilayered $Ti_3C_2T_x$ membranes to evaluate their biocompatibility and osteoinductive potential. These membranes significantly promoted the adhesion, proliferation, and ALP activity of pre-osteoblasts, subsequently inducing new bone formation in a rat calvarial defect model [180]. Moreover, Wan et al. [117] utilized a roll-to-roll assisted scraping and ordered interfacial crosslinking technique to create a high-strength MXene membrane (S-SBM) with a tensile strength of up to 755 MPa. This membrane provided stable structural support for space maintenance while scavenging reactive oxygen and nitrogen species (ROS/RNS). It also induced M2 macrophage polarization, fostering an immune microenvironment conducive to bone formation (Fig. 4A and B) [117]. This strategy successfully integrated mechanical strength, immunomodulation, and osteogenesis through structural control and interfacial functionalization.

Composite designs. Beyond monolithic structures, composite designs represent a key direction in MXene research. Using natural polymer systems, Zhou et al. constructed a bacterial cellulose/$Ti_3C_2T_x$ Janus bilayer membrane. Its hierarchical structure, featuring a "dense protective layer" and a "porous osteogenic layer," combined barrier function with osteoinduction, significantly promoting bone tissue repair in an animal calvarial defect model [118]. In synthetic polymer systems, MXene-bacterial cellulose Janus composites have demonstrated high mechanical strength, antibacterial activity, and osteogenic potential (Fig. 4C) [118]. Furthermore, combining electrical stimulation with an MXene-incorporated electroactive composite dually promoted the osteogenic and angiogenic differentiation of BMSCs, achieving excellent *in vivo* bone defect repair [181]. Collectively, these studies indicate that combining MXenes with polymers or bioceramics amplifies their multifunctionality, integrating mechanical support, electrical conductivity, antibacterial properties, and osteogenic activity (Fig. 4D) [181].

Safety and translational considerations. Current *in vivo* evidence for MXene-based GBR membranes derives predominantly from rat calvarial defect models, with efficacy in alveolar bone defects and larger-animal models still to be established; nevertheless, the field is evolving from single-property optimization toward multifunctional integration. This trend showcases their unique advantages in mechanical reinforcement, osteogenic promotion, electro-stimulatory responsiveness, and antimicrobial defense.

However, compared to established biomaterials, MXene-based systems remain relatively underexplored in GBR applications. Key concerns include long-term biosafety — particularly the reported cytotoxicity associated with -F surface terminations and the well-documented susceptibility of MXenes to oxidative degradation in aqueous environments. The unique oral microenvironment, characterized by saliva-mediated ionic exposure, occlusal pH fluctuations, and continuous microbial activity, may further accelerate this oxidative degradation, yet stability under such conditions remains largely unevaluated. In addition, current GBR-relevant *in vivo* evidence relies primarily on rodent cranial defect models, with no published data from periodontal or alveolar bone defect models. Together, these gaps highlight the limited stability of surface functional groups, and a lack of systematic *in vivo* degradation studies. Further investigations are necessary to clarify their biological interactions and evaluate their translational potential for bone regeneration.

4.1.4. CBPs

Recently, CBPs have emerged as a distinctive class of biodegradable biomaterials owing to their highly tunable molecular architecture and intrinsic biological relevance (Fig. 5A and B). Structurally, citric acid contains three carboxyl groups and one hydroxyl group, enabling versatile esterification and crosslinking reactions with diols and other comonomers. This chemical versatility facilitates precise control over crosslinking density, chain flexibility, and network topology, allowing for the partial decoupling of mechanical properties from degradation kinetics [120].

Tunable mechanical properties. Through rational molecular design, CBPs can be engineered to exhibit a broad spectrum of mechanical properties. Poly(1,8-octanediol citrate) (POC), a representative citrate-based elastomer, exhibits tensile strengths of 6-10 MPa and an elongation at break exceeding 200%, reflecting its elastomeric and damage-tolerant nature [120]. Notably, the mechanical properties and degradation characteristics of CBPs can be readily modulated by varying the diol composition. For instance, using aliphatic diols with chain lengths ranging from C4 to C12 yields diverse polycitrate-diol variants [182,183].

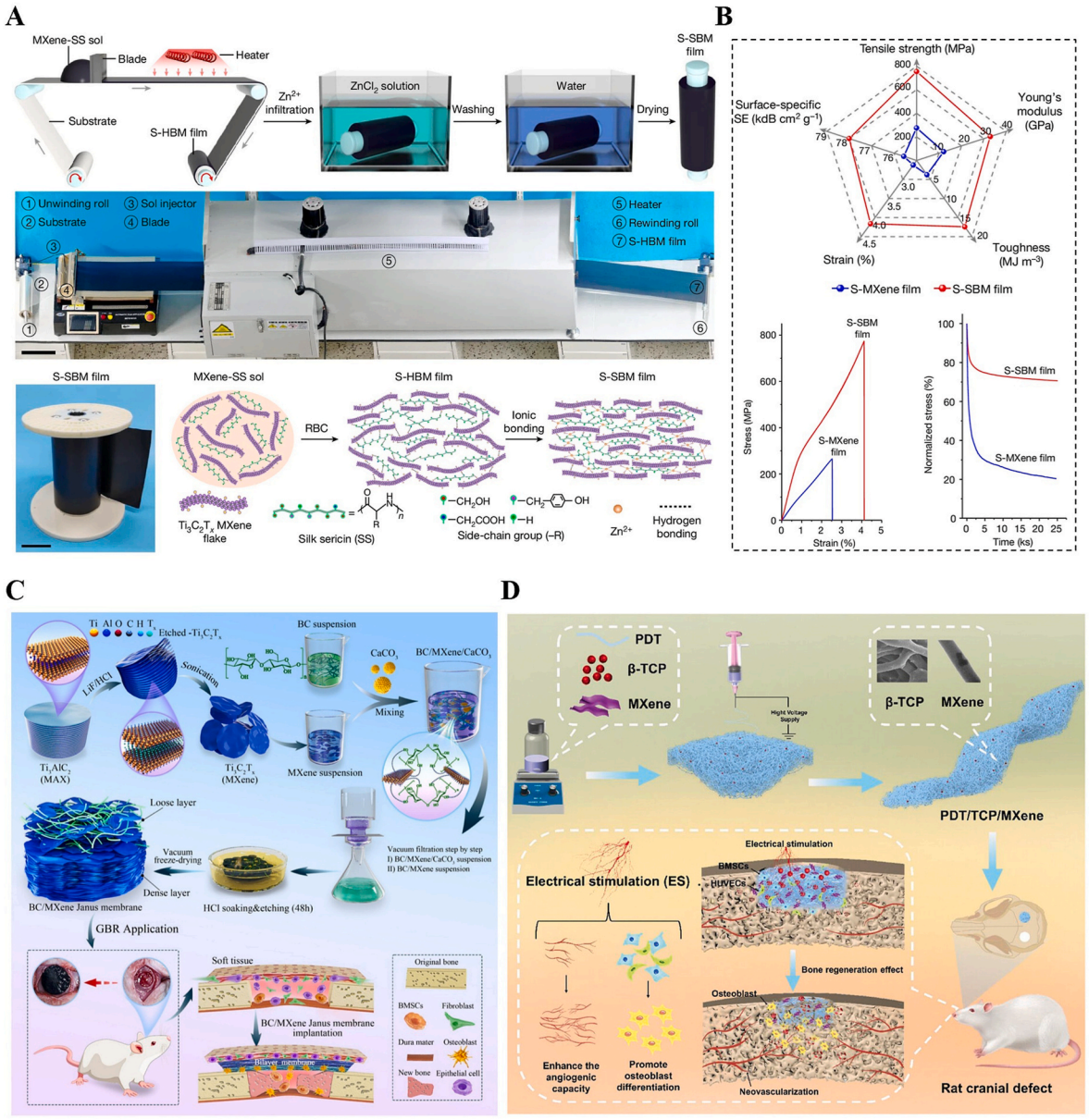

Fig. 4. Research progress on MXene-based GBR membranes. A) Fabrication process and structural model of S-SBM membranes [117]. Copyright 2024. B) Mechanical properties of S-MXene and S-SBM membranes [117]. Copyright 2024. C) Schematic illustration of the fabrication process of Janus BC/MXene membrane and its application as GBR membrane in rat calvarial defect models. A facile strategy of vacuum-assisted filtration and etching was employed to develop the Janus membrane, which could prevent fibroblast invasion and promote osteogenesis with different surfaces. The chemical structures of the used components and possible interactions between them were shown [118]. Copyright 2024. D) Schematic diagram of the preparation of P/T/MXene/ES multifunctional bone regeneration membrane and repair of cranial defects [181]. Copyright 2024.

More importantly, incorporating HA substantially enhances CBP mechanical properties, yielding stress-strain behaviors that more closely resemble those of native bone [184]. For example, POC/HA composite (POCHA) can incorporate up to 60 wt% HA while maintaining elasticity. Specifically for the citrification-processed POC-HA composite (POCHA) recently reported by Wang et al. [184], compressive strengths exceed 250 MPa with elastic moduli of 0.5-0.8 GPa — approaching the upper-cancellous/lower-cortical bone range (cortical: ~14-20 GPa); legacy POC-HA/CUPE-HA composites span ≈ 75-280 MPa across formulations and post-cure conditions. At the interface, citric acid and HA form synergistic chemical bonds, primarily driven by carboxyl group interactions (Fig. 5C). This process, mediated by carboxyl-Ca^{2+} chelation and ester linkages with the HA surface, creates a stable organic-inorganic interface that improves both mechanical stability and cellular attachment [184].

Tunable degradation behavior. In parallel, the degradation behavior of CBPs can be finely tuned from weeks to months by adjusting diol composition, hydrophilicity, and crosslinking density. It was demonstrated that introducing N-methyldiethanolamine (MDEA) into poly(glycol citrate) (POCM) markedly enhanced the degradation rate of the material, which increased proportionally with the ratio of MDEA (Fig. 5D) [183]. Moreover, compared with conventional polyesters like PLA and PLGA, CBPs exhibit a milder degradation profile characterized by reduced local acid accumulation, enabling controllable resorption without provoking pronounced inflammatory responses.

This coupling of mechanical adaptability and degradation control provides a robust foundation for GBR membranes, which are required to maintain space, resist collapse, and degrade synchronously with new bone formation.

Citrate metabolism in osteogenesis. Beyond structural tunability,

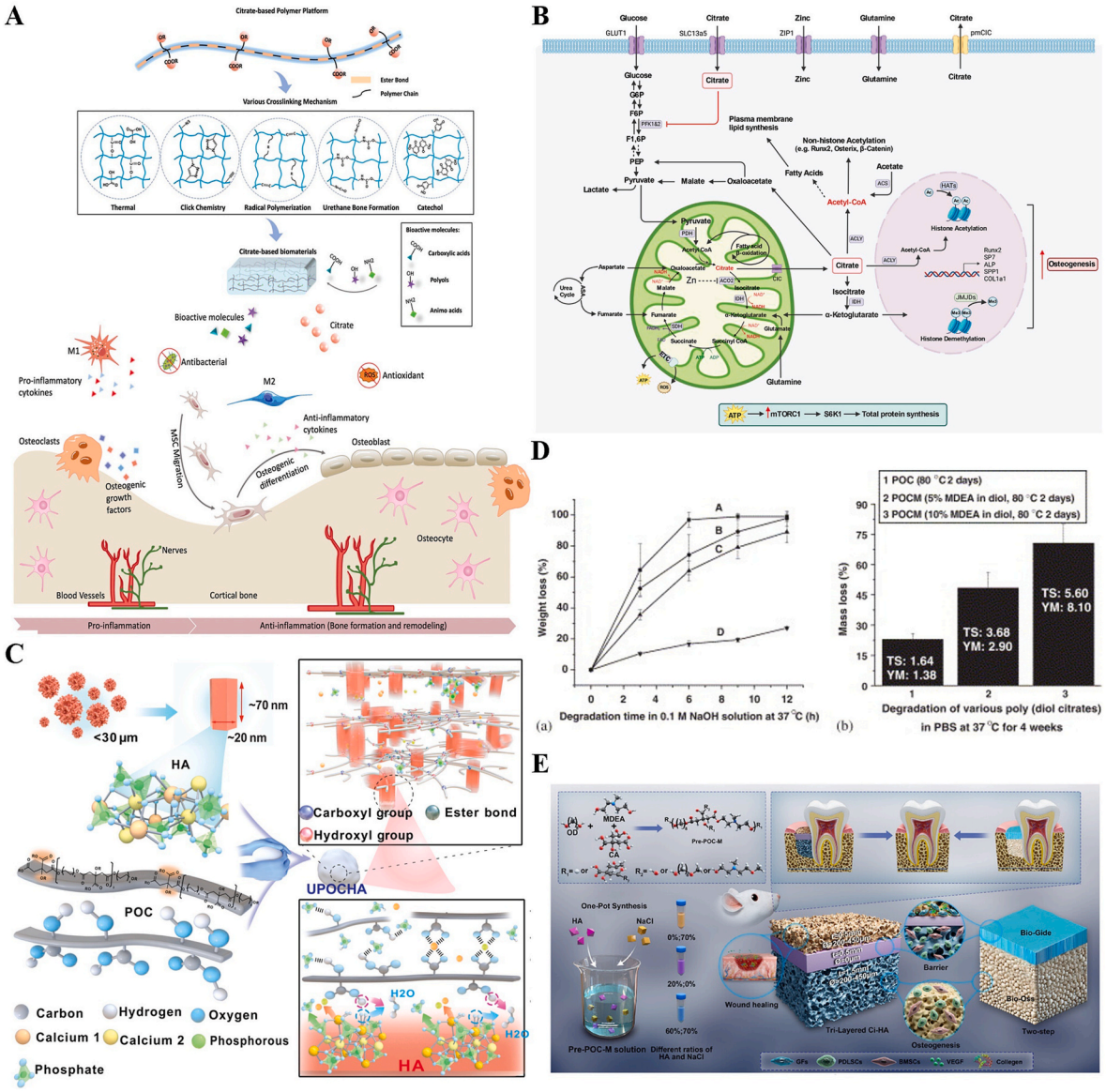

Fig. 5. Development of CBPs and their applications in dentistry. A) Multifaceted functions of citrate-based materials in bone repair [120]. Copyright 2024. B) Overview of citrate metabolic pathways in mammalian cells and metabonegenesis [120]. Copyright 2024. C) Schematic illustration of the fabrication of UPOCHA composites and the dissolution of HA microparticles (blurry HA rods) within the polymer networks with the hypothesized chemical bonding between HA and POC; reaction between POC and HA releases water as dehydroxylation, which is followed by release of calcium and phosphate into polymeric matrix [184]. Copyright 2026. D) Degradation studies of poly(diol citrates) in (a) 0.1 M NaOH solution and (b) PBS at 37 °C (n = 5) [183]. Copyright 2006. E) Schematic of the preparation and function of tri-layered Ci-HA composite scaffold for periodontal-bone defect (PBD) repair in rats [119]. Copyright 2025.

citrate itself is integral to bone biology, conferring CBP with bone-mimetic features. CBPs primarily degrade into citrate and its derivatives, which directly enter the tricarboxylic acid (TCA) cycle and participate in cellular metabolism and biosynthesis. Exogenous citrate supports oxidative phosphorylation (OXPHOS) and fatty acid oxidation while promoting osteogenic differentiation and mineralization through Akt-dependent signaling and HIF-1α stabilization [120,185]. Thus, CBPs provide biologically instructive cues beyond passive structural support.

Furthermore, citrate constitutes approximately 5 wt% of the organic component of bone (equivalent to 1-2 wt% of total bone mass), tightly associating with HA nanocrystals [186]. Through carboxyl-calcium chelation, citrate regulates HA crystal thickness, morphology, and interfacial stability, contributing to the exceptional mechanical strength and toughness of bone. Consequently, incorporating CBPs into mineralized composites recapitulates key aspects of bone's organic-inorganic nanostructure. This offers a bone-mimetic strategy especially relevant for alveolar bone, which exhibits rapid turnover and high metabolic demand.

***In vivo* evidence.** *In vivo* studies further support the osteogenic potential of CBP-based systems. POC/HA composites significantly upregulated osteogenic markers (e.g., RUNX2, ALP, and OCN) while promoting mineral deposition and new bone formation without inducing evident cytotoxicity or chronic inflammation. Importantly, citrate-mediated bioactivity extends beyond osteogenesis. Emerging evidence indicates that CBPs-based scaffolds can simultaneously enhance angiogenesis and modulate the immune microenvironment, both essential processes for successful GBR [120]. For instance, a multilayer CBP/HA composite scaffold (CI-HA) demonstrated *in vitro* pro-angiogenic and osteogenic effects. In a three-wall intrabony defect model, it achieved regenerative outcomes comparable to a commercial collagen membrane combined with bone grafting. Although derived from a GTR model, these findings underscore the translational relevance

of CBPs for GBR applications, particularly in alveolar bone regeneration where coordinated bone formation, vascularization, and immune regulation are required (Fig. 5E) [119].

Translational caveats. Compared to conventional polymers, CBPs introduce biochemical functionality due to the intrinsic role of citrate in bone metabolism and mineralization. Unlike inert polymer matrices, citric acid provides multiple coordination sites for calcium binding and mineral nucleation, actively driving osteogenesis. Furthermore, CBPs exhibit enhanced crosslinking capabilities and highly tunable degradation compared to traditional aliphatic polyesters. Nevertheless, research on CBP-based GBR membranes remains relatively limited compared to more established systems like collagen or PCL composites. Critical issues — including long-term mechanical stability, degradation kinetics, and scalable fabrication strategies — still require systematic investigation prior to clinical translation. It is also worth noting that the GBR-specific evidence base for CBPs remains heavily concentrated within a few research consortia, with sparse independent replication in alveolar bone defect models and limited head-to-head benchmarking against established PCL- and collagen-based platforms; broader engagement of the wider GBR research community will be necessary to consolidate the clinical positioning of CBP membranes.

A cross-platform comparison reveals that current GBR membrane materials cluster into two mechanically distinct regimes with a conspicuous gap between them. Polymer-based composites occupy the low-to-moderate strength range (Table 4). Their mechanical ceiling is fundamentally constrained by the polymer matrix itself; even with substantial inorganic loading (e.g., nano-hydroxyapatite, bioactive glass), strength gains plateau before exceeding approximately 15 MPa wet, beyond which filler aggregation degrades structural integrity. Natural biopolymer composites suffer an additional penalty from rapid enzymatic degradation that erodes mechanical function well before the 12-16-week threshold required for space maintenance.

At the opposite extreme, biodegradable metals provide compressive and tensile strengths orders of magnitude higher than those of polymer systems. Zinc alloys, particularly Zn-0.4Li, achieve tensile strengths up to ~520 MPa, while Zn-0.8Li exhibits brittle fracture before yielding under tensile loading [167].

Magnesium alloys, in contrast, offer values in the hundreds of MPa coupled with an elastic modulus of 41-45 GPa — closer to cortical bone than titanium (~110 GPa) but still sufficient to risk localized stress shielding. Importantly, the rapid corrosion of magnesium can compromise mechanical integrity within 8 weeks *in vivo*, collapsing the effective load-bearing window below clinical requirements. MXene-based membranes bridge this gap in absolute strength — the roll-to-roll fabricated S-SBM membrane achieved 755 MPa in tensile testing — yet all existing data derive from rat calvarial models, which impose negligible masticatory loading. No alveolar bone study has been reported, leaving the functional relevance of these values uncertain. CBPs, conversely, demonstrate tunable mechanics spanning from soft elastomers (1-2 MPa for neat POC) to mineralized composites with reported compressive strengths spanning approximately 75-280 MPa across formulations and post-cure conditions (e.g., POC-HA at 65 wt% HA ≈75 MPa, CUPE-HA ≈116 MPa, with citrification-processed POCHA at 60 wt% HA exceeding 250 MPa [184]), though their application in GBR membranes is supported by only a single direct GTR/GBR study. A critical design-space gap thus persists: materials that combine moderate wet-state tensile strength (15-50 MPa), elastic recovery for conformal fitting, and controlled degradation over 4-9 months remain largely unexplored.

The five platforms differ markedly in degradation mechanism and timeline relative to the 4-9-month clinical window (Table 4): polymer systems span slow PCL hydrolysis [104,139] that risks interference with late-stage remodeling, PLGA bulk hydrolysis with auto-catalytic acidification detrimental to osteogenesis, and rapid enzymatic erosion of collagen, chitosan, and silk fibroin [136,143,144] that typically falls below the therapeutic window unless reinforced.

Biodegradable metals introduce complex corrosion-mediated degradation behaviors: magnesium alloys suffer from rapid hydrogen evolution and localized alkalinity [156,161,187] — creating a kinetic mismatch with surrounding tissue accommodation. While surface treatments like micro-arc oxidation and calcium phosphate coatings can attenuate this phenomenon, a controlled, linear degradation profile has yet to be achieved. Conversely, zinc alloys offer a more moderate degradation timeline, but their tendency toward non-uniform corrosion creates unpredictable structural thinning [115,116,167]. MXene degradation in oral tissues remains uncharacterized [173,176,177], and CBPs' tunable degradation has been validated in only a single GBR-relevant study [119]. A unifying gap across platforms is the absence of feedback-controlled degradation that could self-correct temporal mismatch in response to local biological signals — currently the dominant limitation on clinical predictability.

While material composition determines the intrinsic properties of GBR membranes, their clinical performance is profoundly shaped by spatial organization at multiple length scales. Identical materials can exhibit markedly different mechanical behavior, degradation profiles, and cellular responses depending on their macroscopic architecture and microscopic pore structure. The following sections examine how hierarchical structural design translates material properties into optimized regenerative outcomes.

4.2. Structural designs and spatial construction

In GBR membrane development, macroscopic structural design is as critical as material chemistry innovations. Membrane architecture regulates cellular behavior - including the adhesion, migration, and differentiation of osteoblasts and endothelial cells - while directly dictating space-maintaining capacity, barrier function, and regenerative efficacy [188]. By precisely controlling macroscopic configuration, microscopic pore architecture, and network interconnectivity, researchers can direct cellular behavior, nutrient exchange, and new bone growth. This multiscale design approach is fundamental to optimizing the performance of next-generation GBR membranes (Fig. 6A).

4.2.1. Macroscopic structural design

At the macroscopic scale, bilayer, multilayer, and Janus structures (two functional layers, three or more sequential zones, and asymmetric interfaces, respectively) are widely adopted, inspired by the nano-micro-macro hierarchical organization of native bone [189]. This hierarchical organization - where mineralized collagen nanofibrils self-assemble into lamellar and trabecular architectures with anisotropic mechanics that support adaptive remodeling - has inspired layered GBR membranes that spatially partition barrier function from osteoinductive activity [190].

Bilayer membranes. Among these strategies, bilayer membranes are extensively studied. They typically consist of two functional zones: a dense barrier layer and an osteoinductive layer. The dense layer prevents premature soft-tissue infiltration, whereas the osteoinductive layer provides an osteophilic microenvironment that promotes osteoblast adhesion, migration, and differentiation [191]. For example, Zhang et al. [192] developed a nacre-inspired bilayer nanocomposite membrane combining a compact nacre-like barrier layer, fabricated via evaporation-induced self-assembly to provide mechanical strength and prevent soft-tissue infiltration, with a porous osteoinductive layer, fabricated via ice-templating self-assembly to mimic the trabecular bone microarchitecture and support cell infiltration. This bioinspired hierarchical design conferred mechanical robustness superior to commercial collagen membranes, while preserving effective bacteriostasis, controlled degradation, and biocompatibility.

Janus membranes. Janus architectures extend this concept by making interfacial asymmetry the defining design criterion — whereas bilayer membranes simply imply functional partition into two layers regardless of symmetry, Janus membranes require explicit asymmetry between the two opposing surfaces (Fig. 6A). In these membranes,

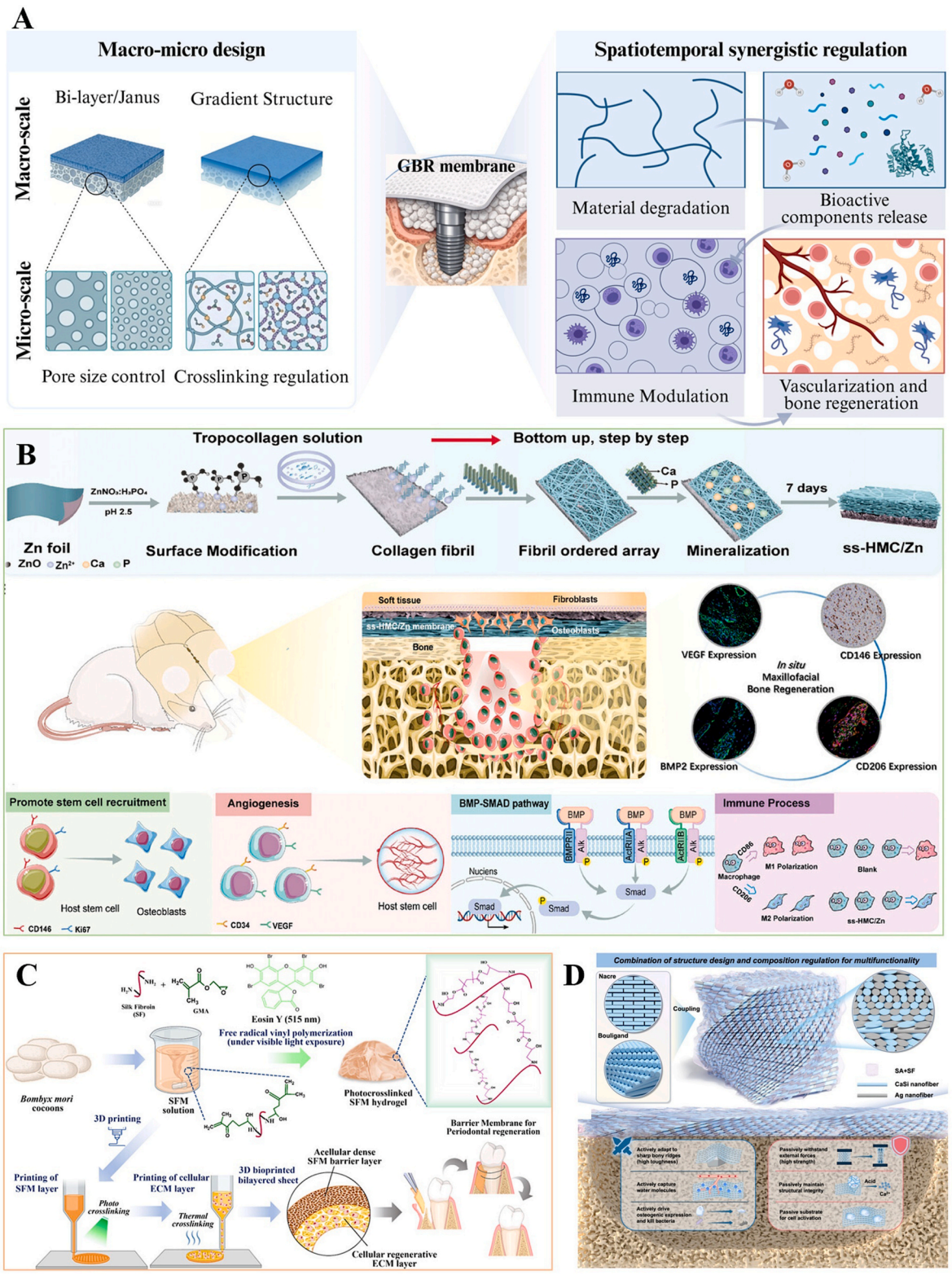

Fig. 6. Novel structural designs and spatial construction of GBR membrane. A) Schematic diagram (original, prepared by the authors) summarizing the principal structural-design and spatial-construction strategies — bilayer/Janus/multilayer/functionally graded/multi-morphology — that modulate alveolar bone regeneration through coordinated barrier function and osteoinductive cueing. B) Conceptual illustration of biomimetic strategy to construct the ss-HMC/Zn membrane and mechanism of osteogenesis [56]. Copyright 2025. C) Schematic of visible light cross-linked methacrylated SF for bioprinting dual-layer GBR membrane [150]. Copyright 2025. D) The combination of structure design and composition regulation for multifunctionality [210]. Copyright 2025.

opposing surfaces differ in chemical composition, morphology, or wettability, enabling spatially separated yet synergistic functionalities [193–195]. Structurally, Janus membranes are classified into three categories [196]: (1) “A on B” or “B on A”, where one layer is significantly thinner than the other. (2) “A and B”, where the layers have comparable thickness or the structure contains three or more layers; and (3) “A to B”, where components A and B are distributed in a gradient across the membrane's cross-section. They can be fabricated from resorbable or non-resorbable polymers and biodegradable metals.

Asymmetric functionalization allows Janus membranes to integrate antibacterial, osteogenic, and immunomodulatory properties. For example, Lin et al. [197] constructed a DA-quaternary ammonium salt (QAS) composite polyurethane Janus membrane via uniaxial electrospinning, distributing DA and an antimicrobial gemini QAS on opposite sides. The DA-functionalized osteogenic side promoted BMSCs adhesion and mineralization, while the QAS side inhibited fibroblast proliferation and exhibited potent antibacterial activity, achieving excellent periodontal tissue regeneration *in vivo*. For immunomodulation, Yan et al. [56] designed an ss-HMC/Zn membrane. The outer Zn layer acted as a soft-tissue barrier, while the inner HMC layer induced endogenous osteogenesis. It achieved this by recruiting stem cells, promoting angiogenesis, inducing M2 macrophage polarization, and activating BMP signaling — mechanisms increasingly recognized as central to osteoimmunological coupling in GBR (Fig. 6B) [46,51].

Janus electro-microenvironment. Structural asymmetry can also be exploited to regulate physical signaling. The Janus electro-microenvironment (JEM) membrane proposed by Lai et al. [198] achieves directional tissue regeneration via an asymmetric electroactive design. The positively polarized side (JEM+) shifts fibroblast metabolism toward the mitochondrial OXPHOS pathway, significantly increasing ATP production to accelerate soft tissue healing. Conversely, the negatively polarized side (JEM-) was shown to induce mitophagy that clears dysfunctional mitochondria in osteoblasts, with subsequent lysosomal release of calcium phosphate to the extracellular matrix to accelerate bone mineralization. These findings demonstrate that Janus structures achieve macroscopic functional spatialization while actively modulating cellular differentiation and micro-level signaling pathways.

Limitations of Janus and multilayer designs. Despite these advances, Janus and multilayer membranes face several challenges. First, weak interfacial bonding risks delamination and the subsequent loss of functional coatings. Second, mutual functional interference remains a concern; for example, excessive ROS from potent antibacterial agents can inhibit osteogenesis [199]. Third, differential control over the degradation rates of individual layers has not yet been achieved, leading to temporal mismatches with bone regeneration. Finally, complex fabrication limits scalability and hinders clinical translation.

Functionally graded membranes. To overcome these limitations, researchers have begun exploring structural optimization strategies that more closely mimic the continuous structural transitions observed in native bone. Functionally graded bilayer membranes (FGBMs) feature gradual compositional and architectural transitions across their thickness (Fig. 6A). This gradient architecture reduces interfacial stress while coordinating barrier and osteoinductive functions, as demonstrated by a PLGA/nHA FGBM [200].

Single-material with multi-morphology. Another emerging strategy uses single-material, multi-morphology composite membranes. By controlling SF morphology into distinct fiber, sponge, and membrane forms, Atila et al. [201] fabricated a self-composite membrane that eliminated peeling risks while promoting osteoblast mineralization. Of the four limitations enumerated above, FGBMs and single-material approaches primarily address interfacial bonding and fabrication complexity; mutual functional interference (e.g., antibacterial-osteogenic antagonism) and layer-specific degradation control remain comparatively unresolved and will likely require integrated strategies that combine gradient architectures with bioresponsive degradation chemistries.

4.2.2. Microstructural design

Pore architecture across length scales. At the microstructural level, pore architecture and crosslinking networks dictate cellular behavior and tissue regeneration. Porous structures provide a scaffold for osteoblast and endothelial cell migration while serving as versatile platforms for releasing bioactive factors and nanoparticles. Porosity and pore size distribution directly impact osteogenic performance. For example, 3D-printed PCL membranes with 30% porosity (~130 μm pore size) exhibited more robust bone formation and mechanics than their highly porous (50-70%) counterparts [202]. Pore sizes of 50-100 μm support cell migration and soft-tissue ingrowth, >100 μm facilitate bone ingrowth, and >200-300 μm are generally required to sustain vascularized bone formation (Fig. 7) [4]. However, excessively large pores compromise mechanical strength and barrier function [4,160]. Conversely, nanoscale pores (<1 μm) are suited for diffusion-controlled release of small-molecule drugs such as antimicrobial peptides via size-exclusion, ensuring sustained therapeutic delivery and mitigating burst-release toxicity. By contrast, nanoparticulate fillers like nHA (20-100 nm) are typically distributed throughout the matrix rather than confined by pore architecture (Fig. 7) [203].

Crosslinking control. Precisely controlling crosslinked networks is essential. Photo-crosslinking is widely adopted for its efficiency. Ghosh et al. [150] used a visible-light activated system to prepare methacrylated silk fibroin (SFM) hydrogels and fabricate a bilayer membrane, providing more flexible and uniform networks than conventional UV curing. Here, the SFM concentration directly determined the protein chain density and pore size. Higher concentrations increased chain interactions, producing a denser network with smaller pores. A ≥10% (w/v) concentration yielded 40-60 μm pores, effectively blocking fibroblasts while permitting osteoblast migration and proliferation. This interconnected architecture significantly elevated ALP activity and regulated staged osteogenic marker genes, balancing barrier function with tissue integration (Fig. 6C).

4.2.3. Macro-micro structural coupling

Multi-scale architecture. Whereas the preceding subsection considered pore architecture and crosslinking as standalone micro-scale features, GBR membrane optimization is increasingly advancing toward genuine multi-scale structural integration in which those microscopic features are explicitly coupled with macroscopic layered or graded designs. Electrospinning has emerged as a particularly versatile method, mimicking the native ECM's nanofibrous topography while controlling functional component distribution. At the micro-scale, encapsulating inorganic nanoparticles can significantly enhance osteogenic activity [204]. At the macro-scale, the porosity and mechanical properties can be tuned by adjusting the fiber diameter, thereby modulating osteogenic performance [205,206]. To achieve the simultaneous integration of mechanical and biological functions at both macro- and micro-levels, advanced techniques such as core-shell coaxial electrospinning and hybridization with 3D printing, which is an effective method for achieving structural control, have been developed [134,207,208]. For example, Jin et al. [209] combined an electrospun PLGA/collagen membrane with a 3D-printed PLGA/nHA scaffold. The 3D printing achieved cancellous bone-like porosity (75%) and large pores (~350 μm) for vascular ingrowth, while the shared PLGA matrix ensured strong interfacial bonding.

Hierarchical biomimicry. Inspired by nature, Yuan et al. [210] developed a biomimetic nanocomposite membrane (d-BLG membrane) coupling nacre's “brick-and-mortar” architecture (where CaSi/Ag nanofibers are dispersed in an SA-SF matrix, allowing energy dissipation through fiber pull-out and sliding) with the Bouligand helical structure (where a 20° twist between layers enhances damage tolerance by forcing crack tortuosity). The resulting membrane exhibited superior hydrated mechanics, including high tensile strength (12.43 ± 0.76 MPa) and toughness. Furthermore, in an infected bone defect model, Ag^{+} release from the smooth surface inhibited bacteria, while Ca^{2+} release from the

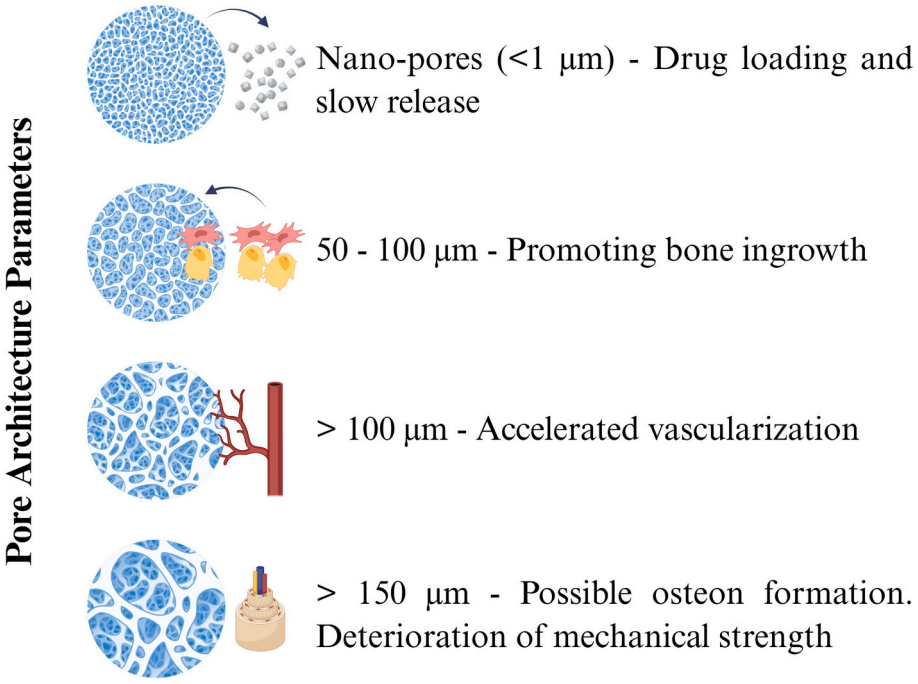

Fig. 7. Effect of membrane pore architecture on GBR-relevant cellular behavior across length scales. Nanoscale pores (<1 μm) restrict diffusion-controlled drug release and exclude soft-tissue infiltration; meso-scale pores (50-100 μm) permit cell migration and early soft-tissue ingrowth; macropores (>100 μm) support osteoblast colonization and woven bone formation; and large macropores (>200-300 μm) sustain vascularized bone regeneration in line with native trabecular architecture.

rough surface promoted BMSCs proliferation (Fig. 6D).

In conclusion, macroscopic layered designs, fine-tuned microporosity, and multi-scale architectures have driven the evolution of GBR membranes from inert structures to active regulatory platforms. However, manufacturing complexity and the translational gap between laboratory and clinic remain. Moreover, structural design alone cannot fully address the dynamic biological demands of bone regeneration, which motivates the integration of drug delivery and stimuli-responsive strategies discussed in the following section.

Across structural strategies, distinct trade-offs emerge: bilayer and Janus architectures offer mature manufacturing routes (electrospinning, layer-by-layer assembly) but face interfacial bonding challenges; multilayer and functionally graded designs achieve smoother mechanical-biological transitions at the cost of more complex fabrication (sequential electrospinning, 3D printing); single-material multi-morphology approaches simplify supply-chain complexity but remain validated in only a handful of studies.

4.3. Functionalization and responsive design

Material selection and structural design establish the physical and architectural foundation of GBR membranes. However, bone regeneration is a dynamic, multi-stage process that demands temporally coordinated biological cues beyond what passive material properties alone can provide. This section examines two progressively sophisticated strategies for active microenvironmental regulation: bioactive delivery systems that supply therapeutic agents within defined release windows, and stimuli-responsive designs that enable on-demand, externally or endogenously triggered modulation of the regenerative process.

4.3.1. Drug delivery and microenvironmental control

Bone regeneration is a dynamic and highly coordinated biological process that progresses through sequential phases of inflammation, tissue formation, and remodeling. Successful GBR therefore depends not only on maintaining a secluded space for bone growth but also on actively regulating the local microenvironment throughout the healing process. Consequently, next-generation membranes are engineered to deliver spatiotemporally controlled biological cues — using growth factors, extracellular vesicles, or matrix-derived components — to favorably modulate immune responses, angiogenesis, and osteogenesis [110].

Growth factor delivery. Growth factors represent one of the most widely investigated bioactive components for enhancing GBR outcomes. Integrating growth factors transforms GBR membranes into delivery platforms capable of releasing therapeutic agents within the optimal therapeutic window. Among the various candidates, BMPs, fibroblast growth factor (FGF), platelet-derived growth factor (PDGF), and stromal cell-derived factor 1α (SDF-1α) have been extensively studied [211]; comprehensive reviews of growth factor delivery strategies in bone tissue engineering provide additional context [212]. For example, incorporating recombinant human BMP-2 at the upper end of the low-dose range tested in canine peri-implant ridge augmentation (rhBMP-2; 0.2 mg/mL — well below the 1.5 mg/mL used in commercial INFUSE products) into an HA/β-TCP/collagen composite significantly enhances osteoblast differentiation while avoiding the inflammatory responses and ectopic ossification associated with high-dose clinical applications [213].

The efficacy of these systems relies heavily on release kinetics. Pure CS showed limited adsorption capacity for BMP-2, whereas composite membranes containing inorganic phases provided larger surface areas for protein immobilization and enabled more sustained release. Moreover, the release of soluble silicon species from silica components could synergistically activate osteogenic signaling. *In vivo*, loading this composite with BMP-2 stimulated significantly higher new bone formation at 2 weeks post-implantation [214].

Vascularization-promoting factors (bFGF, EGF) and growth-factor-derived peptides (BFP-1) extend the membrane's bioactive repertoire beyond osteoinduction. Lee et al. [215] demonstrated that loading a PCL/gelatin membrane with basic fibroblast growth factor (bFGF) promoted hMSCs migration and induced human umbilical vein endothelial

cells (HUVECs) to form tube-like structures - a critical step for vascularization. Growth factor loading can also promote soft tissue healing. Lu et al. co-loaded epidermal growth factor (EGF) and bFGF into a CS sponge/PLGA/PCL scaffold, which stimulated new bone formation and enhanced soft tissue regeneration in the defect area [216]. Growth factor-derived peptides have also gained attention. For instance, modifying PLGA membranes with bone-forming peptide-1 (BFP-1) significantly enhanced BMSC spreading, ALP secretion, and calcium deposition [217].

Beyond osteoinductive factors, vascular endothelial growth factor (VEGF) is increasingly recognized as indispensable, given that the HIF-1α/VEGF axis governs early angiogenic coupling during bone healing [218,219]. Recent studies have therefore embedded VEGF together with BMP-2 in bone-targeted scaffold systems, in which rapid VEGF release

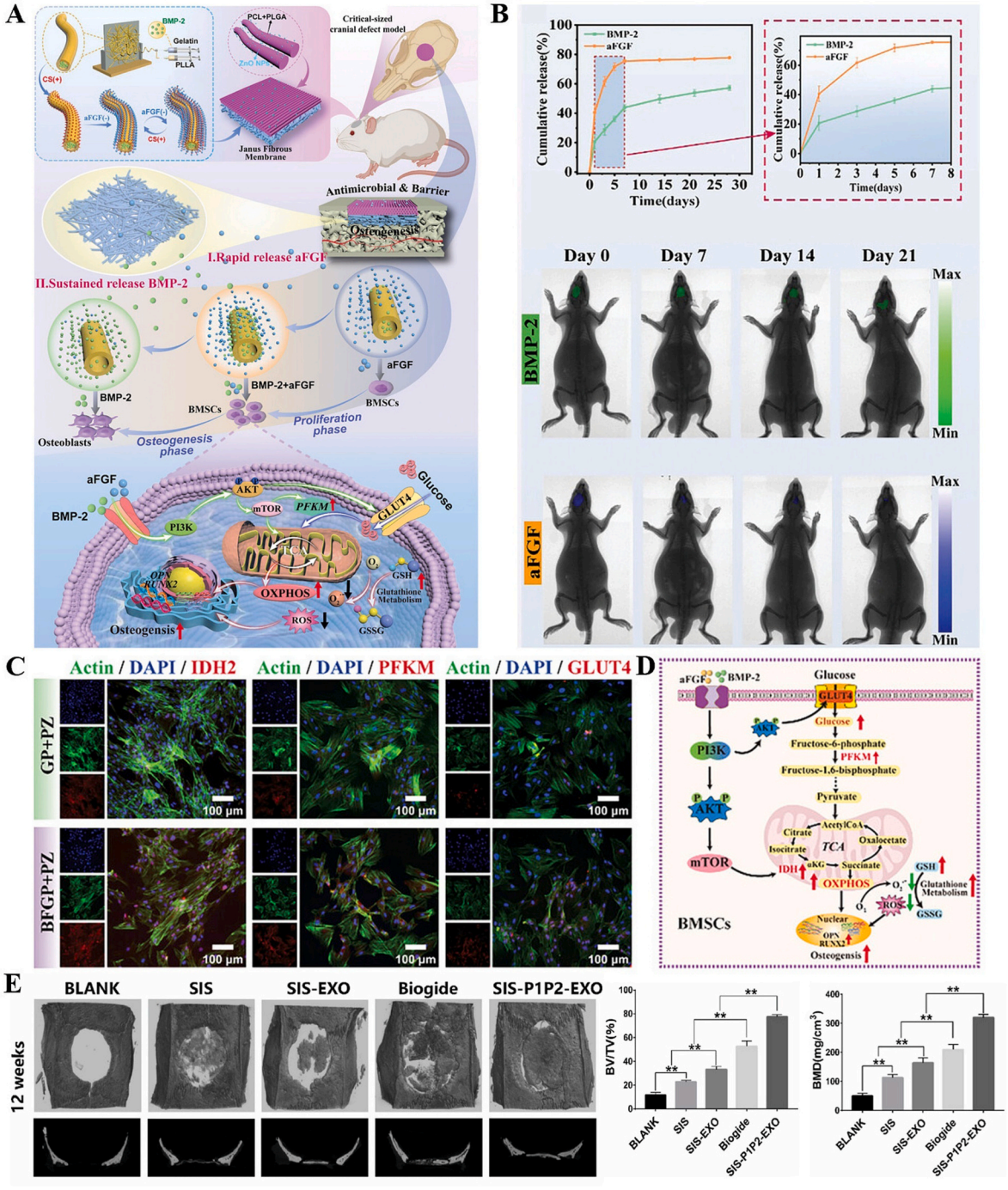

Fig. 8. Design for bioactive release and microenvironment regulation of GBR membranes. A) Fabrication, application, bioactive functions, and mechanisms of Janus multifunctional fibrous membranes [222]. Copyright 2025. B) *In vitro* and *in vivo* release of aFGF and BMP-2 [222]. Copyright 2025. C) Representative images for immunofluorescence staining of IDH2, PFKM, and GLUT4 in different groups [222]. Copyright 2025. D) Schematic diagram of the mechanism of osteogenic differentiation of BMSCs induced by Janus fibrous membranes, showing the metabolic shift from glycolysis — with PFKM catalyzing the phosphofructokinase step (fructose-6-phosphate to fructose-1,6-bisphosphate) followed by downstream pyruvate generation — toward TCA-cycle and OXPHOS pathways (with concomitant glutathione/GSH/GSSG redox balance), driven by AKT signaling and IDH2-mediated isocitrate metabolism [222]. Copyright 2025. E) General evaluation of the *in vivo* performance at 12 weeks after implantation of the SIS, SIS-EXO, Biogide, and SIS-P1P2-EXO membranes. *P < 0.05; **P < 0.01 [227]. Copyright 2022.

for capillary ingrowth, while sustained BMP-2 release for osteogenesis [220]. Adapting these dual-release strategies to GBR membranes remains a largely open opportunity. Equally underexplored within current GBR membrane designs is the co-delivery of antibacterial agents (e.g., antimicrobial peptides, metal ions, photothermal antibacterial nanomaterials), which is critical given the high infection susceptibility of intraoral GBR sites and the routinely contaminated surgical field.

Sequential delivery systems. Bone regeneration and repair are complex physiological processes that are regulated through a cascade of signaling pathways, including Wnt/β-catenin, BMP/TGF-β, MAPK, and PI3K/Akt/mTOR. These pathways participate in the entire process from initial inflammation to bone remodeling. Both natural and synthetic small-molecule drugs can target these pathways to activate them, promote osteoblast differentiation, and inhibit bone resorption, thereby synergistically driving bone defect repair [221]. Consequently, increasing efforts have focused on developing GBR membranes capable of sequential or stage-specific delivery of bioactive factors to better mimic this natural healing cascade.

A representative strategy involves multilayer or Janus membranes. Cheng et al. [222] developed a Janus fibrous membrane for synergistic cascade therapy using coaxial electrospinning and layer-by-layer self-assembly. The outer layer (PCL/PLGA fibers with ZnO nanoparticles) provided antibacterial activity and barrier function. The inner layer (core-shell gelatin/PLLA nanofibers) enabled the rapid release of aFGF for early-stage angiogenesis, followed by the sustained release of BMP-2 for long-term osteogenesis (Fig. 8A and B). Mechanistically, this hierarchical system shifted BMSCs energy metabolism toward OXPHOS and maintained a low-ROS microenvironment. This ultimately promoted BMSC osteogenesis and HUVEC angiogenesis *in vitro*, achieving efficient bone regeneration *in vivo* (Fig. 8C and D).

Comparable sequential strategies have also been established in adjacent scaffold systems. Wang et al. [223] designed a silk fibroin/n-HAp scaffold in which BMP-2 and VEGF were partitioned into separate compartments of SF microspheres, achieving rapid VEGF release for early angiogenesis followed by sustained BMP-2 release for subsequent osteogenesis, bridging rat calvarial defects within 12 weeks at very low growth-factor doses (300 ng BMP-2 + 20 ng VEGF per scaffold). In a complementary approach, Yao et al. [224] used mesoporous silica nanoparticles embedded within a 3D nanofibrous gelatin platform to release the hypoxia-mimetic deferoxamine (DFO) over ~10 days, thereby activating HIF-1α/VEGF signaling, while BMP-2 was released over ~28 days from large-pore MSNs to support sustained osteogenic differentiation. Across these examples, the stage-specific release pattern — fast angiogenic, slow osteogenic — emerges as a generalizable design principle, encoded through distinct carrier compartments such as microspheres, layered fibers, or nanoparticles.

Cell-derived vesicles. Cell-derived extracellular vesicles, particularly exosomes, have emerged as promising bioactive regulators for GBR membranes. Exosomes contain proteins, lipids, and regulatory RNAs capable of modulating osteogenesis, angiogenesis, and immune responses, making them attractive alternatives to direct cell transplantation [225,226]. However, efficient loading and stabilization of exosomes remain major challenges. To address this issue, Ma et al. [227] achieved specific exosome loading onto a small intestinal submucosa (SIS) membrane using an engineered recombinant peptide comprising a collagen-binding domain, a linker, and an exosome-capturing motif. *In vivo*, this SIS-peptide-exosome membrane (SIS-P1P2-EXO) resulted in superior new bone formation compared to unmodified SIS or commercial controls, confirming its enhanced regenerative efficacy (Fig. 8E). To address stability issues, Zhang et al. [228] loaded stromal vascular fraction-chimeric nanovesicles (USE-SCNVs) onto an electrospun PCL membrane. Enriched in specific miRNAs, these USE-SCNVs were efficiently internalized by macrophages, driving polarization toward the pro-healing M2 phenotype. In a rat femoral defect model, this composite promoted the formation of mature, lamellar-like bone within two weeks, presenting a novel strategy for early-stage repair.

More recently, Wen et al. [229] developed a biomimetic periosteum (PEC-Apt-NP-Exo) by coaxially electrospinning PCL/periosteal decellularized ECM fibers and covalently coupling M2 macrophage-derived exosomes functionalized with BMSC-specific aptamers, achieving combined immunomodulation (M2 polarization), endogenous BMSC recruitment, osteogenic differentiation via Rap1/PI3K/AKT, and VEGF-driven angiogenesis in large bone defect repair. Compared with recombinant growth factors, exosomes carry a multimodal payload (proteins, miRNAs, lipids) and avoid burst-release-related ectopic bone formation, but their translation hinges on currently unresolved challenges, including scalable GMP-compatible production, storage stability and cold-chain logistics, and standardized characterization metrics (particle size, surface markers, miRNA content) — issues that growth factor delivery does not face to the same extent.

Matrix-derived components. ECM is an ideal source for biomimetic functionalization. Demineralized dentin matrix (DDM), in particular, provides a sustained release of type I collagen, non-collagenous matrix proteins, and endogenous bone-related growth factors (e.g., BMPs and TGF-β) while exhibiting innate immunomodulatory properties. Incorporating DDM into a PLA/PLGA membrane not only accelerated osteogenesis but also actively remodeled the local macrophage population toward a pro-reparative M2 phenotype [230]. Compared to exogenously administered growth factors, matrix-derived substances like DDM offer superior biological stability and mitigate safety risks such as burst release or dosage toxicity, holding significant translational value.

Despite their therapeutic promise, the bioactive delivery systems discussed above share a fundamental limitation: their release kinetics are largely predetermined by material composition and fabrication parameters, offering limited capacity for real-time adjustment in response to the evolving wound microenvironment. This constraint has motivated the development of stimuli-responsive GBR membranes capable of dynamically modulating their therapeutic output in synchrony with specific biological or externally applied signals.

4.3.2. Stimuli-responsive and adaptive GBR membranes

Stimuli-responsive GBR membranes can be broadly classified according to their triggering mechanism: endogenous microenvironment-responsive systems that exploit biological signals such as local pH changes during inflammation; externally triggered systems activated by ultrasound, near-infrared light, or electrical fields; piezoelectric biomaterials that convert mechanical loading into osteogenic electrical signals; and programmable 4D-printed architectures that undergo predesigned structural transformations over time.

Microenvironment-responsive membranes. Building upon biofunctional membranes, recent research increasingly explores stimuli-responsive biomaterials that dynamically interact with the regenerative microenvironment. These systems utilize endogenous biological signals generated during tissue repair (passive response) to modulate the microenvironment and promote regeneration. Localized acidification at the defect site during the inflammatory phase provides a natural trigger for controlled therapeutic release [231,232]. For example, Gao et al. [233] incorporated a metal-phenolic network (MPN) composed of tannic acid (TA) and Mg^{2+} into an electrospun PCL nanofiber membrane. Under acidic conditions, the material coordinated the release of both components, simultaneously modulating inflammation and enhancing osteogenic differentiation of stem cells. Such designs transformed a pathological microenvironment into a therapeutic trigger, synchronizing drug release with tissue repair (Fig. 9A). Similarly, a pH-responsive PCL/Van-ZIF-8 GBR membrane was developed to rapidly release vancomycin in an acidic infectious environment for bacterial eradication, followed by sustained release under neutral conditions to promote bone regeneration [234].

Beyond pH, the regenerative microenvironment offers several other endogenous triggers that remain comparatively underexplored within GBR membranes. Elevated reactive oxygen species (ROS) at inflamed defect sites can be exploited via thioketal-, phenylboronate-, or

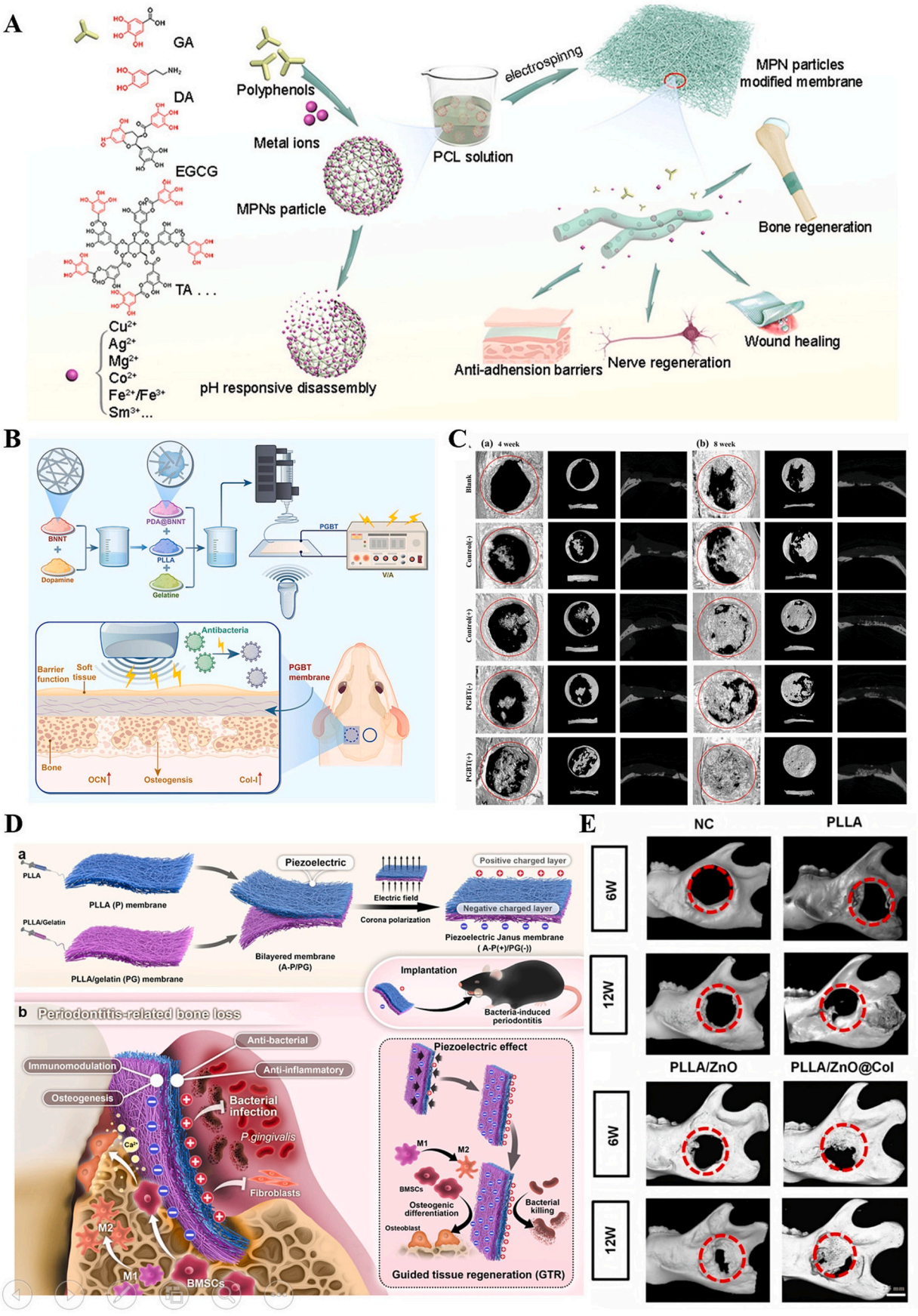

(caption on next page)

Fig. 9. Applications of responsive materials in GBR membranes. A) Schematic diagram of the MPNs as a novel filler to advance multi-functional immunomodulatory biocomposites [233]. Copyright 2021. B) Schematic diagram of the novel ultrasound-driven piezoelectric GBR membrane [236]. Copyright 2025. C) Radiological evaluation in rat cranial defect regeneration after the membrane-covered defect sites [236]. Copyright 2025. D) Design and fabrication of a biodegradable piezoelectric Janus membrane (asymmetric A-P(+)/PG(−) configuration: PLLA piezoelectric layer paired with PLLA/gelatin layer) for simultaneous antibacterial and bone-regenerative therapy in periodontitis, with the piezoelectric effect concurrently driving osteogenic differentiation, immunomodulation, antibacterial action, and matrix synthesis [240]. Copyright 2025. E) Reconstructed 3D micro-CT images of PLLA, PLLA/ZnO, and PLLA/ZnO@Col groups at 6 weeks and 12 weeks. Scale bars: 2.5 mm [241]. Copyright 2025.

thioether-bearing polymers that disassemble under oxidative stress to release encapsulated cargo while simultaneously scavenging ROS — a strategy already validated in adjacent bone-related scaffolds [235]. Likewise, locally upregulated matrix metalloproteinases (MMPs) during the remodeling phase can cleave MMP-sensitive peptide linkers to trigger spatially confined factor release, while temperature-responsive (e.g., PNIPAM) and enzymatically degradable hydrogel coatings have been integrated into wound-healing and periodontal devices yet rarely transposed onto barrier membranes. Translating these mechanisms into GBR contexts could enable membranes that respond to the full repertoire of biological cues encountered during bone healing, rather than relying on acidic pH alone [188,221].

Externally triggered regulatory systems. Beyond endogenous cues, external stimuli offer opportunities to control membrane function with high spatiotemporal precision. Ultrasound-responsive systems have garnered attention due to their non-invasive nature, deep tissue penetration, and ease of control. Zhu et al. [236] reported a piezoelectric GBR membrane based on PLLA/Gelatin/PDA@BNNT (PGBT). Under low-intensity ultrasound stimulation (100 mW/cm^2), the membrane generated a piezoelectric potential of approximately 130 mV without prior poling, with the response primarily originating from the intrinsically piezoelectric BNNT fillers rather than the PLLA matrix. This in situ-generated electrical signal exhibited antibacterial properties and significantly promoted osteoblast differentiation. In a rat calvarial defect model, combining this membrane with ultrasound therapy achieved complete bone filling within 8 weeks, with new bone height in some areas even exceeding the original bone level (Fig. 9B and C). Alternatively, photo-responsive GBR membranes utilize the tissue-penetrating ability of near-infrared (NIR) light to drive localized tissue regeneration via photothermal effects [237].

Direct electrical stimulation serves as another key modality. An electro-stimulable Janus membrane (Col/FA-FAGO) with dense and porous layers was constructed via the one-step electroassembly of collagen, ferulic acid (FA), and rGO. Under a 300 mV field, it activated pro-osteogenic Ca^{2+}/TGF-β/Smad signaling, while FA scavenged ROS and drove M2 macrophage polarization. This quadruple action-antibacterial, antioxidant, immunomodulatory, and osteogenic-significantly enhanced periodontal bone regeneration in diabetic rats [238].

These externally activated systems allow clinicians to modulate therapeutic effects post-implantation, offering an additional level of control over the regenerative process.

Piezoelectric biomaterials. Natural bone exhibits inherent piezoelectricity, generating surface potentials upon mechanical loading that regulate cellular adhesion, proliferation, and differentiation. Inspired by this, researchers have constructed intelligent bio-interfaces capable of actively transmitting electrical signals by incorporating conductive or piezoelectric components into polymer membranes (e.g., piezoelectric PVDF films co-stimulated with low-intensity pulsed ultrasound) [239]. Naturally biodegradable piezoelectric polymers (e.g., PLLA-based systems) combine biocompatibility with tunable, harmless degradation, thereby avoiding the biotoxicity and secondary removal surgeries associated with traditional lead-based ceramics or non-degradable polymers. Moreover, naturally derived biodegradable polymers, such as collagen and SF, offer excellent flexibility and tissue conformability for oral applications.

For instance, Li et al. [240] designed a biodegradable piezoelectric Janus membrane (A-P (+)/PG (−)) composed of a positively charged poly(L-lactic acid) layer (PLLA, A-P (+)) and a negatively charged PLLA/gelatin composite layer (PG (−)). In application, the tissue-facing positive layer inhibited bacteria (e.g., *P. gingivalis*) and alleviated inflammation via electrostatic interactions. Concurrently, the bone-facing negative layer promoted M2 macrophage polarization and matrix mineralization. In a mouse model, bone mineral density (BMD) reached 1637 ± 37 mg/cm^3 at 8 weeks post-implantation — a value that likely reflects localized hypermineralization or methodological factors and warrants verification against the original measurement conditions before its relative outperformance over the collagen-membrane control is generalized (Fig. 9D).

Another study targeting large-area bone defects developed a collagen-enhanced piezoelectric PLLA/ZnO microfiber membrane (PLLA/ZnO@Col). This membrane exhibited piezoelectric responsiveness and upregulated osteogenic genes via Ras and PI3K-AKT, promoting osteoblast proliferation, migration, and differentiation. This osteogenic effect was further enhanced by low-intensity pulsed ultrasound (20 mW/cm^2) stimulation. In a rat mandibular defect model, the membrane's collagen layer facing the bone defect significantly improved BMD and bone volume fraction at both 6 and 12 weeks post-implantation, demonstrating excellent osteoconductivity (Fig. 9E) [241].

Despite these advances, biodegradable piezoelectric materials face critical challenges. Their piezoelectric constants are generally lower than those of traditional ceramics, complicating the trade-off between mechanical flexibility and stable long-term electrical output. Furthermore, the lack of a standardized evaluation system limits their large-scale fabrication and clinical translation [242].

Programmable and 4D-printed biomaterials. Recent advances in programmable biomaterials and 4D printing offer new opportunities to address intrinsic limitations of conventional GBR membranes. 4D printing integrates additive manufacturing with stimulus-responsive materials, enabling printed structures to undergo pre-programmed transformations over time in response to environmental cues [243–246].

In the context of barrier membranes, such programmable behavior enables dynamic regulation of both macro- and micro-scale properties. For example, a recently reported 4D-printed bilayer membrane — combining a hydrogel layer and a shape-memory polymer (SMP) layer — demonstrated sequential structural transformations during bone repair. The hydrogel component enabled time-dependent morphing into a predefined 3D configuration for conformal adaptation to complex defect geometries, while the SMP layer provided switchable surface microtopographies to modulate cell behavior [247]. Importantly, this dynamic microtopography promoted early stem cell proliferation on a temporary flat surface, subsequently enhancing osteogenesis following structural recovery. Such temporal regulation of cell fate resulted in significantly enhanced bone formation compared to static membranes *in vivo* [247].

In a complementary bone-defect-oriented effort, Du et al. [248] fabricated a 4D-printed shape-memory polyester scaffold from a poly(ε-caprolactone)/poly(propylene fumarate) copolymer, in which the PCL/PPF copolymer, with its melting transition tuned to near body temperature via copolymer ratio adjustment (pure PCL Tm ≈ 60 °C is shifted by PPF blocks), served as the molecular switch, enabling on-demand morphological adaptation to irregular defect geometries upon implantation; subsequent post-cross-linking preserved spongy-bone-like porosity (~300 μm) and significantly enhanced osteogenic differentiation *in vivo*. Overall, programmable and 4D-printed

membranes illustrate a paradigm shift toward adaptive and spatiotemporally functional biomaterials, which may better match the evolving mechanical and biological requirements during bone regeneration.

While pH-responsive systems (e.g., PCL/Van-ZIF-8 and MPNs) enable inflammation-triggered drug delivery, their binary "on/off" kinetics prematurely halt therapeutic release once local pH normalizes, neglecting late-stage osteogenesis. Conversely, externally triggered platforms (e.g., electro-activated Col/FA-FAGO membranes) provide precise temporal control but demand repeated clinical interventions, compromising patient compliance. Architecturally, 4D-printed shape-memory bilayers advance sequential tissue modulation via dynamic microtopographical restructuring; however, they lack *in vivo* alveolar validation, and their kinetic reproducibility in the complex oral milieu remains unproven. Ultimately, a critical translational gap across all smart membranes is the absence of closed-loop feedback. Integrating in situ biosensing with adaptive release is essential to evolve these platforms from pre-programmed carriers into truly autonomous, state-responsive GBR systems.

5. Challenges and strategies for novel GBR membranes clinical translation

As the central biomaterial component of GBR, an ideal clinical-grade membrane must balance structural stability with bioactivity throughout healing while meeting regulatory requirements for safety and predictability. The development of GBR membranes is rapidly advancing from laboratory innovation toward clinical application, driven by interdisciplinary collaboration. However, a significant gap remains between laboratory success and widespread clinical use. Deficiencies in performance adaptability, clinical reproducibility, and harmonized international regulatory standards present major obstacles to large-scale application.

5.1. Key bottlenecks

Clinical translation barriers. Despite encouraging preclinical results, many emerging GBR membranes encounter significant obstacles during clinical development. A major limitation is the difficulty of reproducing laboratory performance within the highly variable oral environment. During the critical post-surgical bone regeneration period, the membrane must maintain structural stability while interacting with host tissues, immune cells, and the oral microbiome. Variations in pH, enzymatic activity, and bacterial colonization significantly alter degradation kinetics and biological responses, causing discrepancies between experimental predictions and clinical outcomes.

Magnesium membranes — a case in point. Magnesium-based biodegradable membranes are a prime example. Devices like NovaMag® have achieved CE certification and show preliminary promise for ridge augmentation, periodontal regeneration, and sinus floor elevation [187]. However, studies emphasize a crucial discrepancy: while these membranes exhibit ideal mechanical, degradation, and osteogenic properties *in vitro*, their performance is highly unpredictable within the complex, dynamic *in vivo* environment of the oral cavity. Consequently, variations in degradation, mechanical stability, ion release, and antibacterial activity present a significant obstacle to clinical standardization.

Standardized preclinical evaluation. Another major barrier lies in the lack of standardized preclinical evaluation protocols. Existing frameworks, such as ISO 10993 for biocompatibility (encompassing −1 risk-based evaluation, −6 implantation, −10 sensitization, and −18 chemical characterization), ISO 14155 for clinical investigations, ISO 13485:2016 for quality-management systems, and ISO 14971 for risk management, were primarily developed for inert medical materials [249,250]. Specifically, current ISO and NMPA standards exhibit deficiencies in three areas: first, they lack standardized protocols for evaluating dynamic *in vivo* ion release kinetics; second, they fail to define clear immunomodulatory indicators (e.g., macrophage polarization ratios or inflammatory cytokine profiling); and third, they lack required quantitative endpoints for angiogenesis. Furthermore, the implementation of the European Union Medical Device Regulation (MDR 2017/745) [251] has exposed significant gaps in current evaluations. Under MDR, resorbable GBR membranes — especially those incorporating bioactive ions or biological factors — face stricter scrutiny as high-risk Class III devices. The MDR mandates robust Clinical Evaluation Reports (CER) and rigorous Post-Market Clinical Follow-up (PMCF) to monitor the long-term toxicity of degradation by-products, requirements that most current preclinical studies fail to address adequately.

Regulatory classification. Beyond the aforementioned standards, navigating regulatory classification barriers represents another significant obstacle. For example, the FDA distinguishes three principal pathways — 510(k) clearance (predicate-based), PMA approval (novel high-risk), and de novo classification (low-to-moderate-risk devices lacking a predicate, particularly relevant to MXene-based, piezoelectric, and 4D-printed GBR platforms) — and has updated several guidelines for combination products, including product identification and use-related risk analyses [252,253]. Similarly, the NMPA's *Notice on the Registration of Drug-device Combination Products* clarifies that products primarily functioning as drugs or devices must be submitted for approval under their respective categories [254].

Platform-tailored PMCF. Translating these generic regulatory principles into device-specific actions requires platform-tailored post-market clinical follow-up (PMCF) protocols and pre-clinical endpoint sets. For Mg-alloy GBR membranes, PMCF should monitor (i) hydrogen-gas pocket formation observable on cone-beam CT; (ii) local pH excursion at the implant interface; (iii) systemic Mg^{2+} exposure; and (iv) defect BV/TV at relevant time points (e.g., 8 and 24 weeks). For piezoelectric platforms (PLLA/ZnO and similar), longitudinal tracking of piezoelectric output drift over the relevant healing window and its correlation with peri-implant BMD is essential, as charge-density attenuation directly limits sustained osteogenic stimulation. For MXene-based systems, oxidative stability under saliva-mimicking conditions should be quantified through Ti-species leaching and electrical conductivity decay over the relevant healing window. For CBPs, alveolar pharmacokinetics of citrate-derived metabolites need direct measurement, given that systemic absorption from ester degradation has not yet been evaluated under the unique vascularity and continuous salivary clearance of the alveolar bed. For Zn-alloy GBR membranes, PMCF should track (i) systemic Zn^{2+} via serum or hair sampling, (ii) local Zn accumulation at the alveolar interface (immunostaining or LA-ICP-MS), and (iii) cytotoxicity-related markers given the Zn^{2+} <90 μM *in vitro* cytotoxicity threshold. These platform-specific PMCF endpoints, rather than the generic ISO/MDR checklist alone, define the actionable bottlenecks separating bench validation from regulatory clearance.

5.2. Key strategies for technology translation

Bridging the gap between experimental innovation and clinical application requires coordinated advances in standardized evaluation systems, predictive design tools, and interdisciplinary collaboration.

Tiered evaluation framework. One critical strategy is establishing a standardized, tiered evaluation framework (*in vitro* — small animal — large animal — clinical) to overcome the diagnostic bottlenecks of bioactive membranes. Tier 1 (*in vitro*) should evolve beyond static cytotoxicity to include dynamic degradation models, continuous ion-release profiling, and immune-bone co-cultures for immunomodulatory screening. Tier 2 (small animal) should serve as a high-throughput platform to assess early angiogenesis and osteogenesis. Tier 3 (large animal, e.g., canine alveolar defects) must strictly address translational safety and efficacy. Here, protocols should align with specific regulatory mandates, such as the NMPA guidelines requiring ≥ 6-month observation periods [255] to comprehensively evaluate long-term mechanical

stability, complete degradation pathways, and mature bone remodeling. Finally, Tier 4 (Clinical) requires well-designed randomized controlled trials adhering to ISO 14155 [250] and MDR standards, effectively translating preclinical pharmacokinetic and immunomodulatory data into predictable clinical outcomes.

Engineering technologies. Emerging engineering technologies may also help improve translational predictability [256]. For example, microfluidic organ-on-chip platforms can simulate aspects of the oral microenvironment, including fluid shear stress, salivary components, microbial exposure, and immune interactions. Such systems enable the dynamic, high-throughput evaluation of membrane degradation and biological responses under conditions closely mimicking the *in vivo* environment [257,258]. Concurrently, artificial intelligence (AI) and machine learning (ML) provide data-driven tools to decipher multidimensional structure-property relationships in biomaterials. ML algorithms have already accelerated hydrogel adhesion optimization, antimicrobial polymer discovery, and predictive modeling of scaffold architectures [259–261]. Translating these computational paradigms to GBR membrane engineering enables the predictive optimization of critical parameters, thereby reducing empirical trial-and-error and enhancing material screening efficiency prior to biological evaluation.

Manufacturing standardization. Successful clinical translation requires robust manufacturing standardization and quality control. Many emerging GBR membranes remain confined to laboratory-scale fabrication, with platform-specific sterilization compatibility (e.g., gamma-irradiation acceptable for Mg alloys but accelerating MXene oxidation; ethylene oxide compatible with growth-factor-loaded systems but requiring strict residue control; autoclaving incompatible with thermosensitive citrate or 4D shape-memory polymers) and shelf-life testing (ISO 11607 packaging, accelerated aging at ~55 °C per ASTM F1980) often unaddressed. Fabrication techniques such as electrospinning and customized multilayer assembly frequently produce variable thickness, porosity, and degradation behavior across batches. Scaling these technologies to clinical production requires compliance with Good Manufacturing Practice (GMP) standards, strict batch-to-batch quality control, and traceable material sourcing. Notably, the industrial maturity of native collagen barrier membranes (e.g., Bio-Gide), achieved through standardized cross-linking and regulated tissue sourcing, provides a practical benchmark that next-generation bioactive membranes must approach before robust clinical translation becomes feasible.

GBR-specific computational tools. At the strategy level, AI and microfluidic organ-on-chip approaches must be made GBR-specific to deliver actionable insights rather than generic recipes. AI/ML-driven design should target a defined predictive triad — degradation rate, mechanical retention (% of initial modulus at week 12), and macrophage M2/M1 polarization ratio at days 3 to 14 — using calibrated multimodal training datasets that integrate *in vitro* Hank's-solution corrosion data, *in vivo* small-animal cytokine panels, and clinical histomorphometry. Microfluidic platforms [257] intended to model the oral microenvironment should reproduce key physical parameters relevant to the alveolar bed: physiological salivary flow, pH excursions during occlusal and acidic challenges, dynamic occlusal loading, and bacterial co-culture incorporating oral pathogens to capture both anaerobic dysbiosis and acidogenic challenge. Without these GBR-specific targets and parameters, AI prediction and organ-on-chip readouts risk yielding insights that fail to translate to alveolar-bone-specific clinical outcomes.

In summary, although conventional GBR membranes are well established clinically, translating next-generation bioactive membranes remains constrained by challenges in standardized evaluation, regulatory classification, and manufacturing scalability. Addressing these challenges requires coordinated progress across biomaterials science, regulatory science, and clinical research. By integrating standardized testing pipelines, advanced predictive technologies, and robust manufacturing systems, future GBR membranes will evolve from passive structural materials into clinically reliable regenerative platforms with predictable biological performance.

6. Summary and perspective

The preceding sections demonstrate how vascular, immune, and osteogenic processes converge at the membrane interface. From this synthesis, four design principles emerge for the GBR membrane platforms most likely to translate.

First, spatiotemporal coordination across the four key design requirements (mechanical stability, degradation matching, bioactivity, and immunomodulation) is increasingly recognized as the central paradigm. Despite significant progress, current systems still fall short of achieving quantitative matching between membrane degradation (e.g., 4-6 months vs. ≥9 months), sustained mechanical integrity (≥12-16 weeks), and staged bioactive release, particularly in heterogeneous defect environments. Emerging strategies, including stimuli-responsive materials and nanotechnology-enabled delivery systems, provide promising tools to bridge this gap, yet precise synchronization remains a major translational bottleneck.

Second, hierarchical structural biomimicry has emerged as a strategy to simultaneously enhance mechanical robustness (e.g., compressive resistance) and biological performance (cell infiltration and vascularization). Advanced fabrication technologies, such as 3D/4D printing and electrospinning, enable precise control of multi-scale architectures. However, a critical knowledge gap persists regarding the quantitative relationship between structural parameters (e.g., pore size, fiber alignment, stiffness gradients) and long-term clinical outcomes, limiting their predictive design. Future efforts should integrate multimodal imaging, in situ biomechanical analysis, and clinically relevant large-animal models to establish structure-function-outcome correlations.

Third, immunomodulation-driven design is increasingly recognized as a decisive factor governing regeneration outcomes. Future GBR membranes should achieve controlled macrophage polarization (e.g., M2/M1 balance) and cytokine regulation (IL-10/TNF-α ratios) to promote osteoimmunological coupling. However, precise and sustained immune modulation remains challenging due to the dynamic oral microenvironment and microbiota-associated inflammation, raising concerns about unintended chronic inflammation or oxidative stress. Thus, integrating immunomodulatory materials with real-time monitoring strategies represents an important future direction. Specific implementation routes that warrant systematic investigation include cell membrane-coated GBR membranes (e.g., camouflage of electrospun nanofibers with BMSCs-, macrophage-, or platelet-derived membranes) as a biomimetic immune-evasive interface, zwitterionic surface chemistries that suppress non-specific protein adsorption and bacterial colonization at the soft-tissue interface, and high-resolution bioprinting capable of generating patient-specific membrane geometries with integrated cell-laden compartments and gradient mechanical cues — moving toward more precise regenerative platforms.

Finally, advancing these biomaterial concepts toward clinical reality requires delineating near-term executable goals from long-term visionary concepts. In the near term, AI/ML-driven material screening and data-driven computational modeling serve as pragmatic tools to accelerate prototype optimization. While emerging modalities such as bioelectronics integration and programmable-biomaterial-mediated osteogenic regulation [262,263] offer unprecedented theoretical precision, they remain long-term aspirations. Furthermore, bridging the gap in clinical translation requires moving beyond material synthesis to embrace standardized multicenter clinical trial designs, rigorous health-economic cost-effectiveness analyses, and integrated multidisciplinary collaboration models uniting materials scientists, computational biologists, regulatory experts, and dental clinicians.

Beyond these high-level directions, several specific open mechanistic questions merit systematic investigation. They span the molecular, cellular, and systems levels of GBR biology, together with the closed-loop design tools needed to address them: (i) Can the locally alkaline

microenvironment generated by Mg^{2+} release activate latent TGF-β at alveolar defect sites, and does this pathway couple to peri-implant osteoimmune memory [187]? (ii) What surface potential threshold is required to sustain osteogenic differentiation across the alveolar healing window *in vivo*, and how does this threshold shift in bacterially colonized environments? (iii) Do CBPs reproduce metabotissugenic activity in alveolar BMSCs to the same extent as in long-bone BMSCs, given the periodontal-ligament-derived stem cell niche differences [119] (iv) How do oral microbial metabolites (e.g., short-chain fatty acids from *P. gingivalis*)? interact with stimuli-responsive membrane chemistries, and can this interaction be harnessed as an endogenous trigger rather than a confounder? (v) What macrophage M2/M1 ratio and cytokine ratio thresholds at early post-implantation time points predict long-term bone regeneration outcomes in large-animal alveolar defect models? (vi) Can closed-loop AI/ML-driven membrane design simultaneously satisfy mechanical, degradation, and immunomodulatory constraints that have eluded single-objective optimization to date [256,258]? Addressing these questions will demand integrated efforts spanning materials chemistry, osteoimmunology, oral microbiology, and translational dentistry.

Resolving the scientific and translational challenges outlined above is a prerequisite for moving laboratory innovation into routine clinical use. Future GBR membranes are expected to be more predictable in performance and increasingly individualized to patient anatomy. Material innovation alone will not suffice; coordinated progress across engineering, biology, and clinical validation is required.

CRediT authorship contribution statement

Yue Liu: Writing – original draft, Visualization, Validation, Software, Investigation, Data curation, Conceptualization. **Hao Zhang:** Conceptualization, Investigation, Writing – review & editing. **Lingkun Zhang:** Writing – review & editing, Writing – original draft, Validation, Supervision, Conceptualization. **Jianmin Han:** Writing – review & editing, Supervision, Funding acquisition. **Jian Yang:** Writing – review & editing, Supervision, Funding acquisition.

Ethics approval and consent to participate

This review article does not require any ethical approval or allied consents for publication.

Declaration of competing interest

Jian Yang is an editor in chief for Bioactive Materials and was not involved in the editorial review or the decision to publish this article. All authors declare that there are no competing interests.

Acknowledgements

This work was partially supported by the National Key R&D Program of China (2024YFA1107800) and Tianjin Key Medical Discipline Construction Project (Grant No.TJYXZDXK-3-008B).

References

[1] Z. Gaudimier, S. Tawfik, C. Kerouanton, C. Wulfman, Y. Flottes, Oral bone regeneration and associated complications: a systematic review and meta-analysis, J. Stomatol. Oral Maxillofac. Surg. 127 (2) (2026) 102606, https://doi.org/10.1016/j.jormas.2025.102606.

[2] A. Khojasteh, L. Kheiri, S.R. Motamedian, V. Khoshkam, Guided bone regeneration for the reconstruction of alveolar bone defects, Ann. Maxillofac. Surg. 7 (2) (2017) 263–277, https://doi.org/10.4103/ams.ams_76_17.

[3] P. Aprile, D. Letourneur, T. Simon-Yarza, Membranes for guided bone regeneration: a road from bench to bedside, Adv. Healthcare Mater. 9 (19) (2020) e2000707, https://doi.org/10.1002/adhm.202000707.

[4] R. Dimitriou, G.I. Mataliotakis, G.M. Calori, P.V. Giannoudis, The role of barrier membranes for guided bone regeneration and restoration of large bone defects: current experimental and clinical evidence, BMC Med. 10 (2012) 81, https://doi.org/10.1186/1741-7015-10-81.

[5] S. Xue, N. Tang, C. Zhou, S. Fang, H. Haick, J. Sun, X. Wu, Anti-wound dehiscence and antibacterial dressing with highly efficient self-healing feature for guided bone regeneration wound closure, Adv. Healthcare Mater. 13 (16) (2024) e2304128, https://doi.org/10.1002/adhm.202304128.

[6] D. Buser, I. Urban, A. Monje, M.F. Kunrath, C. Dahlin, Guided bone regeneration in implant dentistry: basic principle, progress over 35 years, and recent research activities, Periodontol. 2000 93 (1) (2023) 9–25, https://doi.org/10.1111/prd.12539.

[7] Y. Zhao, W. Sun, X. Wu, X. Gao, F. Song, B. Duan, A. Lu, H. Yang, C. Huang, Janus membrane with intrafibrillarly strontium-apatite-mineralized collagen for guided bone regeneration, ACS Nano 18 (9) (2024) 7204–7222, https://doi.org/10.1021/acsnano.3c12403.

[8] J.I. Sasaki, G.L. Abe, A. Li, P. Thongthai, R. Tsuboi, T. Kohno, S. Imazato, Barrier membranes for tissue regeneration in dentistry, Biomater Investig. Dent. 8 (1) (2021) 54–63, https://doi.org/10.1080/26415275.2021.1925556.

[9] X. Yang, D. Yang, X. Lin, D. Li, W. Shi, Z. Xiang, C. Mu, L. Ge, D. Li, Z. Xu, Effect of dehydrothermal treatment on the structure and properties of a collagen-based heterogeneous bilayer membrane, ACS Appl. Polym. Mater. 5 (5) (2023) 3427–3438, https://doi.org/10.1021/acsapm.3c00095.

[10] Y. Ren, L. Fan, S. Alkildani, L. Liu, S. Emmert, S. Najman, D. Rimashevskiy, R. Schnettler, O. Jung, X. Xiong, M. Barbeck, Barrier membranes for guided bone regeneration (GBR): a focus on recent advances in collagen membranes, Int. J. Mol. Sci. 23 (23) (2022) 14987, https://doi.org/10.3390/ijms232314987.

[11] H. Pan, Y. Qu, X. Hui, H. Yue, Advances in biological barrier membranes for guided bone regeneration: fabrication, characteristics, multifunctional optimization, and clinical prospects, Mater. Today Sustain. 33 (2026) 101303, https://doi.org/10.1016/j.mtsust.2026.101303.

[12] H. Yu, B. He, Z. Yan, C. Xia, C. Li, W. Xiao, X. Yang, D. Zhang, B. Li, Advances in oral GBR membranes for bone repair and regeneration: materials, mechanisms, and applications, J. Bioact. Compat Polym. 41 (2) (2026) 126–148.

[13] R. Ullah, S. Husain, F. Mohammed, S.A. Khurram, Alveolar Bone, an Illustrated Guide to Oral Histology, 2021, pp. 99–121.

[14] H.E. Schroeder, M.A. Listgarten, The gingival tissues: the architecture of periodontal protection, Periodontol. 2000 13 (1997) 91–120, https://doi.org/10.1111/j.1600-0757.1997.tb00097.x.

[15] G.A. Mandelaris, B.S. Vence, A.L. Rosenfeld, D.P. Forbes, A classification system for crestal and radicular dentoalveolar bone phenotypes, Int. J. Periodontics Restor. Dent. 33 (3) (2013) 289–296, https://doi.org/10.11607/prd.1787.

[16] S.S. Huja, S.A. Fernandez, K.J. Hill, Y. Li, Remodeling dynamics in the alveolar process in skeletally mature dogs, Anat. Rec. A Discov. Mol. Cell. Evol. Biol. 288 (12) (2006) 1243–1249, https://doi.org/10.1002/ar.a.20396.

[17] A. Mavropoulos, R. Rizzoli, P. Ammann, Different responsiveness of alveolar and tibial bone to bone loss stimuli, J. Bone Miner. Res. 22 (3) (2007) 403–410, https://doi.org/10.1359/jbmr.061208.

[18] M.G. Araújo, J. Lindhe, Dimensional ridge alterations following tooth extraction. An experimental study in the dog, J. Clin. Periodontol. 32 (2) (2005) 212–218, https://doi.org/10.1111/j.1600-051X.2005.00642.x.

[19] H.M. Frost, A 2003 update of bone physiology and Wolff's Law for clinicians, Angle Orthod. 74 (1) (2004) 3–15, https://doi.org/10.1043/0003-3219(2004)074<0003:Auobpa>2.0.Co;2.

[20] F. Van der Weijden, F. Dell'Acqua, D.E. Slot, Alveolar bone dimensional changes of post-extraction sockets in humans: a systematic review, J. Clin. Periodontol. 36 (12) (2009) 1048–1058, https://doi.org/10.1111/j.1600-051X.2009.01482.x.

[21] J.D. Hathaway-Schrader, C.M. Novince, Maintaining homeostatic control of periodontal bone tissue, Periodontol. 2000 86 (1) (2021) 157–187, https://doi.org/10.1111/prd.12368.

[22] A. Salhotra, H.N. Shah, B. Levi, M.T. Longaker, Mechanisms of bone development and repair, Nat. Rev. Mol. Cell Biol. 21 (11) (2020) 696–711, https://doi.org/10.1038/s41580-020-00279-w.

[23] W. Lin, Q. Li, D. Zhang, X. Zhang, X. Qi, Q. Wang, Y. Chen, C. Liu, H. Li, S. Zhang, Y. Wang, B. Shao, L. Zhang, Q. Yuan, Mapping the immune microenvironment for mandibular alveolar bone homeostasis at single-cell resolution, Bone Res. 9 (1) (2021) 17, https://doi.org/10.1038/s41413-021-00141-5.

[24] R.P. Settem, K. Honma, S. Chinthamani, T. Kawai, A. Sharma, B-Cell RANKL contributes to pathogen-induced alveolar bone loss in an experimental periodontitis mouse model, Front. Physiol. 12 (2021) 722859, https://doi.org/10.3389/fphys.2021.722859.

[25] S. Li, L. Su, Q. Luan, G. Liu, W. Zeng, X. Yu, Regulatory B cells induced by interleukin-35 inhibit inflammation and alveolar bone resorption in ligature-induced periodontitis, J. Periodontol. 94 (11) (2023) 1376–1388, https://doi.org/10.1002/jper.23-0038.

[26] H. Takayanagi, K. Ogasawara, S. Hida, T. Chiba, S. Murata, K. Sato, A. Takaoka, T. Yokochi, H. Oda, K. Tanaka, K. Nakamura, T. Taniguchi, T-cell-mediated regulation of osteoclastogenesis by signalling cross-talk between RANKL and IFN-gamma, Nature 408 (6812) (2000) 600–605, https://doi.org/10.1038/35046102.

[27] E.M. Cardoso, F.A. Arosa, CD8(+) T cells in chronic periodontitis: roles and rules, Front. Immunol. 8 (2017) 145, https://doi.org/10.3389/fimmu.2017.00145.

[28] K. Bertl, M. Subotic, P. Heimel, U.Y. Schwarze, S. Tangl, C. Ulm, Morphometric Characteristics of Cortical and Trabecular Bone in Atrophic Edentulous Mandibles, 26, 2015, pp. 780–787, https://doi.org/10.1111/clr.12340, 7.

[29] W.L. Tan, T.L. Wong, M.C. Wong, N.P. Lang, A systematic review of post-extractional alveolar hard and soft tissue dimensional changes in humans, Clin. Oral Implants Res. 23 (Suppl 5) (2012) 1–21, https://doi.org/10.1111/j.1600-0501.2011.02375.x.

[30] J. Xu, L. Yu, S. Ye, Z. Ye, L. Yang, X. Xu, Oral microbiota–host Interaction: the Chief Culprit of Alveolar Bone Resorption, 15, 2024 1254516, https://doi.org/10.3389/fimmu.2024.1254516.
[31] G.I. Benic, C.H. Hämmerle, Horizontal bone augmentation by means of guided bone regeneration, Periodontol. 2000 66 (1) (2014) 13–40, https://doi.org/10.1111/prd.12039.
[32] D. De Santis, F. Gelpi, G. Verlato, U. Luciano, L. Torroni, N. Antonucci, F. Bernardello, M. Zarantonello, P.F. Nocini, Digital customized titanium mesh for bone regeneration of vertical, horizontal and combined defects: a case series, Medicina (Kaunas) 57 (1) (2021) 60, https://doi.org/10.3390/medicina57010060.
[33] S.A. Hienz, S. Paliwal, S. Ivanovski, Mechanisms of bone resorption in periodontitis, J. Immunol. Res. 2015 (2015) 615486, https://doi.org/10.1155/2015/615486.
[34] D. Buser, M.M. Bornstein, H.P. Weber, L. Grütter, B. Schmid, U.C. Belser, Early implant placement with simultaneous guided bone regeneration following single-tooth extraction in the esthetic zone: a cross-sectional, retrospective study in 45 subjects with a 2- to 4-year follow-up, J. Periodontol. 79 (9) (2008) 1773–1781, https://doi.org/10.1902/jop.2008.080071.
[35] J.H. Fu, H.L. Wang, Horizontal bone augmentation: the decision tree, Int. J. Periodontics Restor. Dent. 31 (4) (2011) 429–436.
[36] S.-H. Yu, H.-L. Wang, Updated decision tree for horizontal ridge augmentation: a narrative review, Int. J. Periodontics Restor. Dent. 42 (2022) 341–349, https://doi.org/10.11607/prd.5031.
[37] J. Liu, D.G. Kerns, Mechanisms of guided bone regeneration: a review, Open Dent. J. 8 (2014) 56–65, https://doi.org/10.2174/1874210601408010056.
[38] E. Schipani, C. Maes, G. Carmeliet, G.L. Semenza, Regulation of osteogenesis-angiogenesis coupling by HIFs and VEGF, J. Bone Miner. Res. 24 (8) (2009) 1347–1353, https://doi.org/10.1359/jbmr.090602.
[39] A. Grosso, M.G. Burger, A. Lunger, D.J. Schaefer, A. Banfi, N. Di Maggio, It takes two to tango: coupling of angiogenesis and osteogenesis for bone regeneration, Front. Bioeng. Biotechnol. 5 (2017) 68, https://doi.org/10.3389/fbioe.2017.00068.
[40] J. You, M. Liu, M. Li, S. Zhai, S. Quni, L. Zhang, X. Liu, K. Jia, Y. Zhang, Y. Zhou, The role of hif-1α in bone regeneration: a new direction and challenge in bone tissue engineering, Int. J. Mol. Sci. 24 (9) (2023) 8029.
[41] M. Wu, G. Chen, Y.P. Li, TGF-β and BMP signaling in osteoblast, skeletal development, and bone formation, homeostasis and disease, Bone Res. 4 (2016) 16009, https://doi.org/10.1038/boneres.2016.9.
[42] L. Hu, W. Chen, A. Qian, Y.-P. Li, Wnt/β-catenin signaling components and mechanisms in bone formation, homeostasis, and disease, Bone Res. 12 (1) (2024) 39, https://doi.org/10.1038/s41413-024-00342-8.
[43] P.R. Kuzyk, E.H. Schemitsch, The basic science of peri-implant bone healing, Indian J. Orthop. 45 (2) (2011) 108–115, https://doi.org/10.4103/0019-5413.77129.
[44] T.M. Beck, B.L. Mealey, Histologic analysis of healing after tooth extraction with ridge preservation using mineralized human bone allograft, J. Periodontol. 81 (12) (2010) 1765–1772, https://doi.org/10.1902/jop.2010.100286.
[45] I. Elgali, O. Omar, C. Dahlin, P. Thomsen, Guided bone regeneration: materials and biological mechanisms revisited, Eur. J. Oral Sci. 125 (5) (2017) 315–337, https://doi.org/10.1111/eos.12364.
[46] M. Gou, H. Wang, H. Xie, H. Song, Macrophages in guided bone regeneration: potential roles and future directions, Front. Immunol. 15 (2024) 1396759, https://doi.org/10.3389/fimmu.2024.1396759.
[47] H. Wei, J. Cui, K. Lin, J. Xie, X. Wang, Recent advances in smart stimuli-responsive biomaterials for bone therapeutics and regeneration, Bone Res. 10 (1) (2022) 17, https://doi.org/10.1038/s41413-021-00180-y.
[48] Y. Xuan, L. Li, M. Ma, J. Cao, Z. Zhang, Hierarchical Intrafibrillarly Mineralized Collagen Membrane Promotes Guided Bone Regeneration and Regulates M2 Macrophage Polarization, 9, 2022 781268, https://doi.org/10.3389/fbioe.2021.781268.
[49] L. Yi, R. Tang, C. Shao, C. Chen, J. Tang, L. Liao, L. Chen, A Biodegradable Zinc Alloy Membrane with Regulation of Macrophage Polarization for Early Vascularized Bone Regeneration, 29, 2025, p. 223, https://doi.org/10.34133/bmr.0223.
[50] M.L. Zou, Z.H. Chen, Y.Y. Teng, S.Y. Liu, Y. Jia, K.W. Zhang, Z.L. Sun, J.J. Wu, Z. D. Yuan, Y. Feng, X. Li, R.S. Xu, F.L. Yuan, The smad dependent tgf-β and bmp signaling pathway in bone remodeling and therapies, Front. Mol. Biosci. 8 (2021) 593310, https://doi.org/10.3389/fmolb.2021.593310.
[51] L. Chen, Z. Yao, S. Zhang, K. Tang, Q. Yang, Y. Wang, B. Li, Y. Nie, X. Tian, L. Sun, Biomaterial-induced macrophage polarization for bone regeneration, Chin. Chem. Lett. 34 (6) (2023) 107925, https://doi.org/10.1016/j.cclet.2022.107925.
[52] B. Özcolak, B. Erenay, S. Odabaş, K.D. Jandt, B. Garipcan, Effects of bone surface topography and chemistry on macrophage polarization, Sci. Rep. 14 (1) (2024) 12721, https://doi.org/10.1038/s41598-024-62484-3.
[53] H. Atcha, A. Jairaman, J.R. Holt, V.S. Meli, R.R. Nagalla, P.K. Veerasubramanian, K.T. Brumm, H.E. Lim, S. Othy, M.D. Cahalan, M.M. Pathak, W.F. Liu, Mechanically activated ion channel Piezo1 modulates macrophage polarization and stiffness sensing, Nat. Commun. 12 (1) (2021) 3256, https://doi.org/10.1038/s41467-021-23482-5.
[54] T. Yang, Z. Fang, J. Zhang, S. Zheng, Physical cues in biomaterials modulate macrophage polarization for bone regeneration: a review, Front. Bioeng. Biotechnol. 13 (2025) 1640560, https://doi.org/10.3389/fbioe.2025.1640560.
[55] H. Zhan, R. Shi, H. Ni, H. Li, C. Yuan, K. Lin, A. Sculean, R.J. Miron, Functional requirements for guided bone regeneration/guided tissue regeneration membrane design: progress and challenges, Periodontol 2000 (2025) 1–35, https://doi.org/10.1111/prd.70019.
[56] F. Yan, M. Yu, Y. He, F. Wang, F. Yang, X. Zhao, Y. Zheng, Y. Liu, D. Xia, Y. Liu, Hierarchical Mineralized Collagen Coated Zn Membrane to Tailor Cell Microenvironment for Guided Bone Regeneration, 35, 2025 2412695, https://doi.org/10.1002/adfm.202412695, 7.
[57] B. Lima-Sánchez, M. Baus-Domínguez, M.-A. Serrera-Figallo, D. Torres-Lagares, Advances in synthetic polymer membranes for guided bone regeneration in dental implants: a scoping review 16 (5) (2025) 149.
[58] Z. Fu, D. Li, J. Cui, H. Xu, C. Yuan, P. Wang, B. Zhao, K. Lin, Promoting bone regeneration via bioactive calcium silicate nanowires reinforced poly (ε-caprolactone) electrospun fibrous membranes, Mater. Des. 226 (2023) 111671, https://doi.org/10.1016/j.matdes.2023.111671.
[59] X. Chen, T. Zhang, H. Li, Y. Chen, B. Zhang, Y. Wang, W. Zhang, R. Zhang, Y. Wang, Q. Zhou, W. Lu, Y. Guo, J. Wu, Biomimetic multilayer nanofiber membranes with sequential drug release-coupled angiogenesis and osteogenesis for guided bone regeneration, J. Mater. Fut. 5 (1) (2026) 015401, https://doi.org/10.1088/2752-5724/ae315d.
[60] Q. Han, D. Zhao, X. Wang, M. Shang, W. Zhou, Q. Li, H. Song, Composite barrier membrane for bone regeneration: advancing biomaterial strategies in defect repair, RSC Adv. 15 (2) (2025) 1290–1299, https://doi.org/10.1039/d4ra07623k.
[61] C.H. Hammerle, R.E. Jung, Bone augmentation by means of barrier membranes, Periodontol. 2000 33 (2003) 36–53, https://doi.org/10.1046/j.0906-6713.2003.03304.x.
[62] S.A. Jovanovic, R.K. Schenk, M. Orsini, E.B. Kenney, Supracrestal bone formation around dental implants: an experimental dog study, Int. J. Oral Maxillofac. Implants 10 (1) (1995) 23–31.
[63] Y. Xie, S. Li, T. Zhang, C. Wang, X. Cai, Titanium mesh for bone augmentation in oral implantology: current application and progress, Int. J. Oral Sci. 12 (1) (2020) 37, https://doi.org/10.1038/s41368-020-00107-z.
[64] T. von Arx, N. Hardt, B. Wallkamm, The TIME technique: a new method for localized alveolar ridge augmentation prior to placement of dental implants, Int. J. Oral Maxillofac. Implants 11 (3) (1996) 387–394.
[65] I. Konstantinidis, T. Kumar, U. Kher, P.D. Stanitsas, J.E. Hinrichs, G.A. Kotsakis, Clinical results of implant placement in resorbed ridges using simultaneous guided bone regeneration: a multicenter case series, Clin. Oral Invest. 19 (2) (2015) 553–559, https://doi.org/10.1007/s00784-014-1268-4.
[66] L. Ricci, V. Perrotti, L. Ravera, A. Scarano, A. Piattelli, G. Iezzi, Rehabilitation of deficient alveolar ridges using titanium grids before and simultaneously with implant placement: a systematic review, J. Periodontol. 84 (9) (2013) 1234–1242, https://doi.org/10.1902/jop.2012.120314.
[67] J. Gottlow, S. Nyman, J. Lindhe, T. Karring, J. Wennstrom, New attachment formation in the human periodontium by guided tissue regeneration. Case reports, J. Clin. Periodontol. 13 (6) (1986) 604–616, https://doi.org/10.1111/j.1600-051x.1986.tb00854.x.
[68] M. Trobos, A. Juhlin, F.A. Shah, M. Hoffman, H. Sahlin, C. Dahlin, In vitro evaluation of barrier function against oral bacteria of dense and expanded polytetrafluoroethylene (PTFE) membranes for guided bone regeneration, Clin. Implant Dent. Relat. Res. 20 (5) (2018) 738–748, https://doi.org/10.1111/cid.12629.
[69] J.M. Haney, R.E. Nilveus, P.J. McMillan, U.M. Wikesjo, Periodontal repair in dogs: expanded polytetrafluoroethylene barrier membranes support wound stabilization and enhance bone regeneration, J. Periodontol. 64 (9) (1993) 883–890, https://doi.org/10.1902/jop.1993.64.9.883.
[70] S. Almudhi, I. AlSuhimi, K. Almas, F.E. Aljofi, E. AlJoghaiman, A. Alhumaidan, O. Omar, Biological and clinical responses to dense and expanded PTFE membranes in alveolar ridge preservation: a prospective non-randomized cohort study with ex vivo analyses, Clin. Oral Invest. 30 (2) (2026) 84, https://doi.org/10.1007/s00784-026-06777-z.
[71] M. Simion, M. Baldoni, P. Rossi, D. Zaffe, A comparative study of the effectiveness of e-PTFE membranes with and without early exposure during the healing period, Int. J. Periodontics Restor. Dent. 14 (2) (1994) 166–180.
[72] M. Retzepi, N. Donos, Guided bone regeneration: biological principle and therapeutic applications, Clin. Oral Implants Res. 21 (6) (2010) 567–576, https://doi.org/10.1111/j.1600-0501.2010.01922.x.
[73] H.A. Marouf, H.M. El-Guindi, Efficacy of high-density versus semipermeable PTFE membranes in an elderly experimental model, Oral Surg. Oral Med. Oral Pathol. Oral Radiol. Endod. 89 (2) (2000) 164–170, https://doi.org/10.1067/moe.2000.98922.
[74] M.F. Kunrath, G.L. Magrin, C.S. Zorzo, I. Rigotto, H. Aludden, C. Dahlin, Membranes for periodontal and bone regeneration: everything you need to know. https://doi.org/10.1111/jre.70005, 2025.
[75] T.B. Crump, F. Rivera-Hidalgo, J.W. Harrison, F.E. Williams, I.Y. Guo, Influence of three membrane types on healing of bone defects, Oral Surg. Oral Med. Oral Pathol. Oral Radiol. Endod. 82 (4) (1996) 365–374, https://doi.org/10.1016/s1079-2104(96)80299-x.
[76] B.K. Bartee, The use of high-density polytetrafluoroethylene membrane to treat osseous defects: clinical reports, Implant Dent. 4 (1) (1995) 21–26, https://doi.org/10.1097/00008505-199504000-00004.
[77] B.K. Bartee, J.A. Carr, Evaluation of a high-density polytetrafluoroethylene (n-PTFE) membrane as a barrier material to facilitate guided bone regeneration in the rat mandible, J. Oral Implantol. 21 (2) (1995) 88–95.
[78] M.S. Alauddin, N.A. Abdul Hayei, M.A. Sabarudin, N.H. Mat Baharin, Barrier membrane in regenerative therapy: a narrative review, Membranes (Basel) 12 (5) (2022) 444, https://doi.org/10.3390/membranes12050444.

[79] J.M. Carbonell, I.S. Martín, A. Santos, A. Pujol, J.D. Sanz-Moliner, J. Nart, High-density polytetrafluoroethylene membranes in guided bone and tissue regeneration procedures: a literature review, Int. J. Oral Maxillofac. Surg. 43 (1) (2014) 75–84, https://doi.org/10.1016/j.ijom.2013.05.017.
[80] R. Langer, J.P. Vacanti, Tissue engineering, Science 260 (5110) (1993) 920–926, https://doi.org/10.1126/science.8493529.
[81] E. Calciolari, S. Corbella, N. Gkranias, M. Viganó, A. Sculean, N. Donos, Efficacy of biomaterials for lateral bone augmentation performed with guided bone regeneration. A network meta-analysis, Periodontol. 2000 93 (1) (2023) 77–106, https://doi.org/10.1111/prd.12531.
[82] R.E. Jung, G.A. Hälg, D.S. Thoma, C.H. Hämmerle, A randomized, controlled clinical trial to evaluate a new membrane for guided bone regeneration around dental implants, Clin. Oral Implants Res. 20 (2) (2009) 162–168, https://doi.org/10.1111/j.1600-0501.2008.01634.x.
[83] S. Bhagat, P. Jaiswal, P. Bajaj, S. Kotecha, G. Bhandari, Regenerative evaluation of collagen and an advanced platelet-rich fibrin membranes with deproteinized bovine bone matrix in infrabony defects: a randomized controlled trial, J. Contemp. Dent. Pract. 26 (6) (2025) 573–580, https://doi.org/10.5005/jp-journals-10024-3908.
[84] B. Wessing, I. Urban, E. Montero, W. Zechner, M. Hof, J. Alández Chamorro, N. Alández Martin, G. Polizzi, S. Meloni, M. Sanz, A multicenter randomized controlled clinical trial using a new resorbable non-cross-linked collagen membrane for guided bone regeneration at dehisced single implant sites: interim results of a bone augmentation procedure, Clin. Oral Implants Res. 28 (11) (2017) e218–e226, https://doi.org/10.1111/clr.12995.
[85] G. Mizraji, A. Davidzohn, M. Gursoy, U. Gursoy, L. Shapira, A. Wilensky, Membrane barriers for guided bone regeneration: an overview of available biomaterials, Periodontol. 2000 93 (1) (2023) 56–76, https://doi.org/10.1111/prd.12502.
[86] Y. Gao, S. Wang, B. Shi, Y. Wang, Y. Chen, X. Wang, E.-S. Lee, H.-B. Jiang, Advances in modification methods based on biodegradable membranes in guided bone/tissue regeneration: a review 14 (5) (2022) 871.
[87] Y.H. Jiang, Y.Y. Lou, T.H. Li, B.Z. Liu, K. Chen, D. Zhang, T. Li, Cross-linking methods of type I collagen-based scaffolds for cartilage tissue engineering, Am. J. Transl. Res. 14 (2) (2022) 1146–1159.
[88] H. Tal, A. Kozlovsky, Z. Artzi, C.E. Nemcovsky, O. Moses, Long-term bio-degradation of cross-linked and non-cross-linked collagen barriers in human guided bone regeneration, Clin. Oral Implants Res. 19 (3) (2008) 295–302, https://doi.org/10.1111/j.1600-0501.2007.01424.x.
[89] S. Abtahi, X. Chen, S. Shahabi, N. Nasiri, Resorbable membranes for guided bone regeneration: critical features, potentials, and limitations, ACS Mater. Au 3 (5) (2023) 394–417, https://doi.org/10.1021/acsmaterialsau.3c00013.
[90] J. Wang, L. Wang, Z. Zhou, H. Lai, P. Xu, L. Liao, J. Wei, Biodegradable polymer membranes applied in guided bone/tissue regeneration: a review, Polymers (Basel) 8 (4) (2016), https://doi.org/10.3390/polym8040115.
[91] M. Farokhi, F. Mottaghitalab, J. Ai, M.A. Shokrgozar, Sustained release of platelet-derived growth factor and vascular endothelial growth factor from silk/calcium phosphate/PLGA based nanocomposite scaffold, Int. J. Pharm. 454 (1) (2013) 216–225, https://doi.org/10.1016/j.ijpharm.2013.06.080.
[92] A. Emami, I.M. Oskouie, Smart biodegradable polymers for bone tissue engineering: advances, challenges, and future perspective, Polym. Adv. Technol. 36 (12) (2025) e70476, https://doi.org/10.1002/pat.70476.
[93] P. Gentile, V. Chiono, C. Tonda-Turo, A.M. Ferreira, G. Ciardelli, Polymeric membranes for guided bone regeneration, Biotechnol. J. 6 (10) (2011) 1187–1197, https://doi.org/10.1002/biot.201100294.
[94] P. Raz, T. Brosh, G. Ronen, H. Tal, Tensile properties of three selected collagen membranes, Biomed Res. Int. 2019 (2019) 5163603, https://doi.org/10.1155/2019/5163603.
[95] D. Yang, Z. Xu, D. Huang, Q. Luo, C. Zhang, J. Guo, L. Tan, L. Ge, C. Mu, D. Li, Immunomodulatory multifunctional janus collagen-based membrane for advanced bone regeneration, Nat. Commun. 16 (1) (2025) 4264, https://doi.org/10.1038/s41467-025-59651-z.
[96] X. Shi, X. Li, Y. Tian, X. Qu, S. Zhai, Y. Liu, W. Jia, Y. Cui, S. Chu, Physical, mechanical, and biological properties of collagen membranes for guided bone regeneration: a comparative in vitro study, BMC Oral Health 23 (1) (2023) 510, https://doi.org/10.1186/s12903-023-03223-4.
[97] J. Alarcón-Apablaza, K. Godoy-Sánchez, M. Jarpa-Parra, K. Garrido-Miranda, R. Fuentes, Tissue sources influence the morphological and morphometric characteristics of collagen membranes for guided bone regeneration, Polymers 16 (24) (2024) 3499.
[98] J. Caballé-Serrano, A. Munar-Frau, L. Delgado, R. Pérez, F. Hernández-Alfaro, Physicochemical characterization of barrier membranes for bone regeneration, J. Mech. Behav. Biomed. Mater. 97 (2019) 13–20, https://doi.org/10.1016/j.jmbbm.2019.04.053.
[99] E. Ortolani, F. Quadrini, D. Bellisario, L. Santo, A. Polimeni, A. Santarsiero, Mechanical qualification of collagen membranes used in dentistry, Ann. Ist. Super Sanita 51 (3) (2015) 229–235, https://doi.org/10.4415/ann_15_03_11.
[100] A.M. Tanneberger, S. Al-Maawi, C. Herrera-Vizcaíno, A. Orlowska, A. Kubesch, R. Sader, C.J. Kirkpatrick, S. Ghanaati, Multinucleated giant cells within the in vivo implantation bed of a collagen-based biomaterial determine its degradation pattern, Clin. Oral Invest. 25 (3) (2021) 859–873, https://doi.org/10.1007/s00784-020-03373-7.
[101] B. Gedik, M.A. Erdem, Electrospun PCL membranes for localized drug delivery and bone regeneration, BMC Biotechnol. 25 (1) (2025) 31, https://doi.org/10.1186/s12896-025-00965-7.
[102] X. Li, H. Lv, Y. Mou, W. Xiu, L. Han, Z. Chu, H. Dong, Engineering biomedical membranes for guided bone regeneration, Adv. Membr 7 (2026) 100215, https://doi.org/10.1016/j.advmem.2026.100215.
[103] C. Yuan, X. Ren, H. Ye, S. Jin, Y. Zuo, J. Li, Y. Li, Physicochemical and in vitro degradation behaviors of fibrous membranes with different polycaprolactone and gelatin proportions, J. Nanosci. Nanotechnol. 20 (12) (2020) 7376–7384, https://doi.org/10.1166/jnn.2020.18712.
[104] R. Shi, J. Xue, M. He, D. Chen, L. Zhang, W. Tian, Structure, physical properties, biocompatibility and in vitro/vivo degradation behavior of anti-infective polycaprolactone-based electrospun membranes for guided tissue/bone regeneration, Polym. Degrad. Stabil. 109 (2014) 293–306, https://doi.org/10.1016/j.polymdegradstab.2014.07.017.
[105] E. Zhang, C. Zhu, J. Yang, H. Sun, X. Zhang, S. Li, Y. Wang, L. Sun, F. Yao, Electrospun PDLLA/PLGA composite membranes for potential application in guided tissue regeneration, Mater. Sci. Eng., C 58 (2016) 278–285, https://doi.org/10.1016/j.msec.2015.08.032.
[106] F. Wang, Y. Wang, J. Sheng, K. Zhang, Y. Cao, X. Han, K. Yan, X. Wang, A dual-functional Janus nanofibrous membrane as an immunomodulatory barrier for periodontitis regeneration under diabetic conditions, Mater. Today Bio 37 (2026) 102869, https://doi.org/10.1016/j.mtbio.2026.102869.
[107] Y. Wu, S. Chen, P. Luo, S. Deng, Z. Shan, J. Fang, X. Liu, J. Xie, R. Liu, S. Wu, X. Wu, Z. Chen, K.W.K. Yeung, Q. Liu, Z. Chen, Optimizing the bio-degradability and biocompatibility of a biogenic collagen membrane through cross-linking and zinc-doped hydroxyapatite, Acta Biomater. 143 (2022) 159–172, https://doi.org/10.1016/j.actbio.2022.02.004.
[108] X. Zhao, X. Li, X. Xie, J. Lei, L. Ge, L. Yuan, D. Li, C. Mu, Controlling the pore structure of collagen sponge by adjusting the cross-linking degree for construction of heterogeneous double-layer bone barrier membranes, ACS Appl. Bio Mater. 3 (4) (2020) 2058–2067, https://doi.org/10.1021/acsabm.9b01175.
[109] X. Hu, Y. He, Y. Tong, N. Sun, G. Ma, H. Liu, N. Kou, Fabrication and characterization of a multi-functional GBR membrane of gelatin-chitosan for osteogenesis and angiogenesis, Int. J. Biol. Macromol. 266 (Pt 2) (2024) 130978, https://doi.org/10.1016/j.ijbiomac.2024.130978.
[110] S.L. Bee, Z.A.A. Hamid, Chitosan-based dental barrier membrane for periodontal guided tissue regeneration and guided bone regeneration: a review, Int. J. Biol. Macromol. 295 (2025) 139504, https://doi.org/10.1016/j.ijbiomac.2025.139504.
[111] S. Ghafouri, A.R. Sadeghi-avalshahr, A.M. Molavi, H. Hassanzadeh, Fabrication of functionally graded electrospun membranes based on silk fibroin for using as dental barrier membranes in guided bone regeneration, Fibers Polym. 23 (9) (2022) 2549–2556, https://doi.org/10.1007/s12221-022-4304-z.
[112] Y. Yin, X. Zhao, J. Xiong, Modeling analysis of silk fibroin/poly(ε-caprolactone) nanofibrous membrane under uniaxial tension, Nanomaterials 9 (8) (2019) 1149.
[113] S. Ouyang, X. Wu, L. Meng, X. Jing, L. Qiao, J. She, K. Zheng, X. Chen, F. Pan, More than the barrier effect: Biodegradable Mg-Ag alloy membranes for guided bone/tissue regeneration, J. Magnes. Alloys 12 (11) (2024) 4454–4467, https://doi.org/10.1016/j.jma.2024.03.022.
[114] K. Chen, L. Zhao, J. Sun, X. Gu, C. Huang, H. Su, Y. Fan, Utilizing biodegradable alloys as guided bone regeneration (GBR) membrane: feasibility and challenges, Sci. China Mater. 65 (10) (2022) 2627–2646, https://doi.org/10.1007/s40843-022-2118-3.
[115] X. Chu, Y. Dai, Z. Fu, J. Wang, J. Song, Z. Dong, Z. Tang, Y. Yan, K. Yu, Mechanical properties, biodegradation behavior and biocompatibility of novel Zn-based alloy membranes prepared by powder metallurgy for guided bone regeneration, Mater. Today Commun. 42 (2025) 111367, https://doi.org/10.1016/j.mtcomm.2024.111367.
[116] X. Chu, Z. Fu, Y. Liu, Y. Dai, J. Wang, J. Song, Z. Dong, Y. Yan, K. Yu, Mechanical properties, microstructure, degradation behavior, and biocompatibility of Zn-0.5Ti-0.5Fe and Zn-0.5Ti-0.5Mg guided bone regeneration barrier membranes prepared using a powder metallurgy method, ACS Biomater. Sci. Eng. 10 (10) (2024) 6520–6532, https://doi.org/10.1021/acsbiomaterials.4c01068.
[117] S. Wan, Y. Chen, C. Huang, Z. Huang, C. Liang, X. Deng, Q. Cheng, Scalable ultrastrong MXene films with superior osteogenesis, Nature 634 (8036) (2024) 1103–1110, https://doi.org/10.1038/s41586-024-08067-8.
[118] H. Zhou, Y. Zhao, X. Zha, Z. Zhang, L. Zhang, Y. Wu, R. Ren, Z. Zhao, W. Yang, L. Zhao, A Janus, robust, biodegradable bacterial cellulose/Ti(3)C(2)Tx MXene bilayer membranes for guided bone regeneration, Biomater. Adv. 161 (2024) 213892, https://doi.org/10.1016/j.bioadv.2024.213892.
[119] W. Qiu, K. Zhang, M. Wu, M. Fu, H. Wu, R. Tang, Z. Chen, J. Guo, F. Fang, Tri-layer citrate-based hydroxyapatite composite scaffold promoting osteogenesis and gingival tissue regeneration for periodontal bone defect repair, Adv. Healthcare Mater. 14 (13) (2025) e2501002, https://doi.org/10.1002/adhm.202501002.
[120] H. Xu, S. Yan, E. Gerhard, D. Xie, X. Liu, B. Zhang, D. Shi, G.A. Ameer, J. Yang, Citric acid: a nexus between cellular mechanisms and biomaterial innovations, Adv. Mater. 36 (32) (2024) e2402871, https://doi.org/10.1002/adma.202402871.
[121] G. Sui, X. Yang, F. Mei, X. Hu, G. Chen, X. Deng, S. Ryu, Poly-L-lactic acid/hydroxyapatite hybrid membrane for bone tissue regeneration, J. Biomed. Mater. Res. 82 (2) (2007) 445–454, https://doi.org/10.1002/jbm.a.31166.
[122] Z. Yang, C. Wu, H. Shi, X. Luo, H. Sun, Q. Wang, D. Zhang, Advances in barrier membranes for guided bone regeneration techniques, Front. Bioeng. Biotechnol. 10 (2022) 921576, https://doi.org/10.3389/fbioe.2022.921576.
[123] S. Tamburaci, F. Tihminlioglu, Development of Si doped nano hydroxyapatite reinforced bilayer chitosan nanocomposite barrier membranes for guided bone regeneration, Mater. Sci. Eng., C 128 (2021) 112298, https://doi.org/10.1016/j.msec.2021.112298.

[124] V.I. dos Santos, C. Merlini, Á. Aragones, K. Cesca, M.C. Fredel, In vitro evaluation of bilayer membranes of PLGA/hydroxyapatite/β-tricalcium phosphate for guided bone regeneration, Mater. Sci. Eng., C 112 (2020) 110849, https://doi.org/10.1016/j.msec.2020.110849.
[125] J. Liu, Q. Zou, B. Cai, J. Wei, C. Yuan, Y. Li, Heparin conjugated PCL/Gel — pcl/gel/n-ha bilayer fibrous membrane for potential regeneration of soft and hard tissues, J. Biomater. Sci. Polym. Ed. 31 (11) (2020) 1421–1436, https://doi.org/10.1080/09205063.2020.1760700.
[126] X. Deng, C. Yu, X. Zhang, X. Tang, Q. Guo, M. Fu, Y. Wang, K. Fang, T. Wu, A chitosan-coated PCL/nano-hydroxyapatite aerogel integrated with a nanofiber membrane for providing antibacterial activity and guiding bone regeneration, Nanoscale 16 (20) (2024) 9861–9874, https://doi.org/10.1039/D4NR00563E.
[127] N. Barnthip, J. Teeka, P. Kantha, S. Teepoo, W. Damjuti, Fabrication and characterization of polycaprolactone/cellulose acetate blended nanofiber mats containing sericin and fibroin for biomedical application, Sci. Rep. 12 (1) (2022) 22370, https://doi.org/10.1038/s41598-022-26908-2.
[128] H. Shi, Z. Zhou, W. Li, Y. Fan, Z. Li, J. Wei, Hydroxyapatite-based materials for bone tissue engineering: a brief and comprehensive introduction, Crystals 11 (2) (2021) 149.
[129] J. Russias, E. Saiz, S. Deville, K. Gryn, G. Liu, R.K. Nalla, A.P. Tomsia, Fabrication and in Vitro Characterization of three-dimensional organic/inorganic Scaffolds by Robocasting, 83A, 2007, pp. 434–445, https://doi.org/10.1002/jbm.a.31237, 2.
[130] A.G.B. Castro, M. Diba, M. Kersten, J.A. Jansen, J.J.J.P. van den Beucken, F. Yang, Development of a PCL-silica nanoparticles composite membrane for guided bone regeneration, Mater. Sci. Eng., C 85 (2018) 154–161, https://doi.org/10.1016/j.msec.2017.12.023.
[131] J.-H. Shim, J.-Y. Won, S.-J. Sung, D.-H. Lim, W.-S. Yun, Y.-C. Jeon, J.-B. Huh, Comparative efficacies of a 3D-printed PCL/PLGA/β-TCP membrane and a titanium membrane for guided bone regeneration in beagle dogs, Polymers 7 (10) (2015) 2061–2077.
[132] L. Han, J. Huang, Z. Zhang, G. Feng, Y. Zheng, Y. Zhu, H. Li, Restoration of periodontitis-induced bone defects with multifunctional barrier membranes by alleviating oxidative stress and remodelling macrophage metabolism, Chem. Eng. J. 523 (2025) 168205, https://doi.org/10.1016/j.cej.2025.168205.
[133] M. Ren, M. Li, A.R. Boccaccini, Y. Xu, L. Li, K. Zheng, Electrospinning of recombinant human-like collagen-reinforced PCL nanofibrous membranes using benign solvents for periodontal regeneration, Int. J. Biol. Macromol. 284 (2025) 137954, https://doi.org/10.1016/j.ijbiomac.2024.137954.
[134] J. Liu, Q. Zou, C. Wang, M. Lin, Y. Li, R. Zhang, Y. Li, Electrospinning and 3D printed hybrid bi-layer scaffold for guided bone regeneration, Mater. Des. 210 (2021) 110047, https://doi.org/10.1016/j.matdes.2021.110047.
[135] K. Ren, Y. Wang, T. Sun, W. Yue, H. Zhang, Electrospun PCL/gelatin composite nanofiber structures for effective guided bone regeneration membranes, Mater. Sci. Eng., C 78 (2017) 324–332, https://doi.org/10.1016/j.msec.2017.04.084.
[136] M.D. Shoulders, R.T. Raines, Collagen structure and stability, Annu. Rev. Biochem. 78 (2009) 929–958, https://doi.org/10.1146/annurev.biochem.77.032207.120833.
[137] Y. Qian, H. Chen, Y. Xu, J. Yang, X. Zhou, F. Zhang, N. Gu, The preosteoblast response of electrospinning PLGA/PCL nanofibers: effects of biomimetic architecture and collagen I, Int. J. Nanomed. 11 (2016) 4157–4171, https://doi.org/10.2147/ijn.S110577.
[138] S. Türkkan, A.E. Pazarçeviren, D. Keskin, N.E. Machin, Ö. Duygulu, A. Tezcaner, Nanosized CaP-silk fibroin-PCL-PEG-PCL/PCL based bilayer membranes for guided bone regeneration, Mater. Sci. Eng., C 80 (2017) 484–493, https://doi.org/10.1016/j.msec.2017.06.016.
[139] S.W. Tsai, W.X. Yu, P.A. Hwang, Y.W. Hsu, F.Y. Hsu, Fabrication and characteristics of PCL membranes containing strontium-substituted hydroxyapatite nanofibers for guided bone regeneration, Polymers (Basel) 11 (11) (2019) 1761, https://doi.org/10.3390/polym11111761.
[140] X. Han, F. Wang, Y. Ma, X. Lv, K. Zhang, Y. Wang, K. Yan, Y. Mei, X. Wang, TPG-functionalized PLGA/PCL nanofiber membrane facilitates periodontal tissue regeneration by modulating macrophages polarization via suppressing PI3K/AKT and NF-κB signaling pathways, Mater. Today Bio 26 (2024) 101036, https://doi.org/10.1016/j.mtbio.2024.101036.
[141] F. Peng, X. Zhang, Y. Wang, R. Zhao, Z. Cao, S. Chen, Y. Ruan, J. Wu, T. Song, Z. Qiu, X. Yang, Y. Zeng, X. Zhu, J. Pan, X. Zhang, Guided bone regeneration in long-bone defect with a bilayer mineralized collagen membrane, Coll. Leather 5 (1) (2023) 36, https://doi.org/10.1186/s42825-023-00144-4.
[142] Y. Tu, C. Chen, Y. Li, Y. Hou, M. Huang, L. Zhang, Fabrication of nano-hydroxyapatite/chitosan membrane with asymmetric structure and its applications in guided bone regeneration, Bio Med. Mater. Eng. 28 (3) (2017) 223–233, https://doi.org/10.3233/bme-171669.
[143] H.Y. Tai, S.H. Chou, L.P. Cheng, H.T. Yu, T.M. Don, Asymmetric composite membranes from chitosan and tricalcium phosphate useful for guided bone regeneration, J. Biomater. Sci. Polym. Ed. 23 (9) (2012) 1153–1170, https://doi.org/10.1163/092050611x576657.
[144] Y.H. Chen, H.Y. Tai, E. Fu, T.M. Don, Guided bone regeneration activity of different calcium phosphate/chitosan hybrid membranes, Int. J. Biol. Macromol. 126 (2019) 159–169, https://doi.org/10.1016/j.ijbiomac.2018.12.199.
[145] H. Zhang, J. Wu, Y. Wan, S. Romeis, J.D. Esper, W. Peukert, K. Zheng, A. R. Boccaccini, Bioactive glass flakes as innovative fillers in chitosan membranes for guided bone regeneration, Adv. Eng. Mater. 24 (4) (2022) 2101042, https://doi.org/10.1002/adem.202101042.
[146] E.J. Lee, D.S. Shin, H.E. Kim, H.W. Kim, Y.H. Koh, J.H. Jang, Membrane of hybrid chitosan-silica xerogel for guided bone regeneration, Biomaterials 30 (5) (2009) 743–750, https://doi.org/10.1016/j.biomaterials.2008.10.025.
[147] S. Tamburaci, F. Tihminlioglu, Diatomite reinforced chitosan composite membrane as potential scaffold for guided bone regeneration, Mater. Sci. Eng., C 80 (2017) 222–231, https://doi.org/10.1016/j.msec.2017.05.069.
[148] J. Xiang, Y. Li, M. Ren, P. He, F. Liu, Z. Jing, Y. Li, H. Zhang, P. Ji, S. Yang, Sandwich-like nanocomposite electrospun silk fibroin membrane to promote osteogenesis and antibacterial activities, Appl. Mater. Today 26 (2022) 101273, https://doi.org/10.1016/j.apmt.2021.101273.
[149] J. Xu, Y. Xia, H. Song, L. Wang, X. Zhang, J. Lian, Y. Zhang, X. Li, Y. Li, J. Kang, X. Wang, B. Zhao, Electrospun the oriented silk fibroin/bioactive glass @ silk fibroin/polycaprolactone composite bi-layered membranes for guided bone regeneration, Colloids Surf., A 676 (2023) 132224, https://doi.org/10.1016/j.colsurfa.2023.132224.
[150] S. Ghosh, F. Shajahan, J. Adhikari, A.K. Bera, A. Ghosh, F. Pati, Visible light cross-linked methacrylated silk fibroin enables enhanced osteogenic response in bioprinted dual-layer guided bone regeneration membrane, ACS Appl. Mater. Interfaces 17 (16) (2025) 23553–23574, https://doi.org/10.1021/acsami.4c22349.
[151] Q.Q. Wan, K. Jiao, Y.X. Ma, B. Gao, Z. Mu, Y.R. Wang, Y.H. Wang, L. Duan, K. H. Xu, J.T. Gu, J.F. Yan, J. Li, M.J. Shen, F.R. Tay, L.N. Niu, Smart, biomimetic periosteum created from the cerium(III, IV) oxide-mineralized eggshell membrane, ACS Appl. Mater. Interfaces 14 (12) (2022) 14103–14119, https://doi.org/10.1021/acsami.2c02079.
[152] A. Torres-Mansilla, M. Hincke, A. Voltes, E. López-Ruiz, P.A. Baldión, J. A. Marchal, P. Álvarez-Lloret, J. Gómez-Morales, Eggshell membrane as a biomaterial for bone regeneration, Polymers (Basel) 15 (6) (2023), https://doi.org/10.3390/polym15061342.
[153] F.F. Alotaibi, Z.M. AlFaltawi, S.R. Oyhanart, J.C. Knowles, F. D'Aiuto, D.Y. S. Chau, The eggshell membrane as a barrier membrane for guided bone regeneration, Regen. Med. 20 (7) (2025) 285–298, https://doi.org/10.1080/17460751.2025.2542056.
[154] L. Kalluri, J.A. Griggs, A.V. Janorkar, X. Xu, R. Chandran, H. Mei, K.P. Nobles, S. Yang, L. Alberto, Y. Duan, Preparation and optimization of an eggshell membrane-based biomaterial for GTR applications, Dent. Mater. 40 (4) (2024) 728–738, https://doi.org/10.1016/j.dental.2024.02.008.
[155] M. Lin, L. Fan, Y. Qiu, Z. Li, Y. Wang, X. Cai, W. Li, F.R. Tay, X. Huang, Polyethyleneimine-modified eggshell membrane for dual bone and periosteum regeneration: a multifunctional approach for guided bone healing, Acta Biomater. 203 (2025) 604–621, https://doi.org/10.1016/j.actbio.2025.07.044.
[156] S.A. M, S. Jaiswal, A. Dubey, D. Lahiri, A.K. Das, Biocompatibility and biodegradability evaluation of magnesium-based intramedullary bone implants in avian model, J. Biomed. Mater. Res. 109 (8) (2021) 1479–1489, https://doi.org/10.1002/jbm.a.37138.
[157] P. Rider, Ž.P. Kačarević, A. Elad, D. Tadic, D. Rothamel, G. Sauer, F. Bornert, P. Windisch, D.B. Hangyási, B. Molnar, E. Bortel, B. Hesse, F. Witte, Biodegradable magnesium barrier membrane used for guided bone regeneration in dental surgery, Bioact. Mater. 14 (2022) 152–168, https://doi.org/10.1016/j.bioactmat.2021.11.018.
[158] X. Shan, Y. Xu, S.K. Kolawole, L. Wen, Z. Qi, W. Xu, J. Chen, Degradable pure magnesium used as a barrier film for oral bone regeneration 13 (4) (2022) 298.
[159] J. Si, H. Shen, H. Miao, Y. Tian, H. Huang, J. Shi, G. Yuan, G. Shen, In vitro and in vivo evaluations of mg-zn-gd alloy membrane on guided bone regeneration for rabbit calvarial defect, J. Magnes. Alloys 9 (1) (2021) 281–291, https://doi.org/10.1016/j.jma.2020.09.013.
[160] Q. Luo, K. Gao, Y. Li, Z. Zhang, S. Chen, J. Zhou, Osteogenesis activity and porosity effect of biodegradable Mg-Ga alloys barrier membrane for guided bone regeneration: an in vitro and in vivo study in rabbits, Biomedicines 13 (8) (2025) 1940, https://doi.org/10.3390/biomedicines13081940.
[161] C. Zhai, W. Wang, A. Ma, H. Liu, T. Zhu, Y. Zhang, T. Yu, Z. Yang, J. Lan, Z. Wang, Laser powder bed fusion (LPBF) WE43 magnesium scaffold with EGCG/PDA-functionalized silk fibroin membrane for antibacterial osteoinductive guided bone regeneration, ACS Appl. Mater. Interfaces 17 (37) (2025) 51691–51706, https://doi.org/10.1021/acsami.5c11052.
[162] G. Tabanella, P. Rider, S. Rogge, M. Čandrlić, Ž.P. Kačarević, Open wound healing in guided bone regeneration using a magnesium membrane: a paradigm shift, J. Biomed. Mater. Res. 113 (9) (2025) e35642, https://doi.org/10.1002/jbm.b.35642.
[163] M. Frosecchi, Horizontal and vertical defect management with a novel degradable pure magnesium guided bone regeneration (GBR) membrane: a clinical case, Medicina (Kaunas) 59 (11) (2023) 2009, https://doi.org/10.3390/medicina59112009.
[164] M. Barbeck, L. Kühnel, F. Witte, J. Pissarek, C. Precht, X. Xiong, R. Krastev, N. Wegner, F. Walther, O. Jung, Degradation, bone regeneration and tissue response of an innovative volume stable magnesium-supported GBR/GTR barrier membrane 21 (9) (2020) 3098.
[165] Y. Su, I. Cockerill, Y. Wang, Y.X. Qin, L. Chang, Y. Zheng, D. Zhu, Zinc-based biomaterials for regeneration and therapy, Trends Biotechnol. 37 (4) (2019) 428–441, https://doi.org/10.1016/j.tibtech.2018.10.009.
[166] A. Abdal-Hay, E. Xiang, Y. Ali, J. Xu, Y.K. Kim, Environment-dependent degradation pathways of pure zinc induced by acid-alkali surface chemistry, RSC Adv. 16 (22) (2026) 20433–20447, https://doi.org/10.1039/d6ra00345a.
[167] H. Yang, B. Jia, Z. Zhang, X. Qu, G. Li, W. Lin, D. Zhu, K. Dai, Y. Zheng, Alloying design of biodegradable zinc as promising bone implants for load-bearing applications, Nat. Commun. 11 (1) (2020) 401, https://doi.org/10.1038/s41467-019-14153-7.
[168] K. Liu, Y. Hamiti, S. Wang, A. Yalikun, J. Du, K. Duan, J. Liu, Y. Liu, A. Yusufu, Biocompatibility and osteoinductivity of biodegradable zn-li-ca ternary alloys for

bone regeneration: in vitro and in vivo studies, J. Alloys Compd. 1002 (2024) 175396, https://doi.org/10.1016/j.jallcom.2024.175396.
[169] P. Li, J. Dai, E. Schweizer, F. Rupp, A. Heiss, A. Richter, U.E. Klotz, J. Geis-Gerstorfer, L. Scheideler, D. Alexander, Response of human periosteal cells to degradation products of zinc and its alloy, Mater. Sci. Eng., C 108 (2020) 110208, https://doi.org/10.1016/j.msec.2019.110208.
[170] X.-M. Li, Z.-Z. Shi, A. Tuoliken, W. Gou, C.-H. Li, L.-N. Wang, Highly plastic Zn-0.3Ca alloy for guided bone regeneration membrane: breaking the trade-off between antibacterial ability and biocompatibility, Bioact. Mater. 42 (2024) 550–572, https://doi.org/10.1016/j.bioactmat.2024.08.049.
[171] K. Chen, P. Li, Q. Guan, X. Gu, L. Zhao, L. Huang, C. Huang, Y. Qin, C. Yu, T. Zhang, H. Li, Y. Huang, Y. Zheng, Biodegradable zinc-based alloys for guided bone regeneration membranes: feasibility, current status, and future prospects, Adv. Sci. (Weinh.) 12 (40) (2025) e06513, https://doi.org/10.1002/advs.202506513.
[172] X. Huang, M.-C. Zhao, Q. Yin, J. Yao, Y.-C. Zhao, D. Yin, R. Zeng, K. Yang, C. Wen, A. Atrens, Insights into biodegradable Mn-incorporated Fe-based scaffolds in orthopedics: bridging manufacturing techniques, physicomechanical properties, and multifunctional bioapplications, Int. J. Extrem. Manuf. 8 (1) (2026) 012011, https://doi.org/10.1088/2631-7990/ae09e0.
[173] K.N. Alagarsamy, L.R. Saleth, S. Sekaran, L. Fusco, L.G. Delogu, M. Pogorielov, A. Yilmazer, S. Dhingra, MXenes as emerging materials to repair electroactive tissues and organs, Bioact. Mater. 48 (2025) 583–608, https://doi.org/10.1016/j.bioactmat.2025.01.035.
[174] K. Rasool, K.A. Mahmoud, D.J. Johnson, M. Helal, G.R. Berdiyorov, Y. Gogotsi, Efficient antibacterial membrane based on two-dimensional Ti(3)C(2)T(x) (MXene) nanosheets, Sci. Rep. 7 (1) (2017) 1598, https://doi.org/10.1038/s41598-017-01714-3.
[175] S. Iravani, R.S. Varma, MXenes and MXene-based materials for tissue engineering and regenerative medicine: recent advances, Mater. Adv. 2 (9) (2021) 2906–2917, https://doi.org/10.1039/d1ma00189b.
[176] F. Damiri, M.H. Rahman, M. Zehravi, A.A. Awaji, M.Z. Nasrullah, H.A. Gad, M. Z. Bani-Fwaz, R.S. Varma, M.O. Germoush, H.S. Al-malky, A.A. Sayed, S. Rojekar, M.M. Abdel-Daim, M. Berrada, MXene (Ti3C2Tx)-embedded nanocomposite hydrogels for biomedical applications: a review 15 (5) (2022) 1666.
[177] S. Kumar, S.M. Zain Mehdi, M. Taunk, S. Kumar, A. Aherwar, S. Singh, T. Singh, Synergistic effects of polymer integration on the properties, stability, and applications of MXenes, J. Mater. Chem. A 13 (16) (2025) 11050–11113, https://doi.org/10.1039/D4TA08094G.
[178] Y. Yu, Z. You, X. Li, F. Lou, D. Xiong, L. Ye, Z.J.A.a.m. Wang, Interfaces, Injectable nanocomposite hydrogels with strong antibacterial, osteoinductive, and ROS-scavenging capabilities for Periodontitis Treatment, ACS Appl. Mater. Interfaces 16 (12) (2024) 14421–14433.
[179] C. Shuai, X. Long, B. Sun, T. He, X. Shuai, G. Wang, S. Peng, Photothermal and photodynamic synergistic effect of the MXene/SnS_2 heterojunction endows the poly(L-lactic acid) scaffold with antibacterial activity, ACS Appl. Polym. Mater. 6 (13) (2024) 7827–7839, https://doi.org/10.1021/acsapm.4c01336.
[180] J. Zhang, Y. Fu, A. Mo, Multilayered titanium carbide MXene film for guided bone regeneration, Int. J. Nanomed. 14 (2019) 10091–10103, https://doi.org/10.2147/ijn.S227830.
[181] S. Zhang, L. Huang, M. Bian, L. Xiao, D. Zhou, Z. Tao, Z. Zhao, J. Zhang, L. B. Jiang, Y. Li, Multifunctional bone regeneration membrane with flexibility, electrical stimulation activity and osteoinductive activity, Small 20 (47) (2024) e2405311, https://doi.org/10.1002/smll.202405311.
[182] R.T. Tran, J. Yang, G.A. Ameer, Citrate-based biomaterials and their applications in regenerative engineering, Annu. Rev. Mater. Res. 45 (2015) 277–310, https://doi.org/10.1146/annurev-matsci-070214-020815.
[183] J. Yang, A.R. Webb, S.J. Pickerill, G. Hageman, G.A. Ameer, Synthesis and evaluation of poly(diol citrate) biodegradable elastomers, Biomaterials 27 (9) (2006) 1889–1898, https://doi.org/10.1016/j.biomaterials.2005.05.106.
[184] Y. Wang, S. Yan, X. Tan, E. Gerhard, H. Xu, H. Jiang, J. Yang, The genesis of citrated ultrathin hydroxyapatite nanorods, Sci. Adv. 12 (3) (2026), https://doi.org/10.1126/sciadv.aeb6538 eaeb6538.
[185] H. Xu, X. Tan, E. Gerhard, H. Zhang, R. Ray, Y. Wang, S.R. Kothapalli, E.B. Rizk, A.D. Armstrong, S. Yan, J. Yang, Metabotissugenic citrate biomaterials orchestrate bone regeneration via citrate-mediated signaling pathways, Sci. Adv. 11 (30) (2025) eady2862, https://doi.org/10.1126/sciadv.ady2862.
[186] Y.Y. Hu, A. Rawal, K. Schmidt-Rohr, Strongly bound citrate stabilizes the apatite nanocrystals in bone, Proc. Natl. Acad. Sci. U. S. A. 107 (52) (2010) 22425–22429, https://doi.org/10.1073/pnas.1009219107.
[187] P. Li, J. Chen, F. Schmidt, J. Dai, J. Li, S. Xu, A. Li, Z. Yu, F. Witte, Magnesium-based barrier membrane for guided bone regeneration: from bedside to bench and back again, Biomaterials 328 (2026) 123783, https://doi.org/10.1016/j.biomaterials.2025.123783.
[188] B. Wang, C. Feng, Y. Liu, F. Mi, J. Dong, Recent advances in biofunctional guided bone regeneration materials for repairing defective alveolar and maxillofacial bone: a review, Jpn Dent. Sci. Rev. (2022) 233–248, https://doi.org/10.1016/j.jdsr.2022.07.002.
[189] I.B. Leonor, A.I. Rodrigues, R.L. Reis, 13 — designing biomaterials based on biomineralization for bone repair and regeneration, in: C. Aparicio, M.-P. Ginebra (Eds.), Biomineralization and Biomaterials, Woodhead Publishing, Boston, 2016, pp. 377–404.
[190] J. Wang, Q. Liu, Z. Guo, H. Pan, Z. Liu, R. Tang, Progress on biomimetic mineralization and materials for hard tissue regeneration, ACS Biomater. Sci. Eng. 9 (4) (2023) 1757–1773, https://doi.org/10.1021/acsbiomaterials.1c01070.
[191] P. Pan, J. Wang, X. Wang, X. Yu, T. Chen, C. Jiang, W. Liu, Barrier membrane with Janus function and structure for guided bone regeneration, ACS Appl. Mater. Interfaces 16 (36) (2024) 47178–47191, https://doi.org/10.1021/acsami.4c08737.
[192] K.-R. Zhang, H.-L. Gao, X.-F. Pan, P. Zhou, X. Xing, R. Xu, Z. Pan, S. Wang, Y. Zhu, B. Hu, D. Zou, S.-H. Yu, Multifunctional bilayer nanocomposite guided bone regeneration membrane, Matter 1 (3) (2019) 770–781, https://doi.org/10.1016/j.matt.2019.05.021.
[193] Y. Chen, H. Tang, Y. Zhang, L. Wang, J. Zhu, L. Wang, A. Li, X. Zeng, B. Yin, Y. Liang, X. Dong, Q. Bai, Z. Pan, L. Wang, L. Zhang, M. Yang, Y. She, W. Sun, K. Zhang, C. Chen, Multiplexed self-adaptable Janus hydrogels rescue epithelial malfunction to promote complete trachea repair, Nat. Commun. 16 (1) (2025) 5734, https://doi.org/10.1038/s41467-025-61135-z.
[194] Y. Jiang, C. Zhu, X. Ma, D.J.B.s. Fan, Janus hydrogels: merging boundaries in tissue engineering for enhanced biomaterials and regenerative therapies, Biomater. Sci. 12 (10) (2024) 2504–2520, https://doi.org/10.1039/d3bm01875j.
[195] M. Yang, M. Zuo, R. Yang, K. Zhang, R. Jia, B. Yin, Y. Wang, M. Liu, W. Fang, H. Guo, Y. Jin, Q. Fu, K. Zhang, Dynamically urethra-adapted and obligations-oriented trilayer hydrogels integrate scarless urethral repair, Nat. Commun. 16 (1) (2025) 7333, https://doi.org/10.1038/s41467-025-62851-2.
[196] H.C. Yang, J. Hou, V. Chen, Z.K. Xu, Janus membranes: exploring duality for advanced separation, Angew Chem. Int. Ed. Engl. 55 (43) (2016) 13398–13407, https://doi.org/10.1002/anie.201601589.
[197] J. Lin, Y. He, Y. He, Y. Feng, X. Wang, L. Yuan, Y. Wang, J. Chen, F. Luo, Z. Li, J. Li, H. Tan, Janus functional electrospun polyurethane fibrous membranes for periodontal tissue regeneration, J. Mater. Chem. B 11 (38) (2023) 9223–9236, https://doi.org/10.1039/D3TB01407J.
[198] C. Lai, M. Cheng, C. Ning, Y. He, Z. Zhou, Z. Yin, P. Zhu, Y. Xu, P. Yu, S. Xu, Janus electro-microenvironment membrane with surface-selective osteogenesis/gingival healing ability for guided bone regeneration, Mater. Today Bio 17 (2022) 100491, https://doi.org/10.1016/j.mtbio.2022.100491.
[199] A. Nugud, D. Sandeep, A.T. El-Serafi, Two faces of the coin: Minireview for dissecting the role of reactive oxygen species in stem cell potency and lineage commitment, J. Adv. Res. 14 (2018) 73–79, https://doi.org/10.1016/j.jare.2018.05.012.
[200] L. Fu, Z. Wang, S. Dong, Y. Cai, Y. Ni, T. Zhang, L. Wang, Y. Zhou, Bilayer poly (lactic-co-glycolic acid)/nano-hydroxyapatite membrane with barrier function and osteogenesis promotion for guided bone regeneration, Materials 10 (3) (2017), https://doi.org/10.3390/ma10030257.
[201] D. Atila, S. Gurses, A. Tezcaner, Self-composite silk fibroin membranes for guided bone regeneration: 1 material 3 architectures with intrinsic integrity, Mater. Today Commun. 39 (2024) 109215, https://doi.org/10.1016/j.mtcomm.2024.109215.
[202] J.H. Shim, J.H. Jeong, J.Y. Won, J.H. Bae, G. Ahn, H. Jeon, W.S. Yun, E.B. Bae, J. W. Choi, S.H. Lee, C.M. Jeong, H.Y. Chung, J.B. Huh, Porosity effect of 3D-printed polycaprolactone membranes on calvarial defect model for guided bone regeneration, Biomed. Mater. 13 (1) (2017) 015014, https://doi.org/10.1088/1748-605X/aa9bbc.
[203] Y. Li, Y. Lin, T. Xiao, W. Liu, C. Ning, G. Tan, L. Zhou, Recent advances in dual-function Janus membranes for guided periodontal and bone regeneration, Adv. Healthcare Mater. 14 (28) (2025) e2502888, https://doi.org/10.1002/adhm.202502888.
[204] P. Li, Y. Li, T. Kwok, T. Yang, C. Liu, W. Li, X. Zhang, A bi-layered membrane with micro-nano bioactive glass for guided bone regeneration, Colloids Surf. B Biointerfaces 205 (2021) 111886, https://doi.org/10.1016/j.colsurfb.2021.111886.
[205] X. Wen, J. Xiong, S. Lei, L. Wang, X. Qin, Diameter refinement of electrospun nanofibers: from mechanism, strategies to applications, Adv. Fiber Mater. 4 (2) (2022) 145–161, https://doi.org/10.1007/s42765-021-00113-8.
[206] Y.F. Ma, X.Z. Yan, Periodontal guided tissue regeneration membranes: limitations and possible solutions for the bottleneck analysis, Tissue Eng., Part B 29 (5) (2023) 532–544, https://doi.org/10.1089/ten.TEB.2023.0040.
[207] Y. Wang, Y. Jiang, Y. Zhang, S. Wen, Y. Wang, H. Zhang, Dual functional electrospun core-shell nanofibers for anti-infective guided bone regeneration membranes, Mater. Sci. Eng., C 98 (2019) 134–139, https://doi.org/10.1016/j.msec.2018.12.115.
[208] R. Jiao, X. Lin, J. Wang, C. Zhu, J. Hu, H. Gao, K. Zhang, 3D-printed constructs deliver bioactive cargos to expedite cartilage regeneration, J. Pharm. Anal. 14 (12) (2024) 100925, https://doi.org/10.1016/j.jpha.2023.12.015.
[209] S. Jin, F. Sun, Q. Zou, J. Huang, Y. Zuo, Y. Li, S. Wang, L. Cheng, Y. Man, F. Yang, J. Li, Fish fish collagen and hydroxyapatite reinforced poly(lactide-co-glycolide) fibrous membrane for guided bone regeneration, Biomacromolecules 20 (5) (2019) 2058–2067, https://doi.org/10.1021/acs.biomac.9b00267.
[210] S. Yuan, Y. Feng, H. Wang, S.M. Chen, J.H. Li, Y.B. Zhu, S.H. Yu, Z. Wang, Sword and board in one: a bioinspired nanocomposite membrane for guided bone regeneration, Adv. Mater. 37 (37) (2025) e2504577, https://doi.org/10.1002/adma.202504577.
[211] I.B. Darby, K.H. Morris, A Systematic Review of the Use of Growth Factors in Human Periodontal Regeneration, 84, 2013, pp. 465–476, https://doi.org/10.1902/jop.2012.120145, 4.
[212] T.-M. De Witte, L.E. Fratila-Apachitei, A.A. Zadpoor, N.A. Peppas, Bone tissue engineering via growth factor delivery: from scaffolds to complex matrices, Regener, Biomater 5 (4) (2018) 197–211, https://doi.org/10.1093/rb/rby013.
[213] Y.L. Chao, T.M. Wang, H.H. Chang, L.D. Lin, Effects of low-dose rhBMP-2 on peri-implant ridge augmentation in a canine model, J. Clin. Periodontol. 48 (5) (2021) 734–744, https://doi.org/10.1111/jcpe.13440.

[214] E.J. Lee, H.E. Kim, Accelerated bony defect healing by chitosan/silica hybrid membrane with localized bone morphogenetic protein-2 delivery, Mater. Sci. Eng., C 59 (2016) 339–345, https://doi.org/10.1016/j.msec.2015.10.001.
[215] J.H. Lee, Y.J. Lee, H.J. Cho, D.W. Kim, H. Shin, The incorporation of bFGF mediated by heparin into PCL/gelatin composite fiber meshes for guided bone regeneration, Drug Deliv. Transl. 5 (2) (2015) 146–159, https://doi.org/10.1007/s13346-013-0154-y.
[216] X. Lu, S. Sun, N. Li, S. Hu, Y. Pan, L. Wang, X. Zhou, H. Chen, F. Zhang, Janus sponge/electrospun fibre composite combined with EGF/bFGF/CHX promotes reconstruction in oral tissue regeneration, Colloids Surf., B: B, Biointerf. 243 (2024) 114117, https://doi.org/10.1016/j.colsurfb.2024.114117.
[217] Y.J. Lee, J.H. Lee, H.J. Cho, H.K. Kim, T.R. Yoon, H. Shin, Electrospun fibers immobilized with bone forming peptide-1 derived from BMP7 for guided bone regeneration, Biomaterials 34 (21) (2013) 5059–5069, https://doi.org/10.1016/j.biomaterials.2013.03.051.
[218] A.P. Kusumbe, S.K. Ramasamy, R.H. Adams, Coupling of angiogenesis and osteogenesis by a specific vessel subtype in bone, Nature 507 (7492) (2014) 323–328, https://doi.org/10.1038/nature13145.
[219] S. Stegen, N. van Gastel, G. Carmeliet, Bringing new life to damaged bone: the importance of angiogenesis in bone repair and regeneration, Bone 70 (2015) 19–27, https://doi.org/10.1016/j.bone.2014.09.017.
[220] D.D. Dou, G. Zhou, H.W. Liu, J. Zhang, M.L. Liu, X.F. Xiao, J.J. Fei, X.L. Guan, Y. B. Fan, Sequential releasing of VEGF and BMP-2 in hydroxyapatite collagen scaffolds for bone tissue engineering: design and characterization, Int. J. Biol. Macromol. 123 (2019) 622–628, https://doi.org/10.1016/j.ijbiomac.2018.11.099.
[221] K. Zhang, H. Li, T. Wang, F. Li, Z. Xie, H. Luo, X. Zhu, P. Kang, Q. Kang, Z. fei, W. Peng, Mechanisms of bone regeneration repair and potential and efficacy of small molecule drugs, Biomed. Pharmacother. 187 (2025) 118070, https://doi.org/10.1016/j.biopha.2025.118070.
[222] X. Cheng, N. Xu, H. Wu, X. Pan, Y. Zhao, X. Chen, Y. Su, Y. Wei, Q. Jiang, J. Fan, Y. Jiang, Q. Yi, P. Gu, X. Gao, L. Han, J. Li, Y. Bai, A Coordinated Cascade Therapy-based Janus Fibrous Membrane Drives Bone Regeneration Through Mediating the Transformation of Energy Metabolism Pathway, 35, 2025 2423212, https://doi.org/10.1002/adfm.202423212, 23.
[223] Q. Wang, Y. Zhang, B. Li, L. Chen, Controlled dual delivery of low doses of BMP-2 and VEGF in a silk fibroin–nanohydroxyapatite scaffold for vascularized bone regeneration, J. Mater. Chem. B 5 (33) (2017) 6963–6972, https://doi.org/10.1039/C7TB00949F.
[224] Q. Yao, Y. Liu, B. Selvaratnam, R.T. Koodali, H. Sun, Mesoporous silicate nanoparticles/3D nanofibrous scaffold-mediated dual-drug delivery for bone tissue engineering, J. Contr. Release 279 (2018) 69–78, https://doi.org/10.1016/j.jconrel.2018.04.011.
[225] J. Lu, N. Yu, X. Zhang, Y. Wu, D. Fan, L. Zhen, Injectable thermosensitive hydrogel-loaded exosomes promote diabetic periodontal bone regeneration through mitochondrial function regulation, Chem. Eng. J. 519 (2025) 164950, https://doi.org/10.1016/j.cej.2025.164950.
[226] Y. Lu, Z. Mai, L. Cui, X. Zhao, Engineering exosomes and biomaterial-assisted exosomes as therapeutic carriers for bone regeneration, Stem Cell Res. Ther. 14 (1) (2023) 55, https://doi.org/10.1186/s13287-023-03275-x.
[227] S. Ma, Y. Zhao, Y. Yang, Y. Mu, L. Zhang, J. Wu, R. Li, X. Bian, P. Wei, W. Jing, B. Zhao, Z. Liu, J. Deng, Asymmetric SIS membranes specifically loaded with exosomes through the modification of engineered recombinant peptides for guide bone regeneration, Compos Part B 232 (2022) 109571, https://doi.org/10.1016/j.compositesb.2021.109571.
[228] Y. Zhang, Y. Wang, X. Ning, G. Yue, W. Zhang, Y. Chen, X. Jia, Y. Zhang, X. Zhang, Z. Lu, S. Zhu, F. Liu, Y. Zhao, L. Kong, Guided Bone Regeneration Membrane Materials Loaded with Chimeric Nanovesicles Promote Early Bone Defect Regeneration, 14, 2025 e01323, https://doi.org/10.1002/adhm.202501323, 32.
[229] Z. Wen, S. Li, Y. Liu, X. Liu, H. Qiu, Y. Che, L. Bian, M. Zhou, An engineered M2 macrophage-derived exosomes-loaded electrospun biomimetic periosteum promotes cell recruitment, immunoregulation, and angiogenesis in bone regeneration, Bioact. Mater. 50 (2025) 95–115, https://doi.org/10.1016/j.bioactmat.2025.03.027.
[230] W.-H. Zhou, Y.-F. Li, A bi-layered asymmetric membrane loaded with demineralized dentin matrix for guided bone regeneration, J. Mech. Behav. Biomed. Mater. 149 (2024) 106230, https://doi.org/10.1016/j.jmbbm.2023.106230.
[231] Y. Hazehara-Kunitomo, E.S. Hara, M. Ono, K.T. Aung, K. Komi, H.T. Pham, K. Akiyama, M. Okada, T. Oohashi, T. Matsumoto, T. Kuboki, Acidic Pre-conditioning enhances the stem cell phenotype of human bone marrow stem/progenitor cells, Int. J. Mol. Sci. 20 (5) (2019), https://doi.org/10.3390/ijms20051097.
[232] T. Zhu, H. Zhou, X. Chen, Y. Zhu, Recent advances of responsive scaffolds in bone tissue engineering, Front. Bioeng. Biotechnol. 11 (2023) 1296881, https://doi.org/10.3389/fbioe.2023.1296881.
[233] X. Gao, Q. Wang, L. Ren, P. Gong, M. He, W. Tian, W. Zhao, Metal-phenolic networks as a novel filler to advance multi-functional immunomodulatory biocomposites, Chem. Eng. J. 426 (2021) 131825, https://doi.org/10.1016/j.cej.2021.131825.
[234] M.A. Al-Baadani, K. Cai, H. Luo, G. Li, Y. Yuan, X. Shen, J. Liu, X. Zheng, P. Ma, In situ synthesized Van-ZIF-8 functionalized electrospun PCL membrane with pH-responsive dual functionality for oral guided bone regeneration, J. Mater. Sci. Mater. 37 (1) (2026) 22, https://doi.org/10.1007/s10856-025-06996-y.
[235] J.R. Martin, M.T. Howard, S. Wang, A.G. Berger, P.T. Hammond, Oxidation-responsive, tunable growth factor delivery from polyelectrolyte-coated implants, Adv. Healthcare Mater. 10 (9) (2021) e2001941, https://doi.org/10.1002/adhm.202001941.
[236] K. Zhu, R. Li, S. Yin, F. Yang, Y. Sun, Y. Xing, Y. Yang, W. Xu, Y. Yu, A novel ultrasound-driven piezoelectric GBR membrane dispersed with boron nitride nanotubes promotes bone regeneration and anti-bacterial properties, Mater. Today Bio 30 (2025) 101418, https://doi.org/10.1016/j.mtbio.2024.101418.
[237] K. Ma, C. Liao, L. Huang, R. Liang, J. Zhao, L. Zheng, W. Su, Electrospun PCL/MoS_2 nanofiber membranes combined with NIR-triggered photothermal therapy to accelerate bone regeneration, Small 17 (51) (2021) 2104747, https://doi.org/10.1002/smll.202104747.
[238] D. Li, Y. Wang, Y. Tian, Y. Zheng, J. Lv, C. Zhang, Electro-controlled assembled of biphasic guided bone regeneration membrane for healing of diabetic periodontal bone defects, J. Nanobiotechnol. 24 (1) (2026) 289, https://doi.org/10.1186/s12951-026-04224-5.
[239] B. Tandon, J.R. Aguilar Cosme, R. Xue, K. Srirussamee, J. Aguilar-Tadeo, C. Ballestrem, J.J. Blaker, S.H. Cartmell, Co-stimulation with piezoelectric PVDF films and low intensity pulsed ultrasound enhances osteogenic differentiation, Mat. Sci. Eng. C-Mater. 173 (2025) 214283, https://doi.org/10.1016/j.bioadv.2025.214283.
[240] K. Li, J. Song, Y. Lu, D. Zhang, Y. Wang, X. Wang, Y. Tang, Y. Yu, X. Zhang, X. Yang, Q. Cai, Biodegradable piezoelectric Janus membrane enabling dual antibacterial and osteogenic functions for periodontitis therapy, ACS Appl. Mater. Interfaces 17 (16) (2025) 23707–23721, https://doi.org/10.1021/acsami.5c02557.
[241] Y. Zhou, Z. Jiao, H. Zhang, G. Zhao, Z. Zhao, C. Li, P. Zhang, L. Zhao, Y. Zhao, G. Wu, Collagen-enhanced piezoelectric PLLA/ZnO microfiber barrier membranes for superior bone regeneration, Int. J. Biol. Macromol. 319 (2025) 145443, https://doi.org/10.1016/j.ijbiomac.2025.145443.
[242] M. Ali, M.J. Bathaei, E. Istif, S. Karimi, L. Beker, Biodegradable piezoelectric polymers: recent advancements in materials and applications, Adv. Healthcare Mater. 12 (2023) e2300318, https://doi.org/10.1002/adhm.202300318.
[243] S. Olhan, B. Antil, P. Maimí, B.K. Behera, Advances in 4D printing of polymeric composite smart materials, Compos. Struct. 377 (2026) 119859, https://doi.org/10.1016/j.compstruct.2025.119859.
[244] Z. Wang, D. Ma, J. Liu, S. Xu, F. Qiu, L. Hu, Y. Liu, C. Ke, C. Ruan, 4D printing polymeric biomaterials for adaptive tissue regeneration, Bioact. Mater. 48 (2025) 370–399, https://doi.org/10.1016/j.bioactmat.2025.01.033.
[245] M.A. Yousefi, D. Rahmatabadi, M. Ahmadi, A. Bayati, M. Baniassadi, A. Laachachi, V.V. Silberschmidt, D. George, M. Baghani, 4D printing for minimally invasive biomedical applications: programmable smart materials for deployable devices, drug delivery, and tissue regeneration, Mater. Des. 263 (2026) 115555, https://doi.org/10.1016/j.matdes.2026.115555.
[246] J. Chen, C. Virrueta, S. Zhang, C. Mao, J. Wang, 4D printing: the spotlight for 3D printed smart materials, Mater. Today 77 (2024) 66–91, https://doi.org/10.1016/j.mattod.2024.06.004.
[247] D. You, G. Chen, C. Liu, X. Ye, S. Wang, M. Dong, M. Sun, J. He, X. Yu, G. Ye, Q. Li, J. Wu, J. Wu, Q. Zhao, T. Xie, M. Yu, H. Wang, 4D printing of multi-responsive membrane for accelerated in vivo bone healing via remote regulation of stem cell fate, Adv. Funct. Mater. 31 (40) (2021) 2103920, https://doi.org/10.1002/adfm.202103920.
[248] R. Du, B. Zhao, K. Luo, M.-X. Wang, Q. Yuan, L.-X. Yu, K.-K. Yang, Y.-Z. Wang, Shape memory polyester scaffold promotes bone defect repair through enhanced osteogenic ability and mechanical stability, ACS Appl. Mater. Interfaces 15 (36) (2023) 42930–42941, https://doi.org/10.1021/acsami.3c06902.
[249] ISO, Biological Evaluation of Medical Devices – Part 5: Tests for in Vitro Cytotoxicity, 2009.
[250] K. Singh, ISO 14155: clinical investigation of medical devices for human subjects, in: P.S. Timiri Shanmugam, P. Thangaraju, N. Palani, T. Sampath (Eds.), Medical Device Guidelines and Regulations Handbook, Springer International Publishing, Cham, 2022, pp. 1–18.
[251] P. European, U. Council, Of the European, Regulation (EU) 2017/745 on medical devices, Off. J. Eur. Union L 117 (2017) 1–175.
[252] Unique Device Identifier (UDI) Requirements for Combination Products, Draft Guidance for Industry and FDA Staff, U.S. Food and Drug Administration (FDA), Silver Spring, MD, 2025.
[253] Purpose and Content of Use-Related Risk Analyses for Drugs, Biological Products, and Combination Products, Draft Guidance for Industry and FDA Staff, U.S. Food and Drug Administration, Silver Spring, MD, 2024.
[254] N.M.P. Administration, Notice on matters concerning the registration of drug-device combination products (No. 52 [2021]). https://www.nmpa.gov.cn/xxgk/fgwj/xzhgfxwj/20210727154135199.html, 2021. (Accessed 23 July 2021).
[255] N.M.P.A. Center for Medical Device Evaluation, Guidelines for the Registration Review of Oral Repair Membranes, 2025. Announcement No. 6 of 2025.
[256] J.C. Ng, P.S.Q. Yeoh, F. Muhamad, X. Zhao, S. Wu, X. Wu, K.W. Lai, Advancing biomaterial research with artificial intelligence, Mat. Sci. Eng. C-Mater. 180 (2026) 214535, https://doi.org/10.1016/j.bioadv.2025.214535.
[257] S. Fan, Y. Ge, B. Li, P. Liu, X. Liu, Advancements in microfluidic organ-on-a-chip for oral medicine, Int. Dent. J. 75 (5) (2025) 100925, https://doi.org/10.1016/j.identj.2025.100925.
[258] M. Liu, Y. Zhou, X. Mei, Z. Yu, B. Guan, Y. Xiao, S. Liu, H. Wang, Y. Qin, AI-driven biomaterial design: an intelligent closed loop from reverse design to biological response, Front. Cell Dev. Biol. 13 (2025) 1755565, https://doi.org/10.3389/fcell.2025.1755565.

[259] H. Liao, S. Hu, H. Yang, L. Wang, S. Tanaka, I. Takigawa, W. Li, H. Fan, J.P. Gong, Data-driven de novo design of super-adhesive hydrogels, Nature 644 (8075) (2025) 89–95, https://doi.org/10.1038/s41586-025-09269-4.
[260] Y. Wu, C. Wang, X. Shen, Y. Chen, H. Wang, B. Xu, Z. Zhu, Y. Chen, W. Dai, Y. Huang, L. Zou, J. Ji, P. Zhang, Iterative discovery of potent polymeric antibiotics via multi-stage and multi-task learning against antimicrobial resistance, Nat. Commun. 17 (1) (2026) 1878, https://doi.org/10.1038/s41467-026-68682-z.
[261] L.Y. Sujeeun, I.C. Phul, N. Goonoo, N.A. Kotov, A. Bhaw-Luximon, Predicting inflammatory response of biomimetic nanofibre scaffolds for tissue regeneration using machine learning and graph theory, J. Mater. Chem. B 13 (10) (2025) 3304–3318, https://doi.org/10.1039/d4tb02494j.
[262] Z. Meng, B. Gu, C. Yao, J. Li, K. Yu, Y. Ding, P. He, N. Jiang, D. Li, J. He, Enhancing regeneration and functionality of excitable tissues via integrating bioelectronics and bioengineered constructs, Int. J. Extrem. Manuf. 7 (2) (2025) 022004, https://doi.org/10.1088/2631-7990/ad9365.
[263] P. Song, D. Zhou, F. Wang, G. Li, L. Bai, J. Su, Programmable biomaterials for bone regeneration, Mater. Today Bio 29 (2024) 101296, https://doi.org/10.1016/j.mtbio.2024.101296.